Nitrification performance in a novel biofilm process based on external biofilm growth

Effects of carrier surface area and substrate limitations

WATER AND ENVIRONMENTAL ENGINEERING
DEPARTMENT OF PROCESS AND LIFE SCIENCE ENGINEERING | LUND UNIVERSITY
URSULA RONJA ZELLMER | MASTER THESIS 2024

Nitrification performance in a novel biofilm process based on external biofilm growth

Effects of carrier surface area and substrate limitations

by

Ursula Ronja Zellmer

Master Thesis number: 2024-01

Water and Environmental Engineering
Division of Chemical Engineering
Lund University

April 2024

Supervisors: **Maria Piculell, Michael Cimbritz**
Examiner: **Åsa Davidsson**

Picture on front page: Cella aggregate by Giada D'Ambrosio

Preface

This thesis includes a large data set based on many hours in the lab with taking care of the experimental setup, sampling and sample analysis. Therefore, I would firstly like to thank Sara Danielli and Vertika Tiwari, who have taken care of the Cella set up before me. Thank you for your investment in all small and big problems, which occurred on the way, and for the time you invested to take samples as a start for this data set. Thank you Vertika for introducing me to the lab routines and showing me the tricks to solve the puzzle of infinite challenges with the set-up.

Secondly, I would like to thank my supervisors Maria Piculell and Michael Cimbritz. Thank you, Maria, for taking the time to answer all the small and big questions, discussing different points of view, and helping me to structure the knowledge I have gained during the time in this project into a written report. Thank you, Michael, for opening up possibility to perform the thesis work in connection to the department of Chemical Engineering (Lund technical university) and giving feedback to improve the flow in the text.

Additionally, it would like to thank the members of the research and development group from AnoxKaldnes in Lund, who supported me in all different ways. Thank you, Sofia Lind for creating the possibility for me to come and be part of this project. Thank you, Per Magnusson and Susanne Jacobsson for your help with programming and extra sample taking over the course of the experiment. It was a great help to know whom to turn to when timing and technic did not fit together. Thank you, Christian Rosen and Magnus Christensson for discussions about result interpretation and development of the experiment. Thank you, Fabian Hjalmarsson and Radhika Unnikrishnan for analyzing all the samples and reanalyzing them if needed, even if I came late with them or delivered 50 at once.

Finally, I would like to give my profound gratitude to my family, for their never ending support throughout my years of study. I also would like to thank Viktor for his patient, continuous encouragement and never-ending supply of motivation and Romana for her so valuable language feed back, turning "witch" into "which".

This achievement would not have been possible without all of you.

Thank you.

Popular science summary

Refining wastewater treatment: Unveiling the power of external biofilm growth.

Refining the biofilm process in wastewater treatment, showed that external growth of the biofilm gave a distinct nitrification advantage, independent of changes in temperature, oxygen dynamics and loads.

In the field of environmental sustainability, wastewater treatment stands as a crucial frontier, safeguarding our aquatic ecosystems from the threats of pollution. As urban spaces expand, the demand for efficient wastewater treatment solutions intensifies. In wastewater treatment, microbes are used to remove pollutants from the wastewater. They are growing as slime in the water and feed on the remains from faeces and other things transporter in the wastewater. This slime is called biofilm. Biofilm processes in wastewater treatment are using pipe bits to increase the surface for biofilm growth on. The biofilm only grows on the inside, where it does not get rubbed off. Hence, implementing biofilm processes, offering compact and effective treatment options with the possibility to treat large loads of water, but at the same time their space for biofilm growth is limited.

Resent developments allowed external biofilm growth in a novel biofilm technology using pebbles to increase the surface for biofilm to grow on. Allowing biofilm to grow to an unlimited extent, building up on its own previous built structure. In this study, we investigated the microbial activity comparing the novel biofilm technology to a conventional biofilm technology. Over 421 days of experimentation, it was shown that the microbial activity of the novel biofilm technology was constantly higher than in the conventional biofilm technology. Revealing a remarkable increase of microbial activity with up to 40%. The higher activity also led to lower values of pollutants in the effluent water, independent of the pollutant load put onto the system.

Despite fluctuations in biofilm thickness, the novel biofilm system demonstrated robust performance, achieving efficient pollutant removal even under changing conditions. Surprisingly, the flexibility of the biofilm in the novel biofilm technology was so high, that it was able to adapt to whatever conditions it is put into. Even loss of pebbles were compensated in the shortest time and did not affect the microbial activity negatively.

In summary, the study suggests that the novel biofilm technology could potentially improve wastewater treatment permanently, offering a promising solution to the evolving challenges of wastewater treatment in an increasingly urbanized world. By using the potential of external biofilm growth, microbial activity can be enhanced, leading to lower pollutants levels reaching nature and economize wastewater treatment in the future.

Summary

An increasing usage of ammonium through societal and industrial development is threatening the water bodies around the world. To protect the aquatic ecosystem and drinking water resources, ammonium can be removed with biological treatment at wastewater treatment plants (WWTP). The development of WWTPs in the last century is aiming to implement solutions, which are cost and energy efficient, have a small footprint and combine a high removal rate of as many substances as possible. A majority of those requirements can be achieved by implementing biofilm-based biological processes, where the microorganisms grow as biofilms on installed supporting material inside the reactors.

One example of a biofilm process is the Moving Bed Biofilm Reactor (MBBR), in which the supporting material comes in the form of carriers with a large protected surface area for biofilm to grow on. The fact that the growing area for the biofilm is limited to the inner surface of the carriers is a potential drawback for MBBRs.

A recent development in biofilm process technologies is the AnoxKaldnes Cella™ technology (by Veolia Water Technologies). Cella is a biofilm process similar to the MBBR, in which biofilm is retained on suspended material in the reactors. However, in Cella the support material are irregular particles based on stabilized, recycled biomass. In Cella, the biofilm will grow on the outside of the support material. This results in a more exposed biofilm area, which will increase with increasing biofilm thickness, in contrast to conventional MBBR carriers.

To better understand how this new biofilm process behaves and differs from the MBBR, the Cella technology is compared to the conventional MBBR technology, by studying the effect of various operation parameters on nitrification performance in a bench-scale lab system.

The overall reactor performance showed earlier biofilm development in the MBBR but a larger nitrification potential of the Cella reactors, independently of their initial fill rate of 3%, 6% and 9%. The performed cycle studies showed an increase in nitrification rate of 26-36% at 20°C and of 40% at 15°C. In addition, effluent concentrations reached with the Cella reactors can be lower than with MBBR even under higher loads. Furthermore, by performing activity studies at different oxygen levels, it was shown that the nitrification rate depends on the oxygen levels in the reactor as well as the oxygen levels the biofilm in the Cella system is adapted to. The maximum nitrification rate of the Cella was not found due to the high flexibility of the biofilm. This results in an adjustment of the biofilm to the given conditions. Hence, implementing the Cella technology allows a reduction of the ammonium loads in wastewater. It can also be used to extend the existing reduction to meet the new standards of the EU- urban wastewater treatment directive.

Sammanfattning

En ökande användning av ammonium genom samhälls- och industriell utveckling hotar utvatten runt om i världen. För att skydda det akvatiska ekosystemet och dricksvattenresurserna kan ammonium avlägsnas med biologisk behandling vid avloppsreningsverk. Utvecklingen av avloppsreningsverk under det senaste århundradet syftar till att implementera lösningar som är kostnads- och energieffektiva, har en liten fotavtryck och kombinerar en hög avlägsnande grad av så många ämnen som möjligt. En majoritet av dessa krav kan uppnås genom att implementera biofilmsbaserade biologiska processer, där mikroorganismer växer som biofilmer på installerat stödmateriel inuti reaktorer.

Ett exempel på en biofilmprocess är Moving Bed Biofilm Reactor (MBBR), där stödmaterialet kommer i form av bärare med en stor skyddad yta för biofilm att växa på. Det faktum att växande området för biofilmen är begränsat till den inre ytan av bärarna är en potentiell nackdel för MBBR.

En nyare utveckling inom teknik för biofilmprocesser är AnoxKaldnes Cella^{TM}-teknologin (av Veolia Water Technologies). Cella är en biofilmprocess liknande MBBR, där biofilmen behålls på suspenderat material i reaktorerna. Men i Cella är stödmaterialet oregelbundna partiklar baserade på stabiliserat, återvunnet biomassa. I Cella kommer biofilmen att växa på utsidan av stödmaterialet. Detta resulterar i en mer exponerad biofilmområde, vilket ökar med ökad biofilmens tjocklek, till skillnad från konventionella MBBR-bärare.

För att bättre förstå hur denna nya biofilmprocess beter sig och skiljer sig från MBBR, jämförs Cella-teknologin med den konventionella MBBR-teknologin genom att studera effekten av olika driftsparametrar på nitrifieringsprestanda i ett bänkskala laboratorie system.

Den övergripande reaktorprestandan visade tidigare biofilmutveckling i MBBR men en större nitrifieringspotential för Cella-reaktorerna, oberoende av deras initiala fyllnadsgrad på 3%, 6% och 9%. De utförda cykelstudierna visade en ökning av nitrifieringshastigheten med 26-36% vid 20°C och med 40% vid 15°C. Dessutom kan utlopps koncentrationerna som uppnås med Cella-reaktorerna vara lägre än med MBBR även under högre belastningar. Vidare visades det genom att utföra aktivitetsstudier vid olika syrgasnivåer att nitrifieringshastigheten beror på syrgasnivåerna i reaktorn samt syrgasnivåerna som biofilmen i Cella-systemet är anpassad till. Den maximala nitrifieringshastigheten för Cella hittades inte på grund av biofilmens höga flexibilitet. Detta resulterar i en justering av biofilmen till de givna förhållandena. Således möjliggör implementeringen av Cella-teknologin en minskning av ammoniumbelastningen i avloppsvattnet. Den kan också användas för att förlänga den befintliga minskningen för att uppfylla de nya standarderna för EU: s direktiv om behandling av stadsavloppsvatten.

Table Of Contents

Abbreviations

AOB ……………………….. Ammonium oxidizing bacteria

AS ……………………………. Activated sludge

BOD …………………………. Biological oxygen demand

COD …………………………. Chemical oxygen demand

DO …………………………… Dissolved oxygen

EPS ………………………….. Extracellular polymeric substances

FNA ……………………….. Free nitrous acid

HRT ……………………….. Hydraulic retention time

K5 ……………………………. AnoxK™ 5-carriers

MBBR ……………………... Moving bed biofilm reactor

MSPE ……………………..… Mean squared predicted error

NOB ……………………….. Nitrite oxidizing bacteria

R1-R4 ………………..……… Reactor 1 - Reactor 4

SBR ……………………….. Sequencing batch reactor

WWTP ……………………. Wastewater treatment plant

1 Introduction

"Water is the source of all life. It carries in its flow the seeds of change" (Coelho, 1993) leaving us with a good sample of what we waste upstream in the catchment. With the ongoing development on earth, an increasing amount of nutrients are produced and processed. These nutrients are to a large extent transported with the wastewater and could pose a risk to humans and the environment, if released back into the environment untreated. Wastewater treatment plants (WWTP) work as barriers to protect the recipient, by removing nutrients from the wastewater. By that, the nutrients can be prevented from entering the recipients.

Due to rising population numbers in settlements and the compression of city space, one of the main challenges today is found in improving wastewater treatment to meet these growing needs. Treatment processes need to be more compact and allow for larger volumes to be treated on the same area as previously allocated to WWTPs. One solution for this is the use of biofilm processes, which are very compact. A biofilm process that has been developed over the last 30 years is the Moving Bed Biofilm Reactor (MBBR). The MBBR uses plastic carriers to increase the surface for the growth of microorganisms, leading to a more compact and efficient wastewater treatment.

A very recent development in the field of biofilm processes is called Cella^{TM}. Cella is a pure biofilm process similar to the MBBR, but instead of plastic carriers it utilizes a bio-based support material, which differs substantially from the MBBR carriers. One major difference between these carriers is that the biofilm grows on the external surfaces of the Cella material, as opposed to the internal surfaces in MBBR carriers. This gives the potential for an increased nitrification performance. The development of Cella is thereby creating a possibility to provide better effluent results and/or safe even more space in wastewater treatment. To better understand how this new biofilm process behaves and differs from the MBBR, the Cella technology is compared to the conventional MBBR technology, by studying the effect of various operation parameters on nitrification performance in a bench-scale lab system.

1.1 Aim

This study aims to investigate the nitrification performance of the Cella technology compared to a conventional biofilm technology (MBBR) in a controlled, lab-scale environment. For this, the focus is laid on differences related to having an external rather than internal biofilm growth. To address this aim, the nitrification performance of the two technologies was compared, when applying different fill rates (resulting in different area for biofilm growth), in combination with varying loads, temperatures and oxygen concentrations. Nitrification performance was determined by the over-all rector performance (removal and effluent concentrations), as well as kinetic assessments of nitrification as a function of oxygen and substrate availability in controlled activity studies.

It was hypothesized that the external biofilm growth (Cella) could enable an increase in nitrification rate compared to conventional MBBR, due to fewer restrictions in growth and better exchange with the wastewater. Secondly, it was hypothesized that the initial carrier fill will have less importance on the performance of the Cella system with external biofilm growth compared to the MBBR system with internal biofilm growth, due to a larger available surface area for contact to wastewater.

2 Background

The following chapter gives the theoretical basis for the study. To understand the concepts behind nitrification, the different possibilities and effects of wastewater treatment and biofilm technologies are compiled, providing a more in-depth understanding of the different parts involved in this study. Additionally, information about the MBBR and the Cella technologies is included to enable an understanding of the differences and similarities of the two.

2.1 Biological treatment of wastewater

Societies all around the world are producing wastewater containing nutrients, which could pose a risk. If released back into the environment untreated, they could lead to eutrophication, depletion of oxygen in the water bodies and an increase in the growth of algae. These algae blooms can be harmful to the environment, livestock and humans or block drainage and water pipes. At the same time, clean water is becoming an increasingly scarce resource, due to contamination of large water bodies around the world and the constant increase in freshwater usage. Hence, the protection of our surface waters becomes crucial to maintain access to freshwater, which is usable for drinking water, farming and industry as well as for recreational purposes.

To protect water sources, wastewater treatment plants (WWTP) are used as a barrier, by removing nutrients and other pollutants from the wastewater, thereby preventing nutrient contamination of the environment. WWTPs usually contains at least two treatment steps, but more commonly nowadays three. The first step is called the primary treatment, followed by the secondary treatment and the tertiary treatment. The primary treatment is used for the removal of particulate matter. This usually includes physical treatment (e.g. settling and sieves). The secondary treatment is used for the removal of soluble pollutants accounting for the biological oxidation demand (BOD) and nutrients in the wastewater. These can be removed using chemical (e.g. flocculation and coagulation) or biological treatment (e.g. biofilm processes). The tertiary treatment step removes soluble micro-pollutants, typically using some kind of chemical treatment (e.g. chemical precipitation and filtration). The tertiary treatment can be combined with the secondary treatment.

In the biological treatment, a variety of microorganisms utilize the organic matter and nutrients in the wastewater for growth, thereby removing them from the water. For example, ammonium is consumed by bacteria and transformed to nitrogen gas, through several steps. The biological treatment process can take place in different forms, which are divided into categories depending on how the microorganisms are retained in the treatment process.

The most commonly used method is called activated sludge (AS), where the microorganisms grow in free-floating flocs. This process has been used for more than 100 years. In activated sludge, the flocs are transported with the water to the end of the treatment line, which requires a large area (large footprint) to allow a longer contact time between microorganisms and wastewater. In the end of the treatment line, the microorganisms are separated from the water (typically in a clarifier) as sludge. Excess sludge is discharged to the sludge treatment, and a controlled amount of sludge is recirculated to the beginning of the line. By recirculating the flocs, it is possible to control the sludge age, and therefore the retention time of the microorganisms in the system. To enable the growth of slow-growing microorganisms, the AS process requires a high sludge age.

The development of WWTPs over the last century has been aimed towards implementing solutions that are cost and energy efficient, have a small footprint and combine a high removal rate of as many substances as possible, to make wastewater treatment cost-efficient and allow for the treatment of large water quantities. A majority of these requirements can be achieved by implementing biofilm-based biological processes, where the microorganisms grow as biofilms on installed supporting material inside the reactors (di Biase et al., 2019).

2.2 What is a Biofilm?

Biofilms can be found on nearly every possible surface, that is slightly moist, on which they build small-scale ecosystems, containing different types of spontaneously growing microorganisms. In wastewater treatment, the microorganisms in the biofilm are responsible for the breakdown of organic material through biochemical reactions, as well as the degradation and transformation of soluble compounds in the wastewater (Morgenroth, 2008). The microorganisms live in a dense layer, containing organic and inorganic particles, and are held together by extracellular polymeric substances (EPS) produced by them. The EPS accounts for 50-90 % of the biofilm and enables it to grow on different surfaces (Boltz and Daigger, 2010). The biofilm is surrounded by a stagnant layer of water, the boundary layer, separating it from the bulk liquid (Figure 2.1).
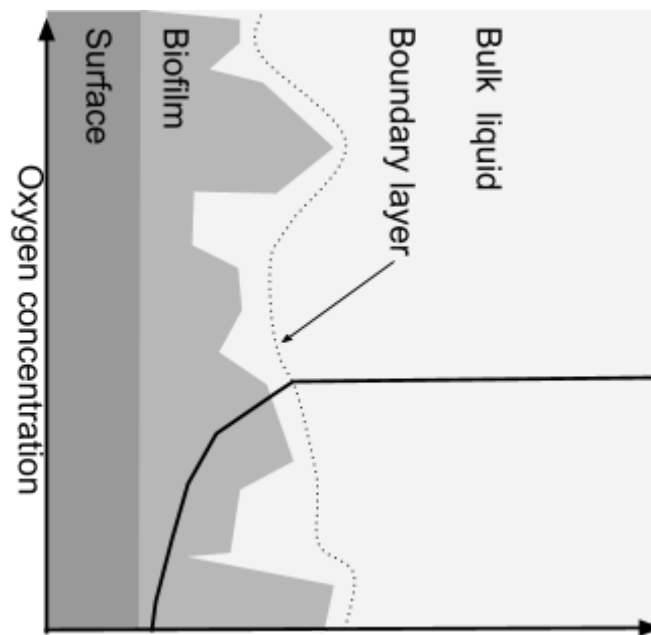

Figure 2.1. Biofilm with surrounding water layers and diffusion gradient of oxygen into the biofilm from the bulk liquid.

Biofilm is formed through free-floating cells from the bulk liquid (Figure 2.2). They attach to a surface through adhesion and EPS production (Deena et al., 2022). When attached, the cells grow and multiply, building a biofilm, which allows higher-order organisms to thrive (Deena et al., 2022). The mature biofilm disperses free-floating cells to colonize new surfaces (Figure 2.2). While growing, new biofilm layers are built on top of the existing ones, leading to less active or dead biofilm in the bottom. These structures are weaker and can lead to abrasion of biofilm, due to collision between particles or erosion due to shear forces. When larger parts of the biofilm are detached, it is called sloughing (Ødegaard, 2006). Due to forces from the water passing the biofilm, smaller particles can also be detached from the surface of the biofilm. This process is called erosion. Biofilm detachment exposes new open areas, which

can be colonized by free-floating cells or used by attached biofilm to extend their growth. Hence, a circle of different phases is created containing: attachment, growth, the mature biofilm in steady-state and detachment (Figure 2.2). In wastewater treatment, the detached biomass, from erosion or sloughing, will leave the reactor of the wastewater treatment with the effluent water (Gapes and Keller, 2009).

The biofilm thickness in the steady-state depends on the balance between growth and detachment, with a thinner and more compact biofilm built under higher turbulence conditions due to stronger shear forces, while lower mixing and higher loads lead to more extensive growth than detachment, promoting a thicker biofilm (di Biase et al., 2019).
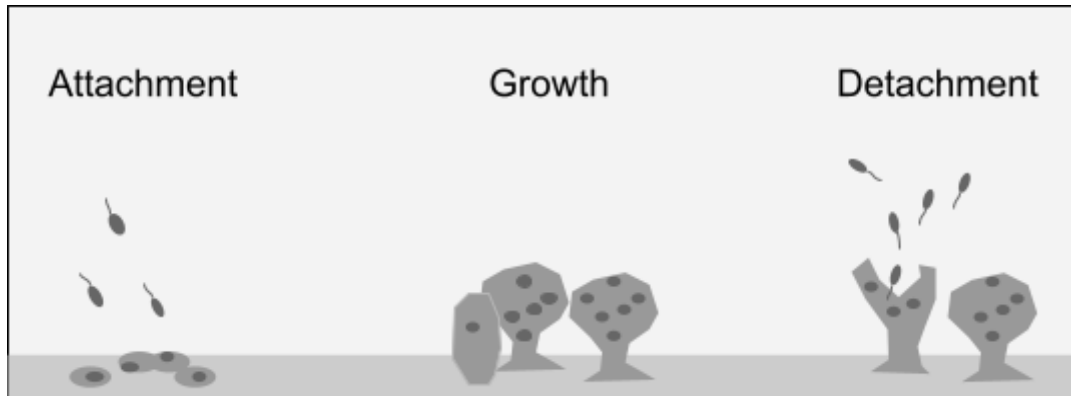

Figure 2.2. Different stages of biofilm built up containing attachment to surface, growth and multiplication and detachments and dispersal (adapted after P. Dirckx, center for biofilm engineering at Montana state university © 2003).

The microorganisms in the biofilm are responsive to local environmental conditions, such as pH, temperature, the presence of electron donors and electron acceptors and the availability of macro-nutrients (Morgenroth, 2008) as well as oxygen. The main transport mechanism in the biofilm is diffusion (Mašić et al., 2010). Diffusion is a spontaneous process of fluids and particles moving to be distributed as evenly as possible in the environment. This leads to a gradual movement of soluble substances from the bulk liquid into the biofilm and vice versa. Within the biofilm, the substances are removed and/or transformed by the microorganisms. As the substance penetrates the biofilm, a concentration gradient is therefore developed, leading to an increase (e.g. for carbon dioxide) or decrease (e.g. oxygen) of the substance from the surface of the biofilm towards the deeper biofilm layers (Figure 2.1). Biofilms can be partially or fully penetrated by any soluble substance (Boltz and Daigger, 2010) including oxygen.

The density and thickness of the biofilm are dependent on external conditions like turbulence in the bulk liquid and load. The biofilm density increases with increasing turbulence, due to larger shear forces, which only a denser, more compact biofilm will withstand (di Biase et al., 2019; Eberl et al., 2000). Larger forces from high turbulence can also lead to the removal of the outer layers of the biofilm, creating a thinner biofilm layer. For example, Hibiya et al. (2004), showed that biofilm density decreased with increasing biofilm thickness, where the thick biofilm had a more heterogeneous structure and larger pores than the thin biofilm. Biofilm thickness is also expected to vary with changes in the concentration of nutrients reaching the biofilm (Boltz and Daigger, 2010), leading to an increase in biofilm thickness in higher loads (di Biase et al., 2019).

2.2.1 MBBR

One example of a biofilm process is the Moving Bed Biofilm Reactor (MBBR), in which the supporting material comes in the form of carriers with a large, protected surface area for biofilm to grow on. The MBBR is often applied in WWTPs that need to keep the footprint of the biological treatment as small as possible.

When introducing free floating carriers into the biological treatment, the surface area available for active biofilm is increased. Hence, a larger biofilm quantity can be contained in a water volume compared to an AS, leading to the possibility of treating more wastewater in the same reactor volume (di Biase et al., 2019). An implementation of an MBBR in an existing WWTP will therefore lead to an increase in volumetric performance with the same footprint, enabling the WWTP to be upgraded with very low additional costs (di Biase et al., 2019).

The carriers are kept moving and in suspension by either aeration or mechanical mixing. A potential drawback with these systems is that strong aeration is needed to keep the carriers in suspension (Rusten et al., 1995). The carriers are maintained in the reactor by the installation of sieves or grids in front of the effluent pipe. Through this, the treated water can be separated from the biomass containing carriers, keeping the microorganisms in the reactor for longer. Hence, the biofilm can grow over a longer time span, allowing the development of slow growing microorganisms, such as nitrifiers, even at a very short hydraulic retention time (HRT).

Due to the retention of the biomass on the carriers, no sludge return is needed to retain the biomass in the reactor, as it is in the activated sludge system with suspended growth. Additionally, the limitation of the system is not based on the biomass amount, but on the diffusion over the available surface area (Boltz and Daigger, 2010).

The MBBR carriers (Figure 2.3) typically have a density < 1 kg/m^3, and can differ in shape and size (typically a few centimetres in diameter). The complex carrier shapes introduce surfaces for biofilm growth, especially on the protected surfaces inside the carriers (di Biase et al., 2019). MBBR carriers are typically made from plastic due to the density and flexibility of the material. However, there are potential draw-backs due to its dependence on non-renewable fossil resources and the risks of contributing to microplastic production through constant abrasion. Another risk with plastic carriers is the potential of accidental release to nature, where the carriers will not degrade and hence pose a risk to the environment.
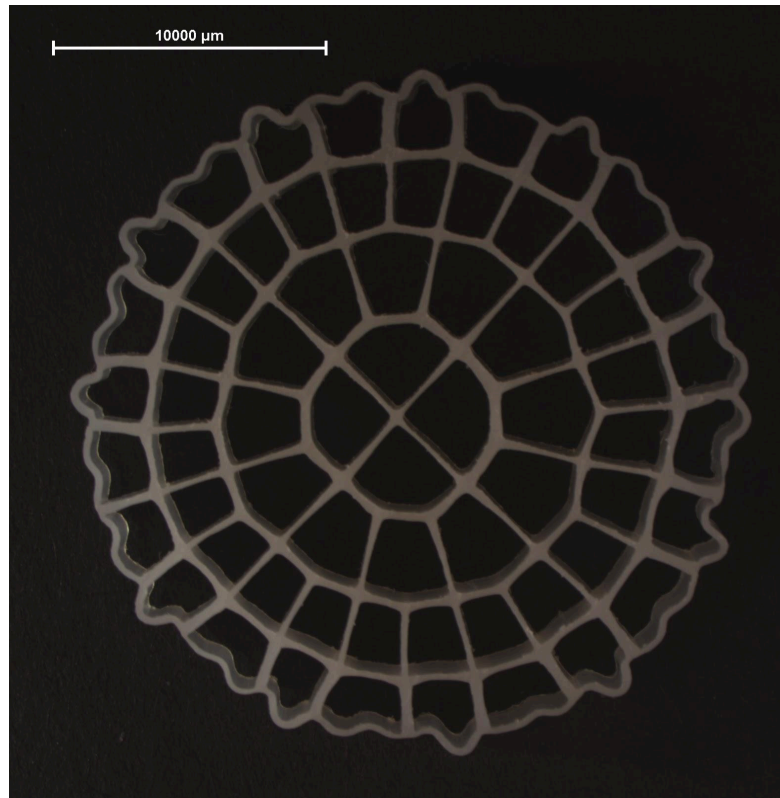
Figure 2.3. AnoxK™ 5-carriers used in conventional MBBRs and in the MBBR reactor of this experiment.

In most MBBR carriers, there is no biofilm growing on the outside of the carriers due to constant erosion caused by collisions between the carriers (Rusten et al., 1995), while at the same time, a large, protected surface is provided on the inside of the carriers. This internal growth limits the exposure of the biofilm to the wastewater, with increasing biofilm thickness decreasing the exposed biofilm area (Young et al., 2016) until pores can be clogged and no internal surface is available (Figure 2.4). In a wastewater treatment using MBBR, the biofilm thickness usually varies between 200-600 μm (Gapes & Keller, 2009; Salvetti et al., 2006). Depending on the carrier used, the biofilm can also be much thinner, with a thickness down to 25 μm (Piculell et al., 2016).

The thickness of the biofilm also limits the diffusion of substrates into the biofilm, which could lead to a decrease in process performance. Independent of the biofilm thickness, Mašić et al. (2010) found that the most inner 100 μm of a biofilm were not oxidized. However, limited exposure together with the layered growth structure of the biofilm has the advantage that the biofilm on the carriers is more protected. Through this, it is more resistant to variations in influent water characteristics, such as shock loads, pH, temperature and toxic compounds (Dezotti et al., 2018).
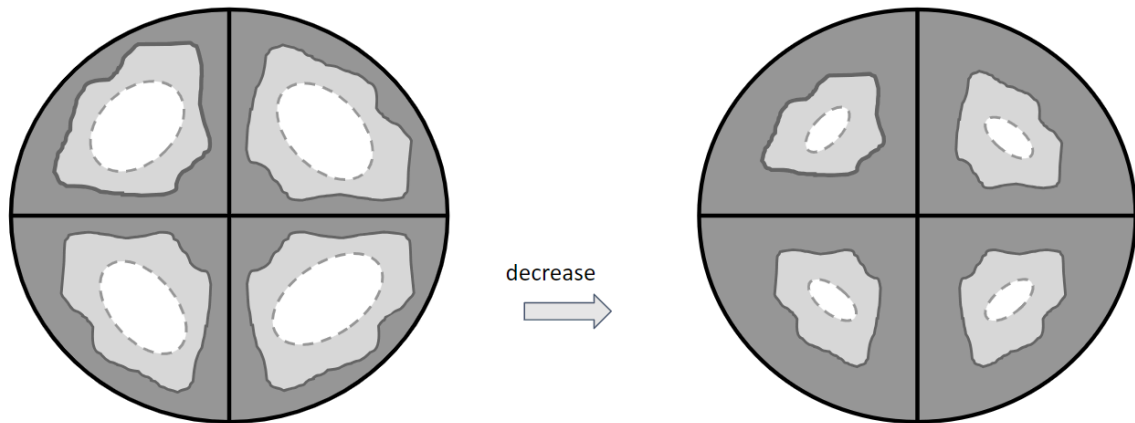
Figure 2.4. Inwards growth of biofilm on the protected surfaces of an MBBR carrier leading to a decrease in cross-section of biofilm surface for contact to wastewater (dashed line), when biofilm (dark gray area) is increasing in thickness, while thickness of the boundary layer (light gray area) stays the same.

The fact that the growing area for the biofilm is limited to the inner surface of the carriers is a potential draw-back for MBBRs. If biofilm could grow on the outside of the carrier, growth of the biofilm would rather extend the contact area to the wastewater instead of limiting it, which could lead to a more effective process. However, the configuration of the carrier must then be adapted to reduce the shear forces and allow external growth.

2.2.2 Cella

Due to the constant increase in awareness of pollution and the need to protect surface waters, more regulations and stricter demands on the regulations for nutrient release have been implemented. This is encouraging the ongoing development of wastewater treatment processes. A recent development in biofilm process technologies is the AnoxKaldnes Cella™ technology (by Veolia Water Technologies). Cella is a biofilm process similar to the MBBR, in which biofilm is retained on suspended material in the reactors. However, in Cella the carriers (from now on referred to as "support material") are irregular particles based on stabilized, recycled biomass which, if released into the environment, are biodegradable.

While the plastics used for MBBR carriers float, the Cella material sinks in water. To ensure sufficient suspension in the Cella process, the size of the support material must therefore be significantly decreased (in the range of 0.5-5 mm) compared to MBBR carriers. This leads to a smaller collision force between the particles, which allows the biofilm to grow on the outside of the support material. Support material surrounded by biofilm is called aggregates. The outward growing biofilm will be exposed to abrasion and erosion. This increased exposure is likely to reduce the boundary layer surrounding the biofilm compared to that of biofilms growing on protected surfaces. Additionally, the available surface area will increase with increasing biofilm thickness in contrast to conventional MBBR carriers (Figure 2.5), where increased biofilm will decrease the available surface area.
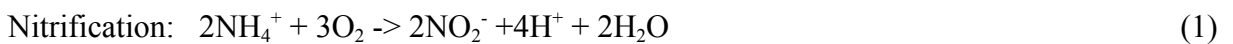
Figure 2.5. Outwards growth of biofilm on the surfaces of Cella support material leading to an increase in cross-section of biofilm surface for contact to wastewater (dashed line), when biofilm (dark gray area) is increasing in thickness, while thickness of the boundary layer (light gray area) stays the same.

2.3 Nitrification in wastewater treatment

Ammonium, present in wastewater, comes from a variety of different sources (e.g. urea, proteins, amino acid products). When released into aquatic ecosystems, it contributes to eutrophication and algae blooms, which pose a hazard to aquatic life and available water sources. Hence, many WWPT have the requirement to remove ammonium to some level, before wastewater can be released.

Biological removal of ammonia in wastewater treatment is typically done through an aerobic and an anaerobic process, referred to as nitrification and denitrification (Equation 1, 2 and 3), where ammonium is transformed into nitrogen gas through several steps by bacteria.

Nitrification: $2NH_4^+ + 3O_2 \rightarrow 2NO_2^- + 4H^+ + 2H_2O$ (1)

$2NO_2^- + O_2 \rightarrow 2NO_3^-$ (2)

Denitrification: $NO_3^- + \text{organic matter} \rightarrow N_2 + CO_2 + H_2O$ (3)

The bacteria responsible for the nitrification, the first part of the nitrogen removal process, are part of two phylogenetically unrelated groups. They are aerobic, autotroph, lithoautotrophic bacteria (Okabe et al., 2002), which are called ammonia oxidizing bacteria (AOB) and nitrite oxidizing bacteria (NOB). AOB oxidize ammonium to nitrite (Equation 1), which is then oxidized to nitrate (Equation 2) by NOB (di Biase et al., 2019). The most common AOB in wastewater treatment are Nitrosomonas and Nitrosospira and the most common NOB in wastewater treatment are Nitrospira and Nitrobacter (Juretschko et al., 1998). Both types of bacteria are slow growing compared to denitrifying heterotroph bacteria. This is due to the low energy content from the ammonia and the nitrite oxidation (Prosser, 1990).

The nitrification rate is correlated with the availability of dissolved oxygen (DO), leading to decreased nitrification with decreased DO (Christensson and Welander, 2004). Similarly, the nitrification rate is also dependent on the available nitrate and nitrite (NH_3^- or NO_2^-) in the water, leading to a decrease in nitrification with decrease of nitrate and nitrite.

Both relationships can be described by the Monod substrate kinetics (Equation 4), leading to a double dependency of nitrification rates (Gapes and Keller, 2009; Sánchez et al., 2001).

$$\text{Monod: } \mu_{(s)} = \mu_{(max)} \times \frac{S_{NH}}{K_{NH}+S_{NH}} \times \frac{S_o}{K_o+S_o} \tag{4}$$

with $\mu_{(s)}$ being the growth rate at ascertain substrate concentration, $\mu_{(max)}$ being the maximum specific growth rate, K_{NH} and K_o are the substrate half-saturation coefficient for ammonium and oxygen respectively and S_{NH} and S_o being the concentration of ammonium or oxygen respectively as the limiting food in solution.

The AOB and NOB are strongly interacting during the nitrification process, due to the NOB depending on the AOB product nitrite as an electron donor. But at the same time, AOB and NOB are competing for the available oxygen in the process (Juretschko et al., 1998). The NOB usually grow faster than the AOB, and therefore the nitrification rate in a WWTP is limited by the activity of the AOB (Sánchez et al., 2001). The higher growth rate of the NOB is due to their oxygen kinetics, where NOB grow faster at high oxygen levels, while the AOB have a growth advantage over the NOB at low oxygen levels, (Pérez et al., 2014; Sánchez et al., 2001). In biological wastewater treatment, there is typically competition for oxygen between the heterotrophs and the nitrifying bacteria, where the slow growing nitrifying bacteria risk being outcompeted. This is avoided by ensuring a low organic matter content in the nitrifying process step. Under such conditions, nitrifying bacteria can consume the oxygen as the heterotrophs lack substrate to feed on.

Other factors, that can affect the nitrification rate are pH and temperature (Prosser, 1990; Wang et al., 2021), as well as high concentrations of non-ionized forms of ammonium and/or nitrite (Anthonisen et al., 1976). The pH and alkalinity are relevant for nitrification due to the release of hydrogen ions during the nitrification process. In municipal wastewater treatment plants, the alkalinity is typically sufficient to meet the nitrification requirements. However, on some occasions, it may be necessary to add alkalinity to avoid inhibiting the nitrification process. Inhibition through non-ionized forms of ammonium and nitrite is also highly dependent on the pH in the system. A inhibition limit value for the non-ionized forms of ammonium was found at 1-5 mgN/l (Zhao et al., 2023) and for nitrite with a level of free nitrous acid (FNA) > 0.0255 mgN/l (Fu et al., 2010). At the same time, NOB and AOB are not necessarily inhibited to the same degree. Gieseke et al. (2003) found an indication for higher NOB sensitivity to free ammonia compared to AOB.

All biological processes are temperature dependent, with the dependency following the Arrhenius relationship (Equation 5). This relationship links the growth rate to temperature, whereby an increase of 10°C results in a doubling of the rate (di Biase et al., 2019). Therefore, reaction rates will increase with increasing temperature between 5-35°C (Hellinga et al., 1998). Comparing the AOB with the NOB shows that the NOB have an advantage in growth over the AOB at temperatures between 5-20°C, while at higher temperatures the AOB grow faster than the NOB (Hellinga et al., 1998).

$$\text{Arrhenius: } \mu_{(T)} = \mu_{T(ref)} \times \theta^{(T-10)} \tag{5}$$

With $\mu_{(T)}$ being the growth rate at a certain temperature, $\mu_{T(ref)}$ being the growth rate at a reference temperature (typically 10°C) and θ being the temperature-activity coefficient.

2.3.1 Nitrification in biofilm technology

Biofilm processes support nitrification due to the long retention time of the biofilm, which allows slow-growing microorganisms to thrive. However, the relationships found for single bacteria strains may not always be directly transferable to the behaviour in a biofilm, due to diffusion limitation of the substrate as well as the growth of different bacteria in a community. This limits the environmental influences and at the same time increases competition for resources, often resulting in a more niche-oriented coexistence of different bacteria stains.

Just as for any microbial process in a biofilm, nitrification in biofilms depends on the availability of substrate, specifically in the form of dissolved oxygen (DO) and ammonium and/or nitrite (di Biase et al., 2019). Nitrification, as an aerobic process, is dependent on the penetration ratio of oxygen into the biofilm, meaning how much depth of the total biofilm gets in contact with oxygen. Hence, the nitrification rate is significantly impacted by the structure of the biofilm, depending on the biofilm thickness and its density, where the oxygen penetration ratio decreases gradually as the biofilm thickness increases (Gapes and Keller, 2009; Hibiya et al., 2004). At the same time, the dependency on ammonium shows that, biofilms grown in high ammonium bulk concentration have a higher activity and thereby larger area-specific rates than biofilms grown in low ammonium-loaded systems (Gapes and Keller, 2009). Thinner biofilms with a higher density have a lower penetration depth for both ammonium and oxygen, resulting in a slower diffusion into the biofilm, but a higher reaction rate (di Biase et al., 2019; Hibiya et al., 2004).

The diffusion gradient of oxygen and ammonium into the biofilm allows the different bacteria to thrive at different depths of the biofilm. Okabe et al. (2002) found that AOB were mostly located at the outer layer of the biofilm, where higher oxygen and nutrient content is present, and that NOB had a higher abundance in the deeper layer of the biofilm, leading to dense clusters of AOB and NOB in the aerobic layer of the biofilm. On the contrary, Gieseke et al. (2003) found that the different nitrifiers can be homogeneously distributed throughout the biofilm with no clear spatial separation between nitrite and nitrate production. The homogenous distribution could be due to the occurrence of nitrite production in the oxic part of the biofilm and its decrease with decreasing oxygen concentration in deeper layers of the biofilm.

One of the goals of wastewater treatment is the transformation of ammonium, hence the ammonium levels in a MBBR are often low. Oxygen, in contrast, can be controlled and used to manage nitrification rates. The oxygen, which penetrates the biofilm, is consumed by the bacteria in the outermost layer of the biofilm and the boundary layer. Hence, it decreases with increasing penetration depth (Gieseke et al., 2003; Hibiya et al., 2004). If oxygen diffuses only partly into the biofilm before it is depleted, the lower layers of the biofilm will be anoxic and not be active in aerobic processes. The total nitrification activity thus depends strongly on the available effective surface area for biofilm growth, as the exchange mainly occurs in the aerobic zone at the biofilm surface (Christensson and Welander, 2004). For MBBRs, it has been shown that increasing dissolved oxygen (DO) concentrations in the reactor leads to a nearly linear increase in nitrification rate (Gapes and Keller, 2009; Gieseke et al., 2003) implying a mass transfer effect depending on the penetration rate of oxygen into the biofilm. Additionally, higher turbulence around the biofilm will also lead to faster transport of oxygen from the bulk liquid into the biofilm (Mašić et al., 2010), due to a thinner boundary layer. Nevertheless, being dependent on diffusion, the limit of the mass transfer rates in a biofilm due to oxygen diffusion is higher, than in suspended biomass, where mass transfer can happen from all dimensions of the flocs, compared to a biofilm, where the mass transfer can only happen from one dimension (Mašić et al., 2010).

Interestingly, Christensson and Welander (2004) found that decreased temperature did not influence nitrification, despite expectations based on nitrifier temperature dependence. This was explained by lower temperatures allowing a higher DO-concentration in the bulk-liquid, leading to higher penetration of oxygen into the biofilm and hence a thicker active layer.

As previously mentioned, the organic load in the wastewater must be removed upstream to avoid interference with the nitrification (Rusten et al., 1995). Hence, the organic loading rate is one of the main factors determining the nitrification rate in an MBBR and should be kept as low as possible (di Biase et al., 2019). Alternatively, one can rely on the diffusion gradient into the biofilm, creating niches for heterotrophs and nitrifiers to co-exist. For this, the biofilm has to be thick enough to give space to the nitrifying bacteria in the lower biofilm layers, and there must be enough oxygen to diffuse down to where the organic matter concentration is low (Hibiya et al., 2004). However, if the organic matter is removed in a primary treatment step, more favourable conditions can be created for the nitrifying bacteria, and thus, a larger depth of the biofilm can be used by the nitrifiers and the nitrification process can be more effective.

While the biofilm is growing in an MBBR, the penetration ratio decreases with increasing biofilm thickness. This leads to the possibility of a larger anaerobic zone in the bottom of the biofilm, allowing for microbial denitrification (Hibiya et al., 2004). At the same time, the contact area between wastewater and biofilm is reduced due to the biofilm covering increasing portions of the flow channels through the carrier spaces (Figure 2.4). This can be limiting for nitrification due to the surface dependency, especially for inwards growing biofilm.

3 Methods

To investigate the nitrification capacity of Cella, a bench scale experiment was set up and run between 2023-02-01 and 2024-03-28 comparing the Cella biofilm process to a conventional MBBR process. For this, reactors one, two and three (R1, R2, R3) were equipped with Cella support material and reactor four (R4) was equipped with AnoxK™ 5-carriers ("K5").

3.1 Reactor set-up

The bench-trial was set up with four sequencing batch reactors (SBRs), with one liter each. SBRs are non-continuous and have four different phases during a cycle, including filling, mixing, settling and draining. The mixing phase can be divided into different sub-periods of aeration and non-aeration, depending on the process wanted (Gieseke et al., 2003). In this study, the volume was aerated over the whole mixing phase. Both the MBBR and the Cella processes are continuous in full-scale applications, however SBR operation was applied in this study to simplify operation at a small scale. To avoid the accumulation of suspended solids in the lab reactors, the cycle operated with a very short settling time (one minute), to ensure that the process was biofilm dependent only.

The different phases were programmed and controlled via an Energenie power manager plug, to ensure that the different phases occurred at the same time in all four reactors and did not overlap. The cycle time was set to two hours, for which 500 ml of reactor volume was replaced with new feed (Table 3.2). This resulted in 12 cycles per day. Each cycle consisted of a filling phase of five minutes, a mixing phase of 111 minutes, a settling phase of one minute and a draining phase of three minutes.

Each reactor was equipped with aeration, an inflow pump and an effluent pump. For the aeration, air was supplied through the bottom of the reactor via an aquarium pump, to keep the carriers suspended. The air flow was regulated using a rotameter. The inflow of the feed was managed through a pump, where the pumping rate could be adjusted individually for each reactor, to ensure the inflow of 500 ml per cycle. The effluent was pumped out of the reactor via a PVC-pipe inserted into the reactor and fixed just above the bed volume to ensure that the effluent was pumped from just above the bed to avoid the accumulation of suspended solids. To regulate the effluent volume, a hole was drilled into the PVC-pipe and adjusted to a height of 500 ml of the reactor volume. Through this, the effluent volume of 500 ml per cycle could be ensured and a distance to the settled carriers could be established to avoid loss of carriers together with the effluent water (Figure 3.1). The outflow pump rate was adjusted separately for each pump and set to a speed to ensure that 500 ml would be removed during the programmed three minutes of pumping.

Each effluent was discharged into a reservoir, which was used to collect aggregates in case of failure of the effluent pump. Additionally, each reactor set-up was placed in a 20 liter container to ensure that aggregates would be contained in case of influent pump failure, as well as to protect the pumps from water.

To maintain a constant temperature in the reactors, all reactors were connected to a water bath that was adjusted to the experimental target temperature. Water was then led through a pipe system connecting the water jackets of the reactors, by coupling them in series, starting at R4 and continuing to R3, R2, R1 and then returning to the water bath.
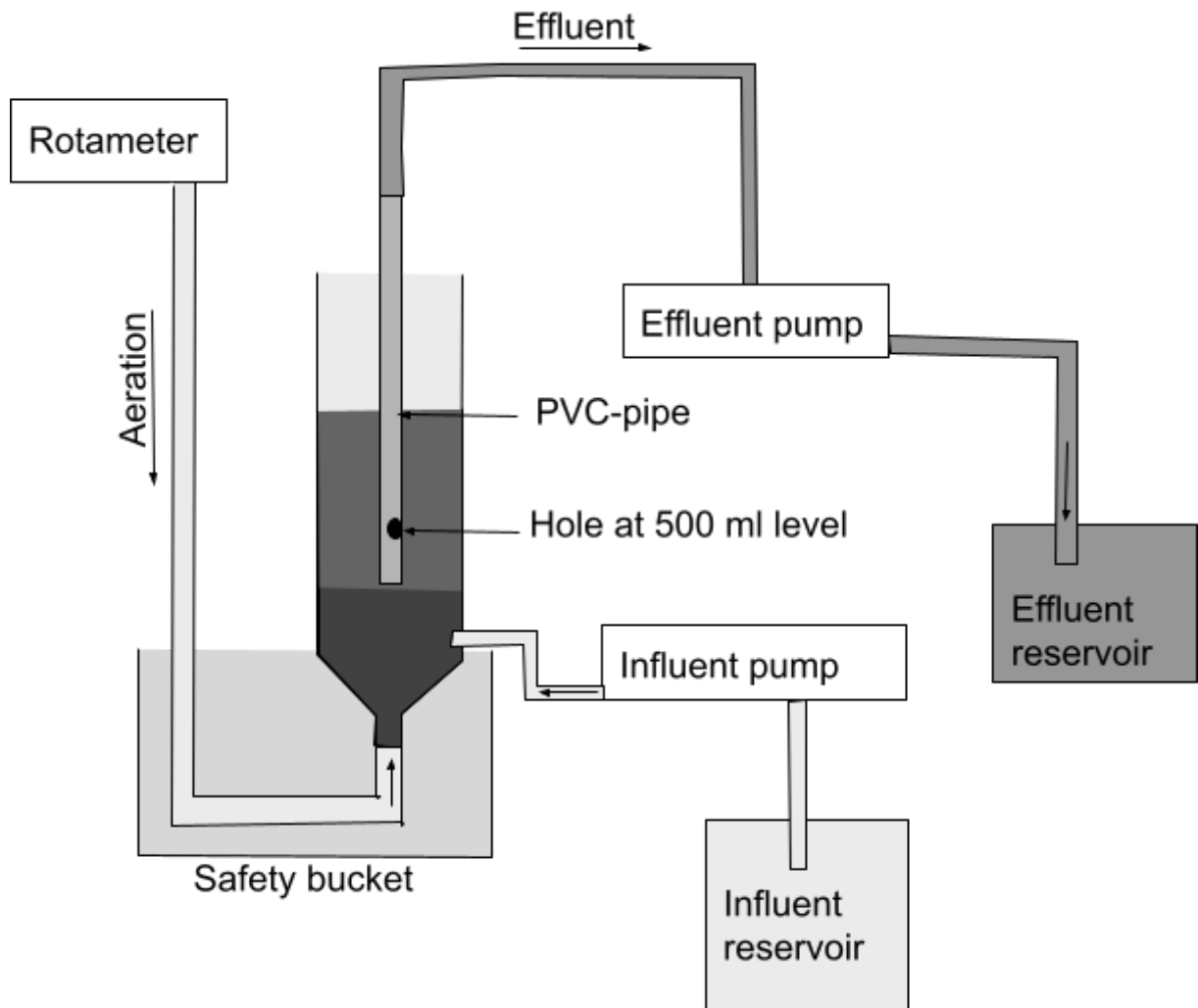
Figure 3.1. Scheme for the reactor set up including the 1 litre reactor with bed volume and water level above. Feed inflow via inflow pump from the influent reservoir. 500 ml removal of the effluent through the PVC pipe, limited by the height of the hole in it. The effluent reservoir was used to capture aggregates, which were pumped out and a safety bucket of 20 litres was used to capture aggregates washed over the edge of the reactor due to pump failure and to protect the pumps from water.

3.2 Carriers

The reactors R1-R3 were filled with Cella support material of different fill rates (3, 6 and 9% virgin material respectively) to determine the effect of surface area within the Cella process. Reactor 4 was filled with 50% (166) K5-carriers as a conventional MBBR reference. Consequently, the physical and chemical parameters of the carriers differed (Table 3.1). The K5-carriers and the Cella support material were fully suspended during the mixing phase. The difference in size and density led to the floating behaviour of the K5 even with biofilm growing on them, and the Cella support material sunk rapidly to the bottom even with biofilm growing on them, during non-aeration phases.

Table 3.1. Differences between the Cella and MBBR support material in the study.

Parameter	Cella	K5
Material	stabilized, recycled biomass	plastic (HDPE)
Size	irregular shape with an average diameter around 1 mm	3.65 mm height, 25 mm diameter
Density	> 1kg/l	< 1kg/l
Volumetric fill of virgin material	3-9%	50%
Protected surface area	N/A	0.4 m^2

3.3 Reactor operation

The support material was added to the reactors on the 1st of February 2023. In the following two days, all reactors were seeded each day with 100 ml activated sludge from a local municipal WWTP, to enhance microbial growth. The experiment ran for a total of 421 days with different loads, aeration/mixing speeds and target temperatures (Figure 3.2).

During the start-up phase (day 0-63) the load and the aeration was gradually increased to match the reactor performance and to allow biofilm growth. In the following days, the load and aeration were decreased prior to a stable period (day 64-98) to allow the NOB in the biofilm to grow and thereby lower the nitrite content in the effluent. The next phase (day 99-152) was used to increase the load and aeration in all the reactors to establish the maximum nitrification rate for the Cella reactors. This period was followed by a period (day 153-212) with stable conditions in the reactors, while the first set of analytical experiments were run. This phase contained a very high load of 1.20 gNH$_4$-N/l*d for the Cella reactors and was run as all the previous phases at 20°C (Figure 3.2).

To further challenge the Cella reactors without increasing the load, the temperature was lowered to 15°C in all the reactors from day 215. This led into an adjusting phase (day 213-242) with a lowered load for a short time, allowing the biofilm to adjust to the new conditions, followed by an increase to the same conditions as in the previous phase. On day 243-347, the load to R4 was lowered to 0.60 gNH$_4$-N/l*d to adjust the load to the possible nitrification rate in the reactor and avoid a buildup of nitrite. At the same time, the Cella reactors were returned to a load of 1.20gNH$_4$-N/l*d and run under these conditions until day 347, to test if the maximum nitrification rate had been reached and allow stable conditions during the second set of experiments.

Finally, a last adjusting period (day 348-370) was initiated, where the aeration was lowered from 6 l/min to 3 l/min for two of the Cella reactors (R1 and R3). To allow for adjustment, the load was again lowered for a short time and then increased again (day 371-386) to meet reactor performance. Reactor R2 was set to the same conditions as the MBBR reactor (R4)

during the last adjustment period (day 348-370), in order to study how the system responds to a reduced load and to be able to directly compare a Cella reactor to the MBBR reactor. During these adjustments, a significant increase in ammonium in the R2 effluent was detected. Monitoring of the alkalinity (Figure 3.2) showed that it was insufficient in the reactor. Hence, alkalinity was increased in the feed to both R2 and the MBBR reactor (R4) leading to the same conditions in both reactors. The load in the final stable phase (day 387-421) was kept at 1.06 gNH_4-N/l*d in R1 and 1.20 gNH_4-N/l*d in R3, with an aeration of 3 l/min, and at 0.60 gNH_4-N/l*d in R3 and R4 with an aeration of 5 l/min. The last set of experiments was then performed under these conditions.
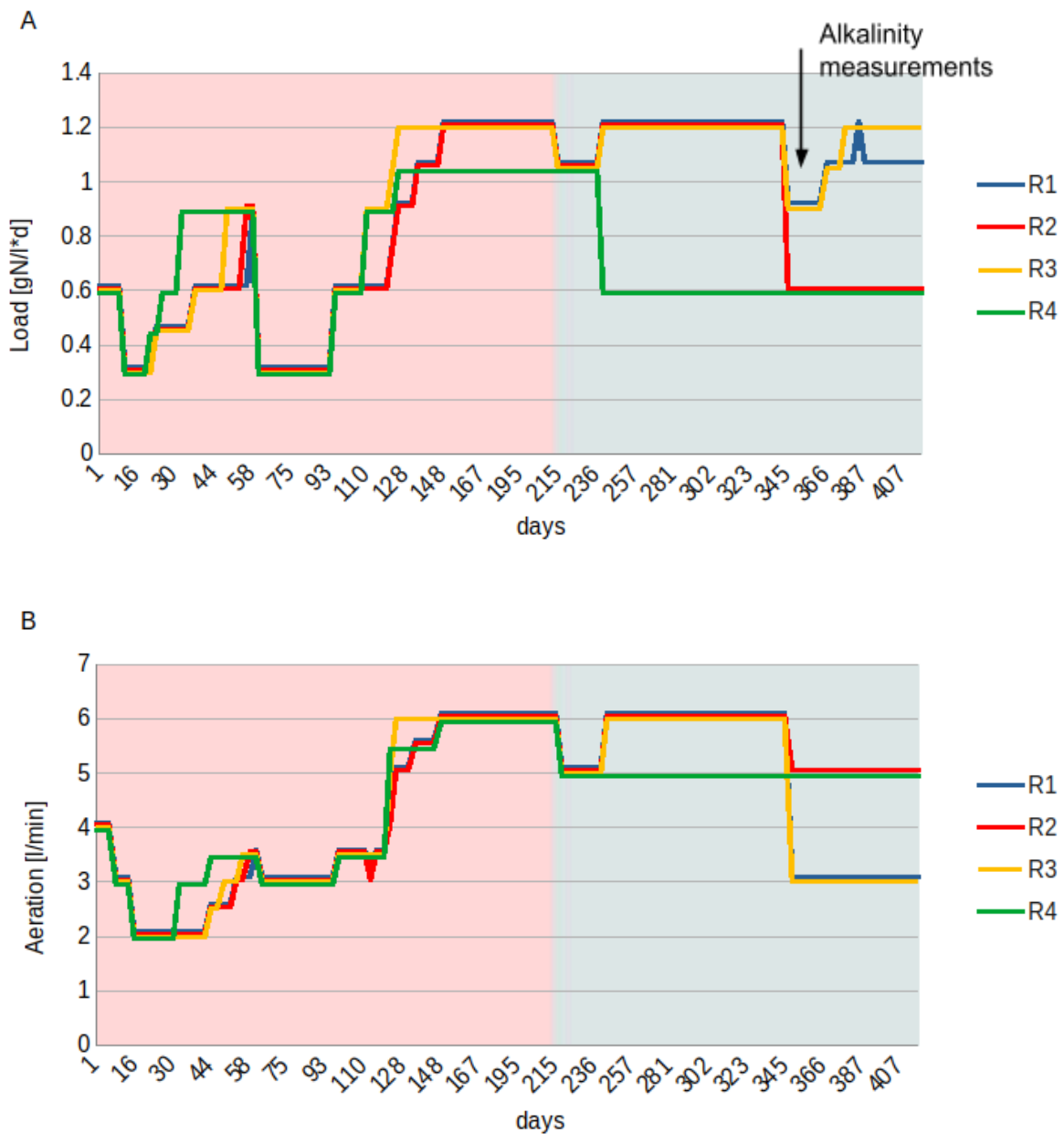
Figure 3.2. Applied loads (Figure A) and aeration (Figure B) to the four bench-scale reactors over time. Pink colour marking the operation time at 20°C and blue colour at 15°C. Alkalinity monitoring was initiated at the end of the study, as indicated with black arrow.

26

3.3.1 Feed composition

The reactors were supplied with artificial wastewater, with a low carbon to nitrogen ratio, to mimic conditions in wastewater after carbon removal treatment. The following basic recipe (Table 3.2) was used and modified for different experimental periods by changing the ammonium and alkalinity content. The alkalinity was increased and decreased together with the ammonium load, to ensure a sufficient buffer capacity in the reactor throughout a cycle. Note that the C:N and P:N ratios thus varied throughout the trial.

By using artificial wastewater, the reactors were supplied with stable loading rates. To minimize the feed volume needed, the artificial water contained higher concentrations of the different compounds to still reach comparable loads.

Table 3.2. Basic feed recipe for 25 litre artificial wastewater

Substance	Volume	Description
Peptone from meat	2250 mg	
NaHCO3	50-75 g	buffer
P-solution	7.50 ml	containing 56 g/l KH_2PO_4 corresponding to 12.75 g/l phosphorus
N-solution	100-200 ml	containing 95.50 g/l NH_4Cl corresponding to 25 g/l N
T1	5.00 ml	trace solution 1 (content s. Appendix 1)
T2	5.00 ml	trace solution 2 containing 5.80 g/l CaCl2x2H2O

3.3.2 Changes in aeration and temperature

The dissolved oxygen (DO) in each reactor could be regulated independently by varying the aeration through a rotameter. Variations in air flow, activity and load resulted in different DO-concentrations in the different reactors over the course of the experiment. Besides providing oxygen, the aeration also kept the carriers suspended and constantly rotating. During the start-up phase (day 0-63) all reactors were set at the same target aeration varying between 2-4 l/min (Figure 3.2). All reactors were operated with a target aeration of 3 l/min during the first stable period (day 64-98) and 6 l/min during the second stable phase (day 153-212). The aeration until day 98 was aiming for high DO levels in the reactor to avoid limitation in nitrification due to oxygen. For the time until day 212 the goal was to have the same aeration in all the reactors and ensure a minimum DO of 2 mg/l, which is needed to operate an aerobic suspended biomass reactor (Tchobanoglous et al., 2014). For the time following, the target aeration differed between R1-R3 and the MBBR reactor (R4). Reactor 4 was set on a target aeration of 5 l/min from day 213 until the end of the experiment (Figure 3.2). R1-R3 continued to operate with a target aeration of 6 l/min until the end of the second last stable period (day 348). After that, R1 and R3 were reduced to a target aeration of 3 l/min until the end of the experiment and aeration to R2 was reduced to match R4 at a target aeration of 5 l/min until the end of the experiment.

The temperature was regulated by a water bath and target temperature was the same for all reactors over the course of the experiment, with 20°C from day 0-215 and 15°C from day 216-421 (Figure 3.2). Both reduction in aeration and temperature were used to test the boundaries of the nitrification ability.

3.4 Sampling

Samples were taken regularly over the course of the experiment, with more intensive sampling periods during the stable periods with nitrification kinetic investigations. The monitoring of the reactors varied slightly over the course of the experiment due to the change in operation personnel. Monitoring with consistent methods can be ensured from day 208 until the end of the experiment, as the author had responsibility for the experiment during this time.

3.4.1 Reactor monitoring

Dissolved oxygen (DO), pH and temperature were measured each working day using a HACH HQ DO meter for the DO and a HACH HQ11d portable meter for pH and temperature. Measurements were taken approximately 45 minutes into the cycle, before water samples were taken. It should be noted that this sampling routine was kept stable from day 208 but could have varied in the preceding time, especially during the start-up phase. Water samples were taken up to 3 times a week and analyzed for nitrite and nitrate (NO_2-N and NO_3-N combined as NOx-N), NH_4-N, PO_4-P and TNb for the reactor effluent and for NH_4-N, PO_4-P and TNb for the feed according to ISO 15923-1:2013. From day 352 alkalinity was also analysed from the effluent of all reactors.

Prior to analysis, all samples were filtered through Munktell Micro-glass fibre paper pore size 1.6 μm (Ahlstrom Munksjö, Ahlstrom Falun AB), to reduce the effect of particles and suspended solids on the analysis. Additionally, unfiltered samples were taken once a week from the influent, and COD (chemical oxygen demand) was analysed for both filtered and unfiltered samples from the feed and effluent.

3.4.2 Cycle studies

To investigate the nitrification rate during a full SBR-cycle, cycle studies were performed with sampling every 15 minutes during the full aeration phase. For each sample, approximately 10 ml were removed from the reactor using a 6x8 mm PVC pipe attached to a 200ml syringe and filtered through a Munktell Micro-glass fibre paper pore size 1.6 μm (Ahlstrom Munksjö, Ahlstrom Falun AB). The carriers extracted with the sample were washed from the filter into a separate container and collected there to be returned to the reactor after the study. The samples were then analysed for ammonium (NH_4-N), nitrite (NO_2-N) and nitrate (NO_3-N). For each sample, DO and pH were measured, using the same DO-meter and pH-meter as for the reactor monitoring (Appendix 2).

3.4.3 Activity studies

To investigate the nitrification rate independently of the changes in DO-concentration and pH during the reactor operation, activity studies were performed at fixed conditions (Sánchez et al., 2001). For this, the removal rate of a predefined amount of substrate (ammonium) is measured, while the dissolved oxygen concentration is kept stable. Through this, the dependency of the nitrification process on substrates in the form of oxygen and ammonium can be separated (Equation 4).

To set up the experiment for the measurements, a fixed volume of 100 ml randomized aggregates was extracted from R1-R3 and washed to remove remains of the feed. For R4, all carriers were used and washed in the same way as the aggregates from R1-R3. The aggregates and the carriers were added to a new reactor for each original R-reactor, with a start feed concentration of 50 mg/l NH_4-N and a pH of 7.5± 0.4. DO was adjusted to 4 or 2 mg/l in the different studies and kept at this level using a fixed gas flow rate of 6 l/min by adjusting the air volume against N2-gas volume. Samples for nitrogen compounds were taken in the same way as in the Cycle studies (Appendix 4). The sample intervals were adjusted to the expected points of interest during the nitrification process, until the biofilm had reduced the ammonium as far as possible.

3.5 Additional measurements

To complement the analytical results, other measurements were taken to investigate the shape and density of the aggregates and the K5-carriers with biofilm, as well as the thickness of the biofilm itself. Through that, information about the biofilm growth as well as potential differences in biofilm structure and density could be captured.

3.5.1 Microscopy

A randomly selected number (n= 13-38) of aggregates from R1-R3 were measured and documented in pictures using a stereo microscope (Nikon SMZ1270) and an attached camera (Nikon, TV Lens 0.55 x DS) every second week. To estimate the biofilm thickness of the aggregates, measurements of the aggregates were taken, analysing mean Area [µm²], EqDiameter [µm] and MaxFeret [µm] as well as the standard deviation using the program NIS-Elements D5.41.01 (Equation 7). The estimate was calculated using the difference between a high and a low contrast picture and dividing the received number by two, to get an average biofilm thickness. Additionally, four randomly selected K5-carriers from R4 were documented at the same time points.

EqDiameter is the equivalent diameter if the object measured would have been a sphere. For this, the area of the object is used and a circle with the same area as the measured object is produced above (Figure 3.3). The diameter from the circle is recorded by using the following Equation 6:

$$EqDiameter = \sqrt{\frac{4xArea}{\pi}} \tag{6}$$

$$Biofilm\ thickness = (\frac{EqDiameter\ (low\ contrats) - EQDiameter\ (high\ contrast)}{2}) \tag{7}$$
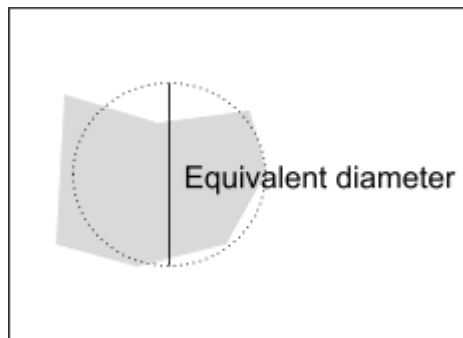
Figure 3.3. Calculation of the equivalent diameter using a circle with the area as the object.

3.5.2 Bed volume

To document the development of the biofilm, the bed volume in the different Cella reactors were measured over the course of the experiment. For that, the airflow was stopped and the aggregates were removed from the reactor using a syphon. Excess water was saved and poured back into the reactor. The aggregates were poured into a measurement cylinder and were allowed to settle for 30 seconds. Then the maximum level of aggregates, defined as bed volume, was noted and the aggregates and reactor water were returned to the reactor.

3.6 Data analysis

Data from the experiment and analysis were digitalized using google sheets to store them and make them available for everyone in the project. Data analysis was carried out in LibreOffice Calc (version 7.3.7.2).

The maximum nitrification rate during the cycle studies was determined by calculating the slope of the line fitted through the measured values of removed ammonium and produced nitrite and nitrate (NOx-N) over time. To estimate the maximum nitrification rate, by ensuring no limitation in ammonium, values from the end of the experiment with NH_4-N < 20 mg/l were excluded. The linear trend line was fitted through the remaining measured values (Appendix 2).

The maximum nitrification rate during the activity studies was determined as for the cycle-studies, with a linear correlation of removed ammonium or produced nitrite and nitrate over time, using all data where ammonia exceeded 20 mg/l, ensuring no limitation in ammonium. The estimated removal rate throughout the test was also calculated as the difference between each sampling point. These rates could then be plotted against the stepwise mean ammonium concentration, to study the ammonia-dependency of the removal rate.

To determine the kinetics for each activity study, two Monod-curves were fitted to the calculated rates (Figure 4.14) according to the Monod equation (Equation 4). The first curve was based on the best fit to all points in the curve, by calculating the smallest possible mean squared predicted error (MSPE) between each measured ammonium and nitrite-nitrate rates from the experiment and the calculated values from the Monod-curve at the same time point. To find the smallest MSPE, the mean of the maximum nitrification rate from the values of the nitrogen compounds was calculated in the same way as for the cycle studies, was used as $\mu_{(max)}$ and the Ks parameter in the Monod equation was adjusted until the smallest difference between the calculated and the measured ammonium and nitrite-nitrate rates were found. This method is from now on referred to as the statistical method. The second curve was fitted against the same data as the curve of the statistical method, but adjusting both $\mu_{(max)}$ and Ks for the best fit through visual judgment. This judgment included a weighing of the data points based on knowledge about errors and deviations in the tests. This method will from now on be referred to as the adjusted fit. The ammonium dependency was investigated through the dependency between DO and ammonium at different points along the Monod-curve (Figure 4.14). Fitting a line along the point through adjustment of the parameters from the Monod-curve will give the kinetic parameters for the nitrification rate (Appendix 5).

4 Results

To determine the differences in behaviour, data from the weekly measurements together with the data from the cycle- and activity studies was analysed. For this, differences in the behaviour of the Cella system were compared to the conventional MBBR system. Additionally, differences in behaviour within the Cella system were investigated, based on an initial fill rate of 3, 6 and 9 %.

4.1 Reactor operation

The reactors were operated for 421 days, with varying temperature, air volume and load. Running the experiment as a bench-scale trial relied on the punctuality of several pumps per reactor to coordinate inflow and outflow and allow for aeration and settling times. The pumps were controlled by a programmable Energenie power manager plug, which during certain times caused failures in turning on or turning off pumps, leading to several issues during the experiment. Over the course of the experiment disturbances in the system occurred on day 152, 204, 208, 215, 217, 222-230, 236, 264, 266, 273-278, 322, 420 and 421, due to pump failures.

One of the issues, which occurred several times in unpredictable intervals, was that the influent or effluent pumps did not stop at the dedicated time. For the influent pumps, this led to a loss of the remaining feed from the storage container via the reactor, leading to the aggregates being washed into the safety bucket the reactor was placed in (Figure 3.1). As a consequence, some sampling occasions were missed, but all aggregates could be recovered. Failure of effluent pumps in combination with the aeration led to a loss of half the reactor volume during mixing, which in the case of the Cella reactors meant that at least half of the aggregates were pumped out of the system. For most cases, the liquid and the aggregates were captured in effluent reservoirs, but on day 322, about 9% of the total bed volume from R1 and 19% of the total bed volume from R3 were lost. Even in the case when the aggregates could be retrieved, the biofilm may have been impacted by the strong forces in the pump head and/or by the long retention in un-aerated areas of the reservoirs, which might have affected biofilm thickness and biofilm activity.

4.2 Oxygen, pH and alkalinity

The pH differed over time depending on load and the performance of the reactors (Figure 4.1), but also depending on the time of monitoring into the cycle. In the start-up phase (day 0-63) the measured pH varied largely, after which it stabilized between 7.0 and 8.2 in the different reactors (Figure 4.1). During day 213-347, after the adjustment of the reactor temperature and the load in R4, the pH of R4 was lower than that of the Cella reactors.

The pH was measured once a day to check that the pH was stable over the course of the experiment. Cycle studies were also performed to check for the pH throughout a cycle. Both showed a pH above 7.0, which was taken as an indicator that there was a sufficient amount of alkalinity in the reactor throughout the cycle. Decreasing the load and with it the buffer solution (Table 3.2) in R2 at day 348 led to a significant increase of the ammonium effluent values. On day 352 it was observed, that the feed to R2 and R4 contained insufficient alkalinity. Consequently, the alkalinity was adjusted in the feed and alkalinity was monitored for the remaining duration of the test. To determine if the reactors had been limited by alkalinity prior to day 352, the theoretical alkalinity need for previous phases was estimated from the feed. Based on this, it can be suspected that the reactors could have been somewhat

limited in alkalinity at times, especially towards the end of each cycle. This limitation is, however, most prominent before day 96, after which the pH becomes more stable, except for R4. A very consequent pH phase can be seen in the end of the experiment, where the alkalinity in the reactors was measured and the alkalinity in R2 and R4 was increased (day 352), so all reactors had sufficient alkalinity in the reactor until the end of the cycle (Figure 4.1).
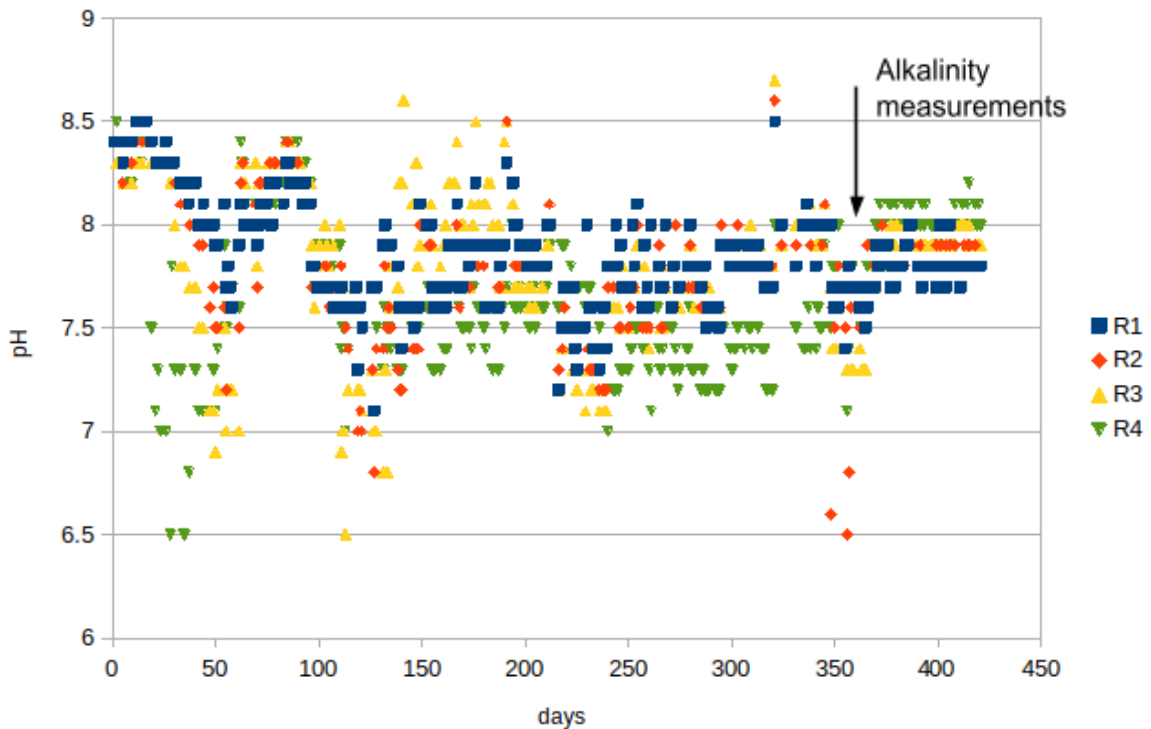

Figure 4.1. Measured pH in the reactors over time. Measurement time point was 45 minutes after aeration start of a cycle from day 208 and expected to be the same as the time before, but undocumented.

The reactors were operated with different air flows over the course of the experiment to reach different dissolved oxygen (DO) concentrations. The DO in the different reactors followed the adjustments of the aeration and the load (Figure 3.2 and Figure 4.2), where a decrease in air flow led to a decrease in DO and an increase in air flow led to an increase in DO in the reactors (Figure 4.2), while a decrease in load could lead to an increase in DO (Figure 3.2). Even under operation with the same airflow, the DO differed between the different reactors, with very similar results in the three Cella reactors but very different results compared to the MBBR reactor. From day 147, the DO in the MBBR reactor (R4) was constantly higher than in the Cella reactors, even when R4 and R2 were operated at similar conditions (day 348-421).

The DO varied largely during the start-up phase (day 0-63) and stabilized more quickly in the MBBR reactor (R4) than in the Cella reactors in the following phases. The DO results also depend on what time in the cycle the measurement was taken, and before day 208 the measurement time point is not documented and may have been sampled at a different time point during the cycle, which could also explain some of the observation variation.
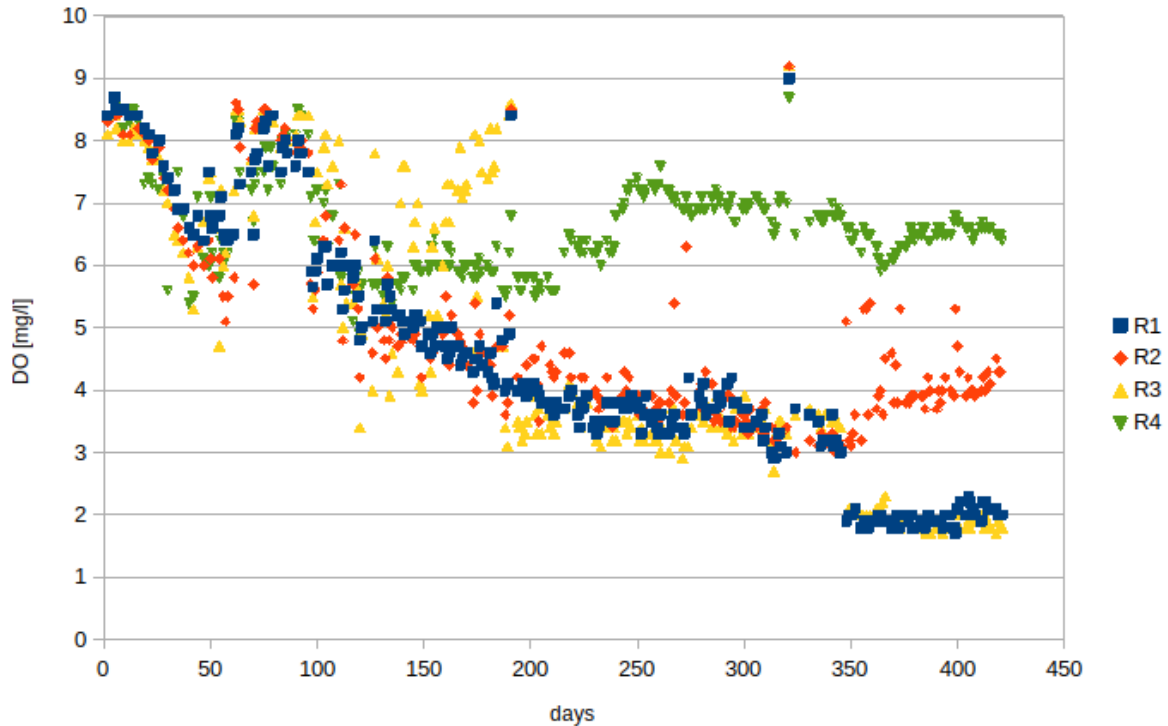
Figure 4.2. Dissolved oxygen concentration (DO) measured in the reactors over time. Measurement time point was 45 minutes after aeration start of a cycle from day 208 and expected to be the same as the time before, but undocumented.

4.3 Reactor performance

The overall reactor performance is shown in Figure 4.3, plotting the effluent composition from the four reactors over time and the corresponding applied load, as previously shown in Figure 3.2. During the start-up phase (day 0-63) the effluents were high in ammonium, as biofilm was not yet established in the reactors. It can be seen that the load gradually increased, and ammonia removal was observed through a decrease of ammonia and an increase of nitrate and nitrite in the effluent. An earlier reduction of ammonium allowed for an increased load in the MBBR reactor earlier in the process compared to the Cella reactors. In the MBBR, a reduction of ammonium was seen from day 12, while the ammonium reduction in the Cella reactors started between day 16-19. After the establishment of the biofilm, the load was reduced to lower the nitrite concentrations and allow the development of NOBs.

When low nitrite concentrations were seen in the reactors, the load was again increased to meet ammonia removal rates in the reactors (day 99-152), leading to a maximum load of 1.20 gNH_4-N/l*d in the Cella reactors and 1.06 gNH_4-N/l*d in the MBBR reactor. The lower load in the MBBR reactor was due to the occurrence of high nitrite values in the effluent when the load was increased. High nitrite levels in the reactor can cause inhibition of the nitrifiers due to FNA. The FNA values were calculated from the effluent nitrite and the pH measured in the system. Due to the variation of nitrite and pH throughout a cycle and the different measurement points of the two values in the cycle, the exact amount of FNA at each point cannot be determined. However, estimated FNA values above the inhibition values of 0.0255 mgN/l (Fu et al., 2010) were only found in R3 and R4 during a few days in the start-up phase, therefore the risk for FNA inhibition is low.

The stable periods during the experiment were used to get to a stable state in the biofilm, to estimate the lowest achievable effluent values. Looking at the period (day 153-212) with an aeration of 6 l/min, average ammonium effluent values of 0.10 mg/l or smaller in the Cella reactors and 4.63 mg/l for the MBBR reactor were found. The average nitrite effluent value was also found to be lower in the Cella reactors than in the MBBR reactor, leading to an average of 1.09, 0.09 and 0.06 mg/l in R1, R2 and R3 with respectively and an average nitrite effluent value for the MBBR reactor of 40.67 mg/l. The awaited reduction in nitrite in the MBBR reactor never occurred.

As a consequence, in the next stable period (day 243-347) the load and aeration in the MBBR reactor were reduced, to avoid nitrite buildup, while the load and aeration for the Cella reactors were kept the same. This phase also included a temperature decrease at day 215 to 15°C (Figure 3.2), to meet the reactor performance. The average ammonium effluent value in all three Cella reactors R1 to R3, was found to be 0.07, 0.06 and 0.09 mg/l respectively, while the average ammonium effluent value in the MBBR was 9.48 mg/l. Average nitrite effluent values for R1, R2 and R3 were found to be 0.06, 0.22 and 0.02 mg/l respectively, while the MBBR reactor showed an average nitrite effluent of 2.05 mg/l. The awaited reduction in nitrite in the MBBR reactor occurred, but very slowly compared to the expectations based on the behaviour of the Cella system.

In the last stable period (day 387-421), the aeration of the Cella reactor R1 and R3 was lowered to 3 l/min with a load of 1.06 and 1.20 gNH_4-N/l*d respectively, and the operating parameters in R2 were adjusted to match the MBBR reactor leading to an aeration of 5 l/min and a load of 0.60 g/l*d. At the beginning of this phase, high effluent concentrations in R2 occurred due to a lack of alkalinity. As a consequence, the alkalinity was increased at day 352 in the feed to R2 as well as R4, leading to a reduction of the effluent values for both reactors (Figure 4.3 D). The average value of the ammonium effluent in the Cella reactors R1, R2 and R3 was 0.31, 0.15 and 1.62 mg/l respectively and the average ammonium effluent in the MBBR was 0.32 mg/l. The average nitrite effluent concentrations for the R1, R2 and R3 Cella reactors were 12.83, 0.01 and 19.81 mg/l respectively, and the MBBR reactor had an average effluent value of 2.13 mg/l.

Certain times were excluded from the calculations of the average effluent concentrations, due to high effluent values caused by problems with the reactor setup (see 4.1 Reactor operation). These times were the following days: 216-238, 247, 254, 268, 273.
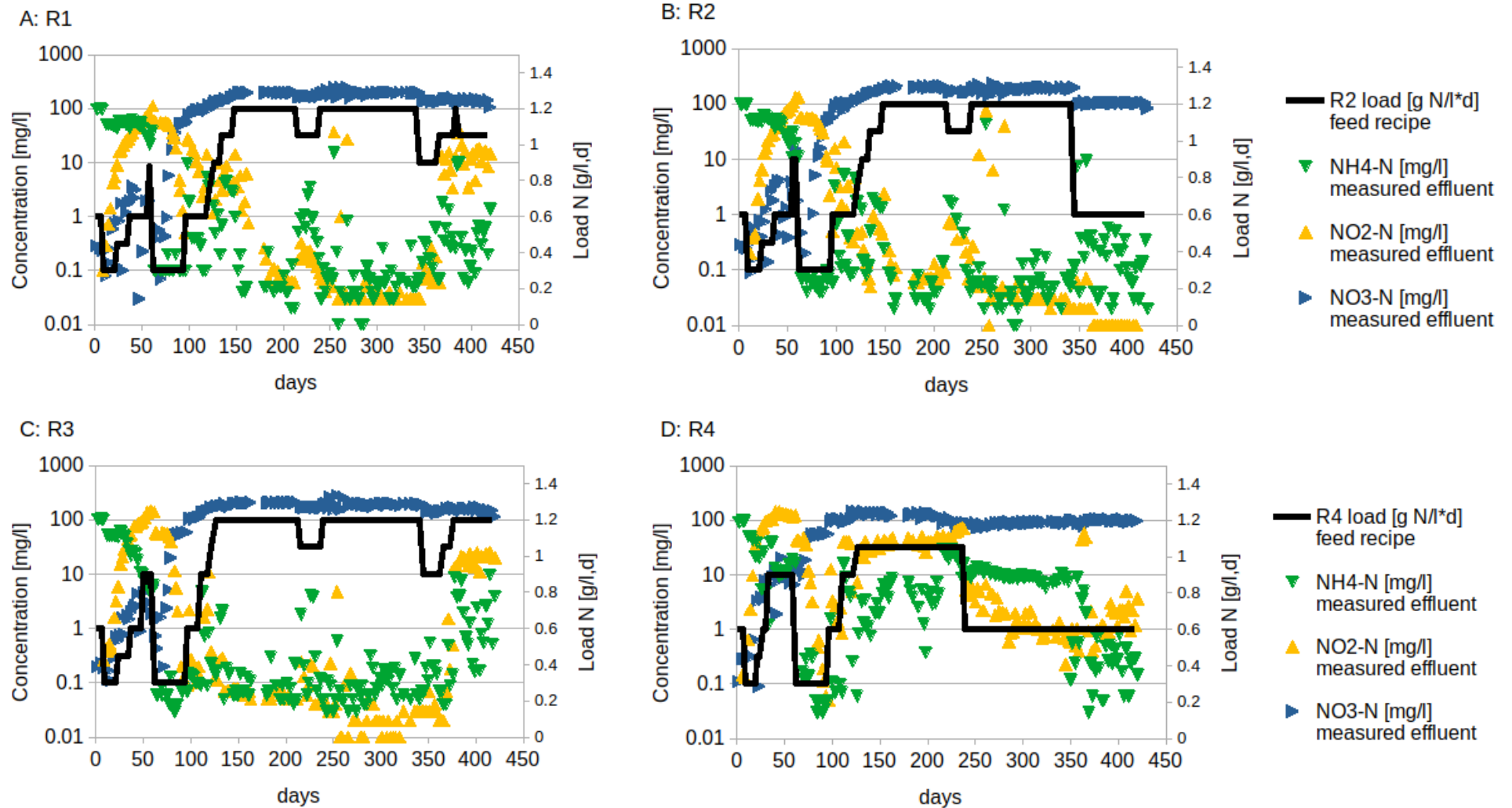
Figure 4.3. Effluent values from the reactors (logarithmic scale on the left) and applied loads to the different reactors (scale on the right). The change in temperature occurred at day 215. Aeration was changed several times over the course of the experiment (see Figure 3.2).

Using the results from the effluent nitrite and nitrate measurements, the nitrification performance in each reactor can be calculated (Figure 4.4). Figure 4.4 shows how the nitrification increased during the start-up period as the biofilm established. A very similar nitrification performance was observed between all four reactors at the beginning of the experiment (day 64-98) with low load. During the stable period at 20°C (day 153-212), with a load of 1.20 gNH_4-N/l*d for the Cella reactors and 1.06 gNH_4-N/l*d for the MBBR reactor the nitrification performance was found to be higher in the Cella reactors with approximately 1.20 gNOx-N/l*d, compared to the MBBR reactor with an approximate nitrification performance of 1.0 gNOx-N/l*d.

Lowering the temperature from 20°C to 15°C (day 215) and the load and aeration for the MBBR reactor (Figure 3.2) led to an approximate nitrification performance just below 0.60 gNOx-N/l*d for the MBBR reactor. At the same time, lowering the temperature from 20 °C to 15°C in the Cella reactors, resulted only in a slight decrease in the nitrification performance (Figure 4.4). The data between day 216 and 274 were removed from the graph due to unstable cycles, triggered by malfunctioning of different pumps. Consequently, the direct effect of the temperature change from 20°C to 15°C on the nitrification performance can not be observed.

Looking at the last period (day 371-421), characterized by the decrease in air flow from 6 l/min to 3 l/min in R1 and R3 and an adjustment of the reactor operation parameters from R2 to operate under the same conditions as the MBBR reactor (Figure 3.2), differences between all the reactors can be found. Although operated at similar conditions, R3 showed a higher nitrification performance with slightly above 1 gNOx-N/l*d, than R1 with slightly below 1 gNOx-N/l*d (Figure 4.4). The approximate nitrification performance for R2 and R4 was found to be very similar at slightly above 0.60 gNOx-N/l*d, potentially with a slight advantage for R2.
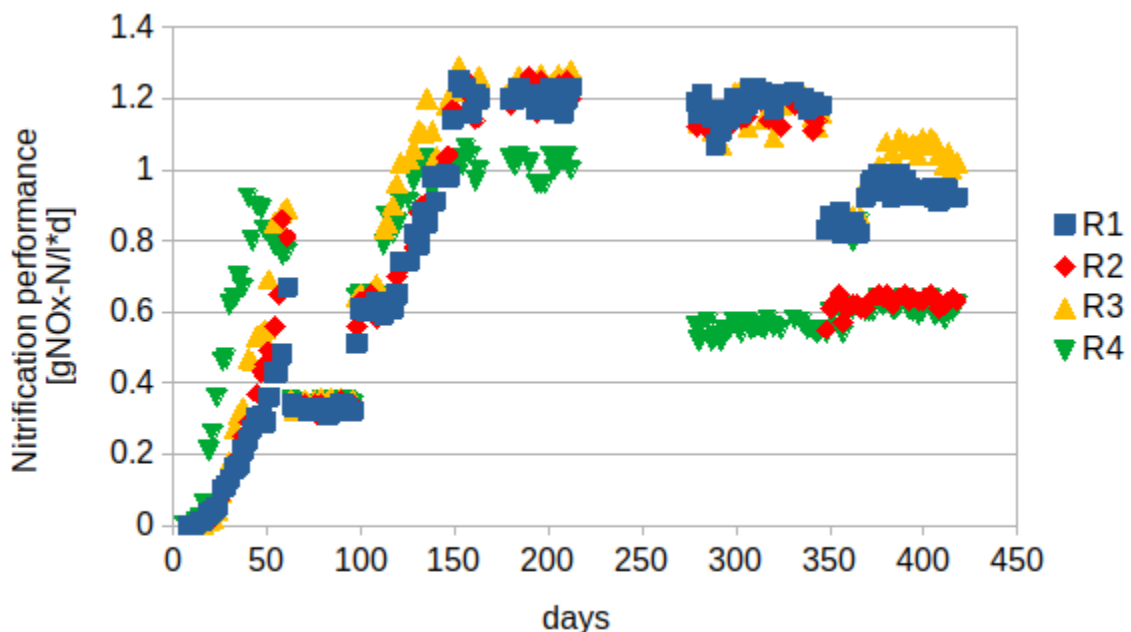
Figure 4.4. Nitrification performance defined as volumetric NO_3-N and NO_2-N (NOx-N) production based on the mass balance over each reactor. Calculated from effluent values of NOx-N taken at the end of an SBR cycle.

4.3 Biomass development

Biofilm developed gradually on the support material of the Cella and on the protected surface of the MBBR carriers (Figure 4.5). The establishment of biofilm varied in the reactors, where biofilm was first observed on the carriers in R4 on day 12. On day 16-19 biofilm was also observed in reactor R1-R3, with R1 developing biofilm earliest and R3 developing biofilm the latest. Figure 4.5 and Figure 4.6 show the gradual development of biofilm in the reactors.

The biofilm thickness in the Cella reactors and the MBBR reactor varied over time. At the beginning of the experiment, a constant increase in biofilm thickness was found, while it seemed to stabilize in the late course of the experiment (Figure 4.6). The measurements of the biofilm thickness include large standard deviations due to the varying size of both the support material and the biofilm. A general trend of a thicker biofilm in R1 and R2 can be seen, resulting in the thinnest biofilm layer in R3 throughout the experiment. A sharp decrease in biofilm thickness can be observed in R2 in the last measurements, after the reduction of load and aeration in R2 at day 348.

During the end of the study, the biofilm in R1 was the thickest with an estimated average of 430 µm, while the biofilm thickness in R2 and R3 did not differ widely with 320 µm and 330 µm respectively. The biofilm thickness in the K5-carriers was documented with pictures only (Figure 4.5). The pictures show how the thickness increased in the beginning of the experiment and varied with the load and the temperature, leading to an increase in biofilm thickness after day 336, when temperature had been decreased to 15°C and the load to 0.60 gNH_4-N/l*d.

Day	1	91	204	336	415
R1					
R2					
R3					
R4					
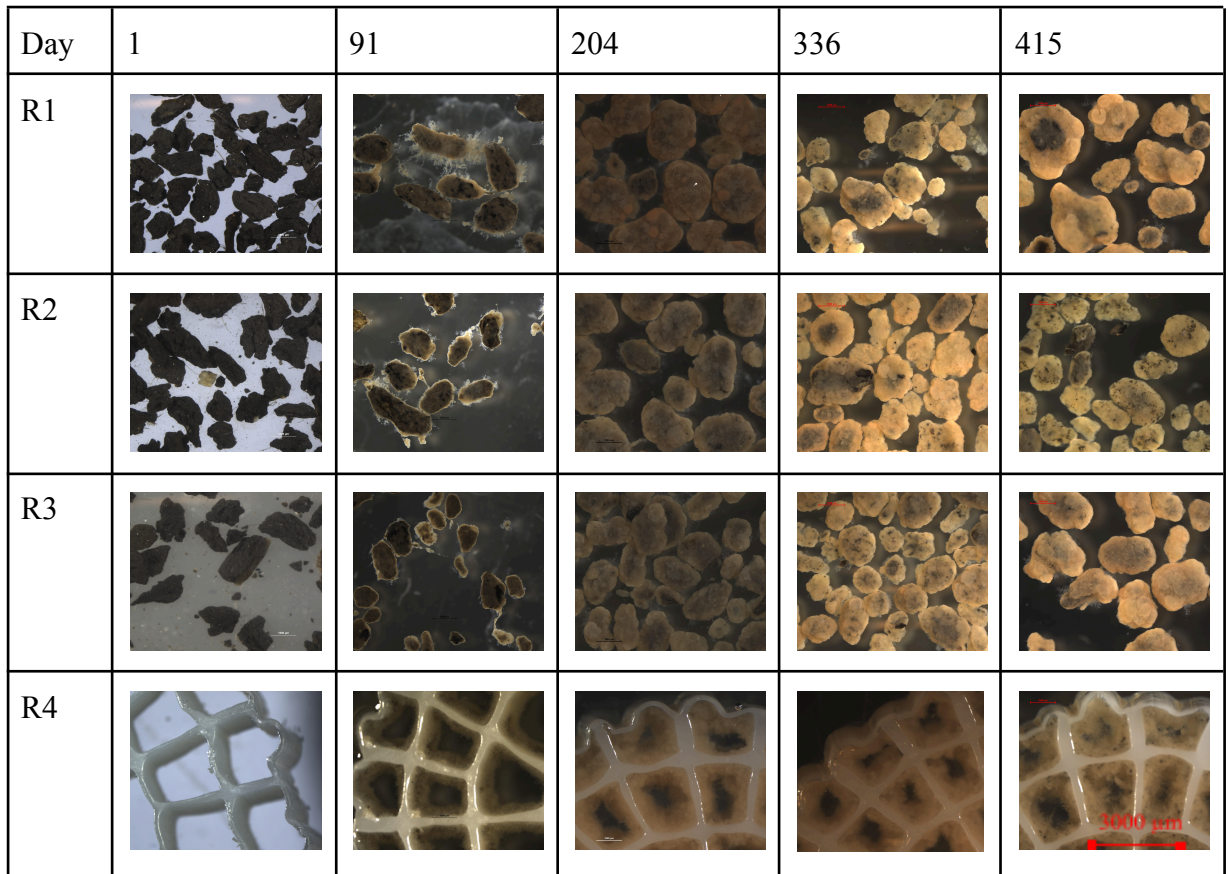
Picture 4.5. Pictures of biofilm development over the course of the experiment taken with a microscope (Nikon SMZ1270) and an attached camera (Nikon, TV Lens 0.55 x DS). The pictures were taken with the same resolution and scale (see picture R4 day 415).
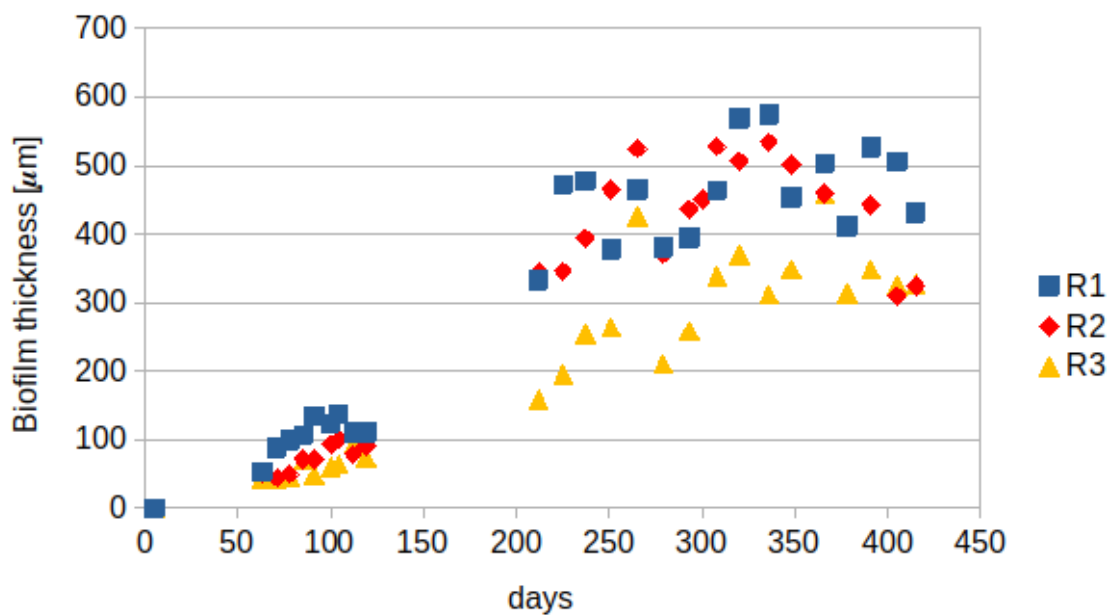
Figure 4.6. Average biofilm thickness measured as) EqDiameter in the low contrast picture - EqDiameter in the high contrast picture)/2 as a measurement of N=13-38.

Bed volume was only measured at the very beginning and end of the experiment. At the beginning of the experiment, a constant increase in biofilm thickness was found (Figure 4.6), which led to an increase in bed volume (Figure 4.7). It is noticeable that the initial 3-9% fill of support material resulted in a final bed volume of 300-450 ml aggregates in the three Cella reactors at the end of the study. The bed volume not always mimicked the changes in biofilm thickness. This is shown for example in R1 and R3, where the bed volume increased towards the end of the experiment (Figure 4.7), even though the biofilm thickness stayed more or less the same (Figure 4.6). The expansion rate of the bed volume seemed rather stable, especially in R1 and R3.

One unexpected change in bed volume occurred due to the loss of aggregates on day 322 from reactor R1 and R3, caused by a pump failure (Figure 4.7). Nevertheless, the bed volume kept on growing with the same speed as before the event. During the last stable phase (day 387-421) the bed volume in R1 and R3 reached the maximum capacity of the reactor setup. Hence, some aggregates were pumped out of the reactor each time the effluent pump started. Those effluent aggregates were collected, and their volume was measured, but not returned to the reactor. The total volume is indicated by the stars for R1 and x for R3 in Figure 4.7, leading to a bed volume limitation in the end by the volume of the reactor.
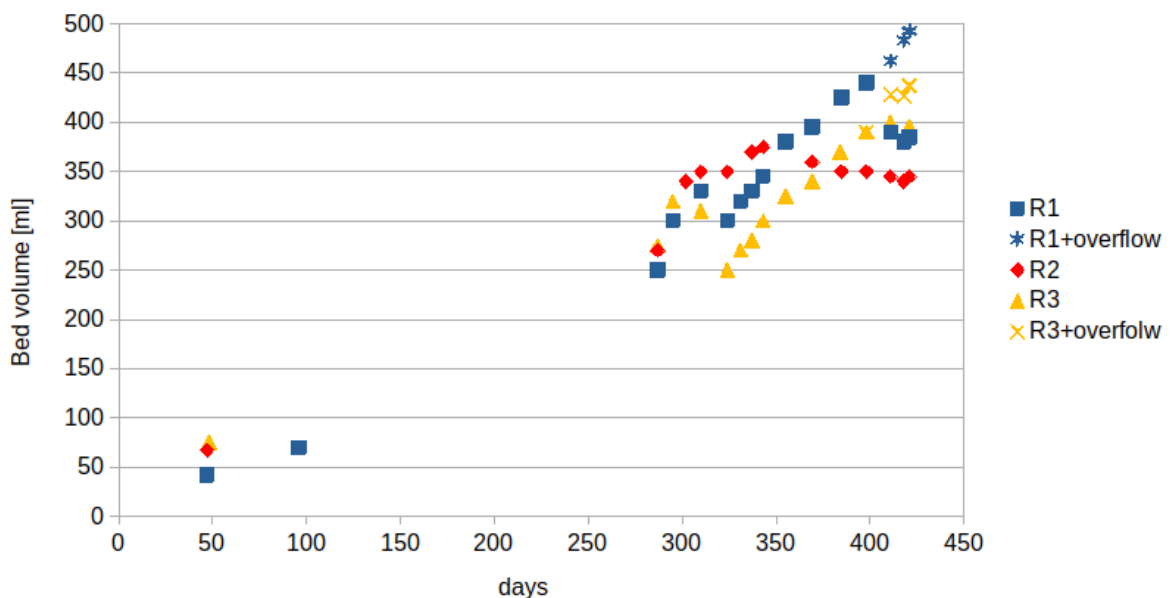
Figure 4.7. Measurements of bed volume change over the course of the experiment, with an allowed settling time of 30 seconds. Overflow was measured as aggregates which were removed from the reactors due to limitation in the reactor volume. Their measured volume was added to the measured bed volume.

4.4 Cycle studies

Over the course of the experiment, four cycle studies were performed (Appendix 2), giving valuable information regarding how pH, DO and the different nitrogen compounds varied over time in an SBR-cycle. Figure 4.8 shows an example of a cycle study with the decrease in ammonium and the simultaneous increase of nitrate and nitrite over time. As soon as the ammonium reached a level close to zero, the DO in the reactor increased drastically, as the bacterial activity dropped. Nitrite increased slightly in the first half of the experiment and then decreased again to levels close to zero, due to the activity of the NOB. Also, the pH was more

or less stable throughout the experiment with slightly lower levels during the higher nitrite levels and a slight increase towards the end of the cycle.
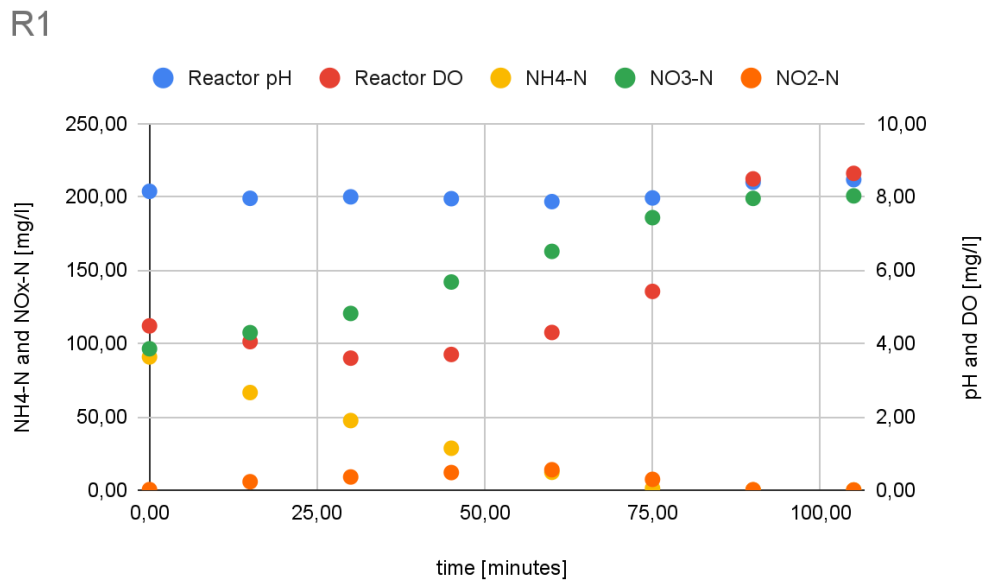
Figure 4.8. Example cycle study from day 204 R1 at 20 °C. Showing a stable pH, next to the decrease of ammonium, the increase of nitrate and DO as well as the increase and decrease of nitrite over the course of a cycle. All other results, see Appendix 2.

From the cycle-studies it was also possible to determine the maximum nitrification rate at operating conditions, which is defined as the nitrification at high substrate concentrations (ammonia > 20 mg/l) at the beginning of the cycle (Appendix 3). Figure 4.9 shows the maximum nitrification rates in each reactor, represented as ammonia removal and nitrate as well as nitrite (NOx-N) production.

The cycle studies at the beginning of the experiment at 20°C show a higher maximum nitrification rate compared to the cycle studies performed after the temperature was changed to 15°C (day 215). While the last cycle study, which was performed during the last stable state (after reduction of the load and aeration in the Cella reactors, and increase of alkalinity in the MBBR reactor), showed the lowest maximum nitrification rate for the Cella and an increase in maximum nitrification rate for the MBBR (Figure 4.9).

40
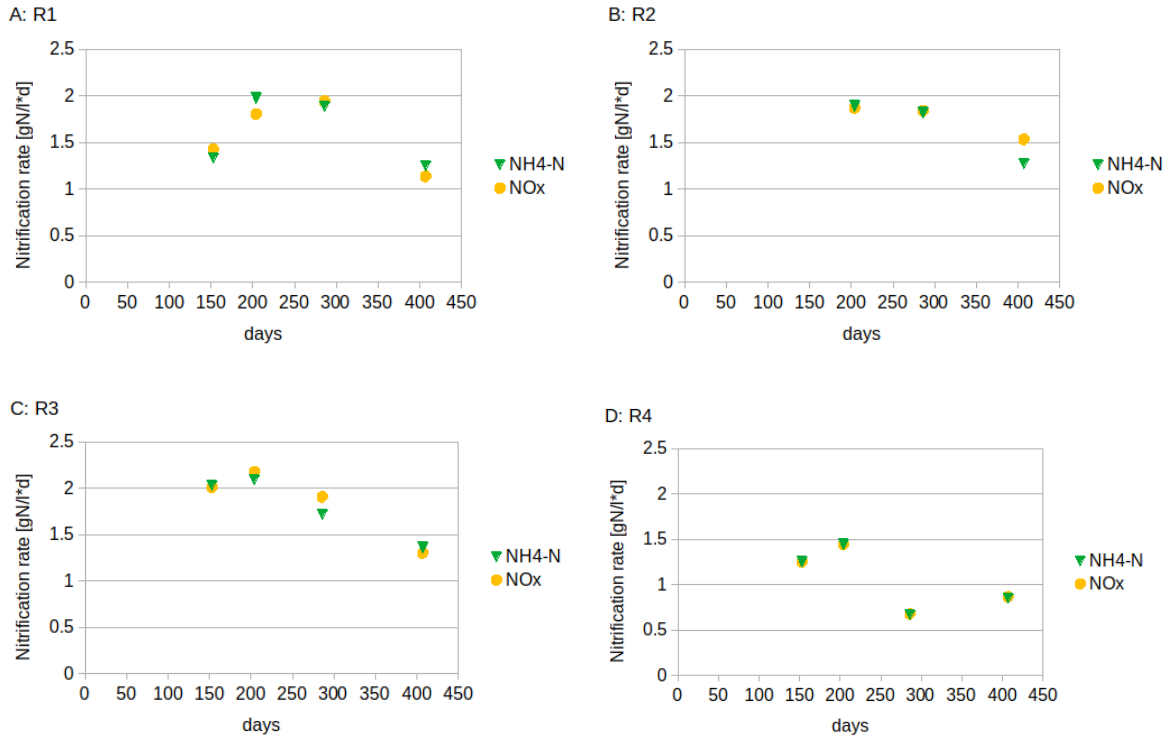
Figure 4.9. Maximum nitrification rates at operating conditions from the cycle studies over the course of the experiment (day 153, 204, 286, 407), represented as NH₄-N removal and NOx-N production. With Figure A showing R1, Figure B showing R2, Figure C showing R3 and Figure D showing R4.

4.5 Kinetic assessments of nitrification

To investigate the ammonium and oxygen dependency of nitrification, activity studies were performed at fixed DO. For the activity studies, the same amount (100 ml) of Cella aggregates were studied in each test, and thus these results cannot be directly compared to the results obtained in the full reactor systems described above. Similar to the cycle studies the different nitrogen components have been analysed. In contrast to the cycle studies, the activity studies were performed under stable DO concentrations and until ammonium was depleted in the reactor (Figure 4.10). For all data from the activity studies, see Appendix 4.
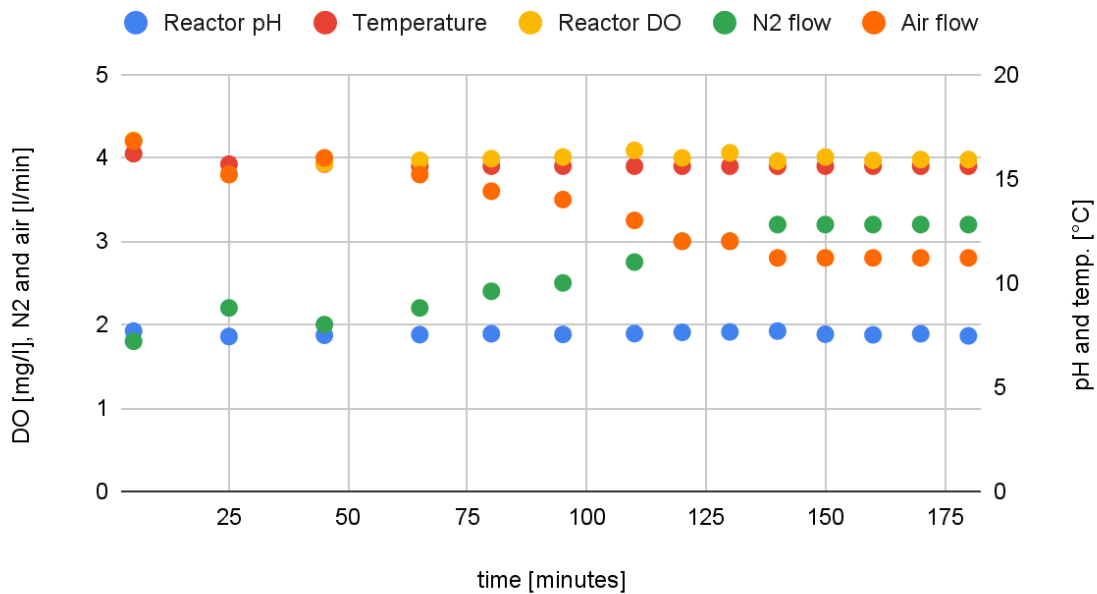
Figure 4.10. Example activity studies from day 273 R1 with high aeration at 15 °C. Showing a stable pH, next to the decrease of ammonium, the increase of nitrate and DO as well as the increase and decrease of nitrite over the course of a cycle. All other results, see Appendix 4.

Two different levels of DO were used in the activity studies to study the oxygen dependency of nitrification for the Cella and the MBBR systems. Additionally, the tests were repeated after the aeration and load change of the experiment on day 348 (Appendix 6). This implied during the first experiments (second last stable period day 243-347, from now on called high aeration phase) a load of 1.20 gNH_4-N/l*d for the Cella reactors and a load of 0.60 gNH_4-N/l*d for the MBBR reactor. Aeration was 6 l/min and 5 l/min for the Cella and the MBBR respectively. For the second set of experiments (last stable period day 387-421, form now on called low aeration phase) it was given a load of 0.60 gNH_4-N/l*d for R2 and the MBBR reactor and a load of 1.06 and 1.20 gNH_4-N/l*d for R1 and R3 respectively. Aeration during this phase was 5 l/min for R2 and the MBBR reactor and 3 l/min for R1 and R3 (Figure 3.2). Figure 4.11 shows the maximum nitrification rate from the activity studies, as a function of DO, at both stable conditions. Higher maximum nitrification rates were retrieved at DO=4 mg/l than at DO=2 mg/l, and a difference was observed between the Cella aggregates with a higher nitrification rate in R3. Additionally, it can be seen that the MBBR carriers had a lower nitrification rate than the Cella aggregates during the majority of the tests.
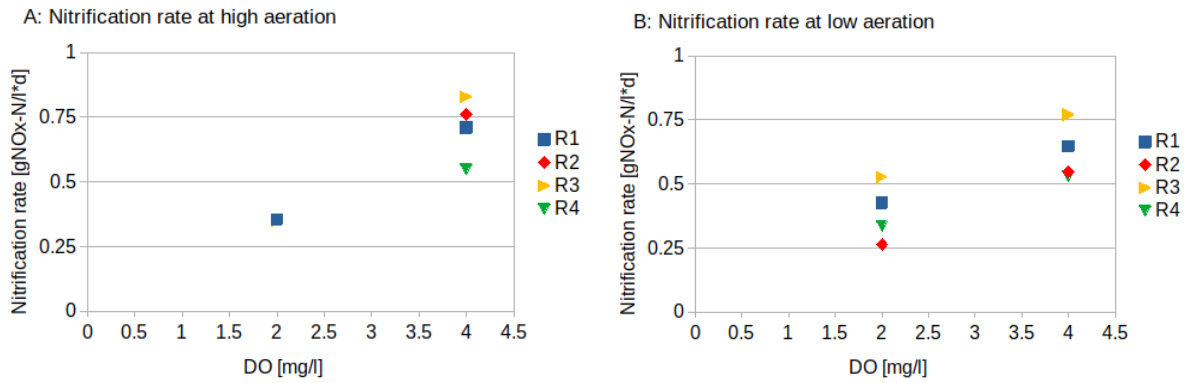
Figure 4.11. Maximum nitrification rate from the activity studies at 15 °C with high aeration in the Cella reactors (Figure A) and 15 °C with low aeration in the Cella reactors (Figure B) performed at DO=2 mg/L and DO=4 mg/L showing the oxygen dependency of the nitrification for MBBR carriers from R4 and Cella aggregates from R1-R3.

To investigate the impact of the aggregate loss from R1 and R3 on day 322 activity studies were performed on day 337 and day 344 to compare with the previous results from the activity studies before the loss (Figure 4.12).
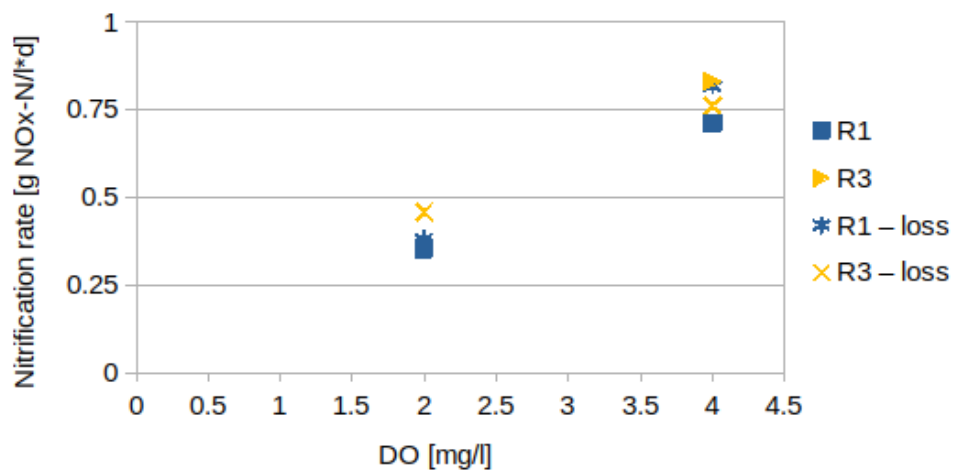
Figure 4.12. *Maximum nitrification rate from the activity studies at 15 °C and high aeration, before and after the loss of aggregates from R1 and R3. Performed at DO=2 and DO=4 showing the impact of aggregate loss on the maximum nitrification rate from the same amount of aggregated from R1 and R3.*

An additional activity study was performed on day 419 with the full bed volume of R2 (340 ml). These results were then adjusted for the bed volume and plotted together with the nitrification rates obtained during the activity studies for R2 on days 412 and 414 (Figure 4.13). This was done to investigate the reliability of the maximum nitrification rates when scaling up from 100 ml of the bed volume to larger quantities. Figure 4.13 shows a linear relationship of the measurements with increasing DO, even though the tests were conducted with different bed volumes.
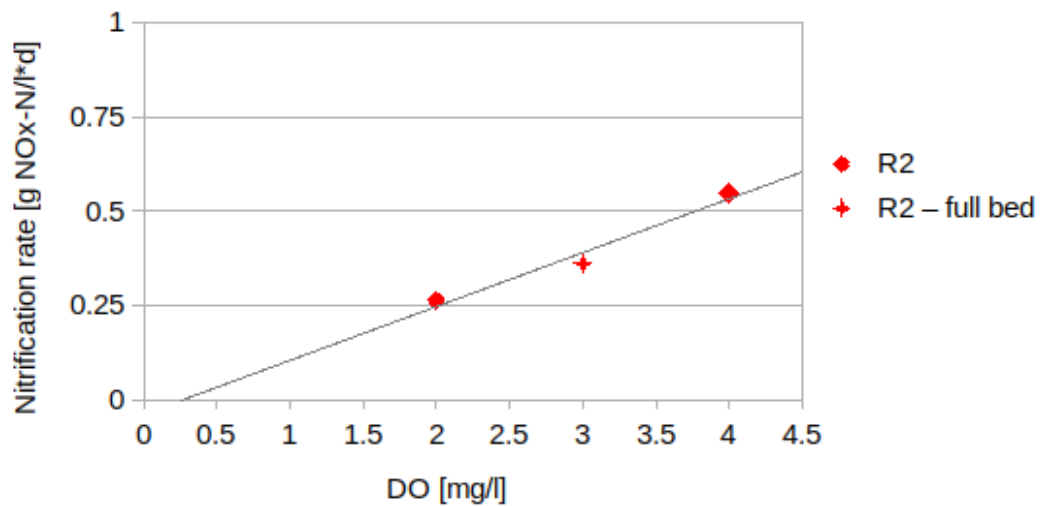
Figure 4.13. Maximum nitrification rate from the activity studies at 15°C with low aeration and DO between 2 and 4 mg/l, using 100 ml aggregates at DO=2 and at DO=4 and the full bed volume (340 ml) at DO=3 (result adjusted to 100 ml).

To investigate the ammonium dependency, the measured nitrogen compound concentrations per step were plotted against the mean ammonium concentration per step, together with Monod-curves (Figure 4.14) based on an adjusted fit and a statistical approach (see 3.6 Data analysis).
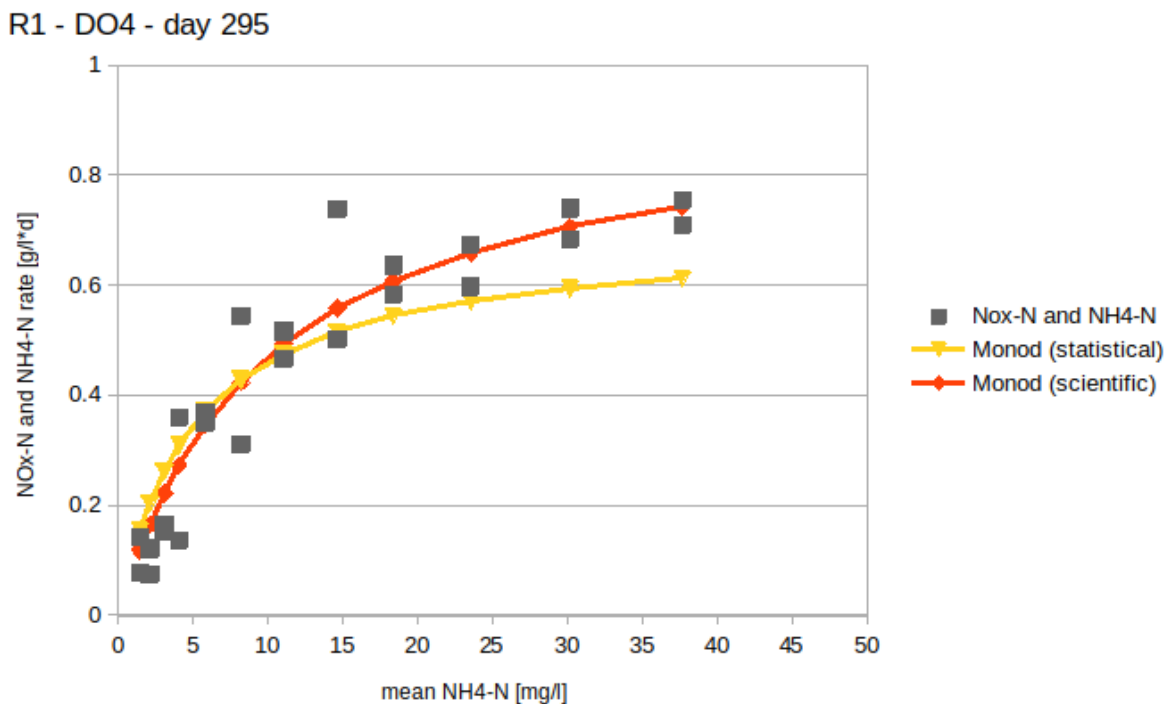
Figure 4.14. Monod curve example with statistical method and adjusted fit. All other results, see Appendix 4.

The different Monod-curves from the adjusted fit for high and low aeration at 15°C were plotted at the two different DOs (Figure 4.15). The DOs are indicated in continuous lines for DO=4 and dashed lines for DO=2 in Figure 4.15. At high aeration, the Cella reactors were all operated under the same conditions, while the MBBR reactor was operated with a lower aeration and a lower load compared to the Cella reactors. Figure 4.15.**A** shows similar maximum nitrification rates at high aeration, which differ between the DOs but not so much between the reactors (similar μmax). The μmax varied between 1.10 $gNH_4-N/l*d$ (R2) and 0.70 $gNH_4-N/l*d$ (R4), while the slope of the curves differs between and even within a DO (different Ks). This results in a Ks of 10 $mgNH_4-N/l$ for all activity studies at high aeration before aggregate loss, besides R3-DO4 and R3-DO2, which have a Ks of 4 $mgNH_4-N/l$ (Apprendix 6).

For low aeration, activity tests were performed from day 412-421 showing both differences between the reactors at the DO2 (dotted line) and the DO4 (continuous line). These activity tests resulted in a slope (Ks) varying between 4 and 9 $mgNH_4-N/l$ with the larger Ks found in the studies with higher DOs and the smaller Ks found in the studies with lower DO (Appendix 6). Differences in maximum nitrification rate (μmax) differed between 0.90 and 0.29 $gNH_4-N/l*d$, following the same pattern as the Ks with higher values in the studies at DO=4 and lower values in the studies with DO=2 (Appendix 6). For both Ks and μmax the values were always highest for R1 and R3. This high nitrification rates can also be seen in Figure 4.15.B, where R1 and R3 have the highest nitrification rates independent on the DO.

A: scientific method day 295 - 310
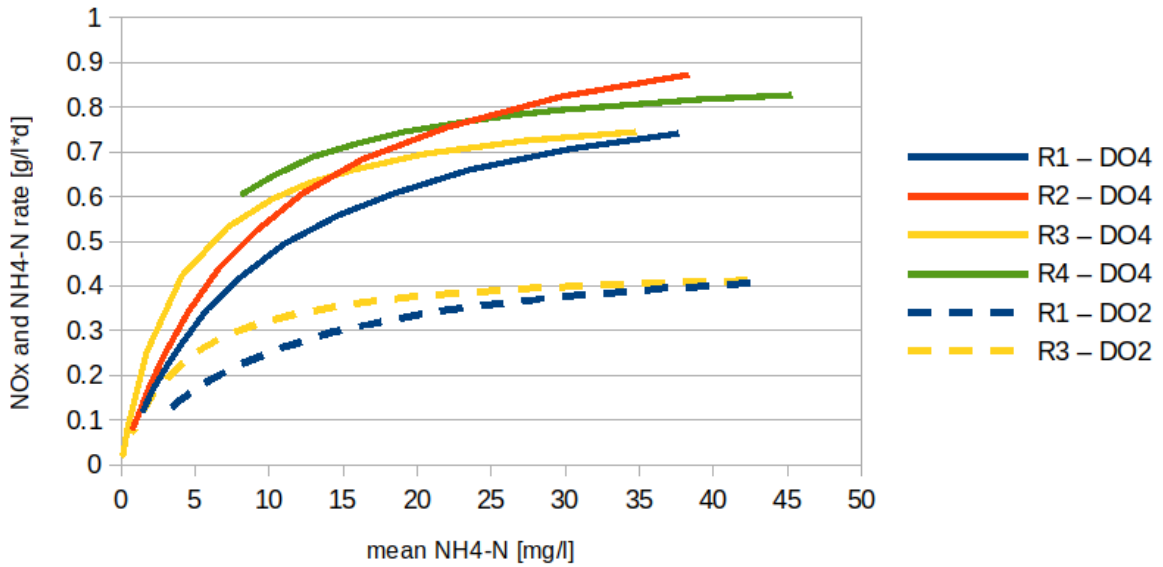
B: scientific method day 412-421
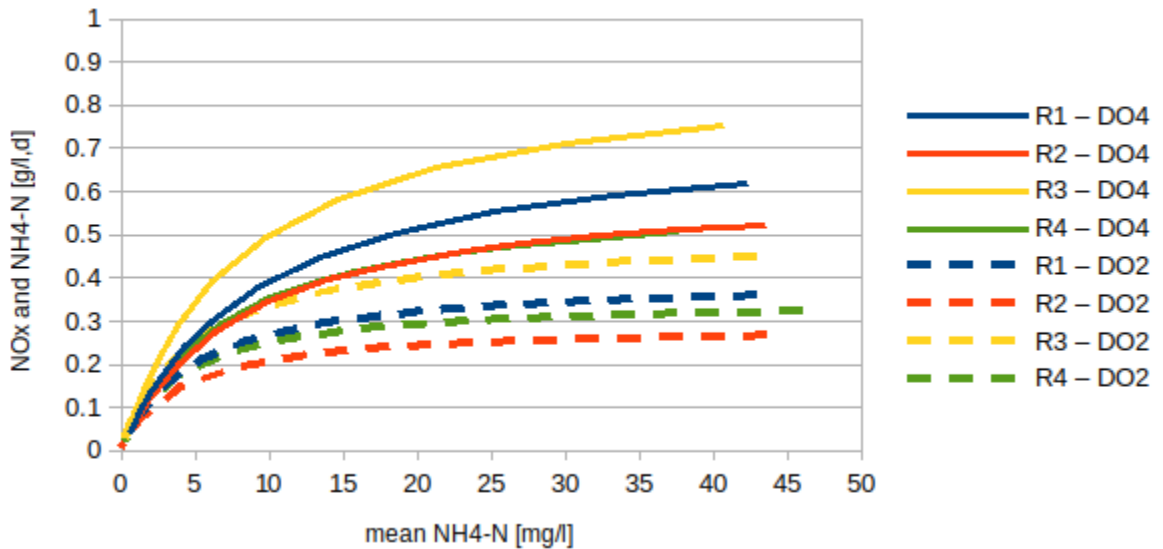
Figure 4.15. Monod curves after the adjusted fit day 295-310 with high aeration in Cella reactors (Figure A) and day 412-421 with low aeration in Cella reactors (Figure B). Data from activity studies performed at DO=2 (dashed lines) and DO=4 (continuous lines), showing the ammonium dependency of the nitrification. Notice that R4 - DO4 is situated under R2 - DO4.

To investigate the effect of the aggregate loss on day 322 from R1 and R3 the Monod-curved from the experiments before the loss on day 264-310 were compared to the results of day 337-344 after the loss. It showed that the ammonium dependency for R1 was impacted at DO4, where there was a higher nitrification rate after the loss, but not at DO2, where there was no difference between the curves. While the effect for R3 was vice versa with an impact at DO2, with an increase in nitrification rate, but not at DO4 (Figure 4.16).
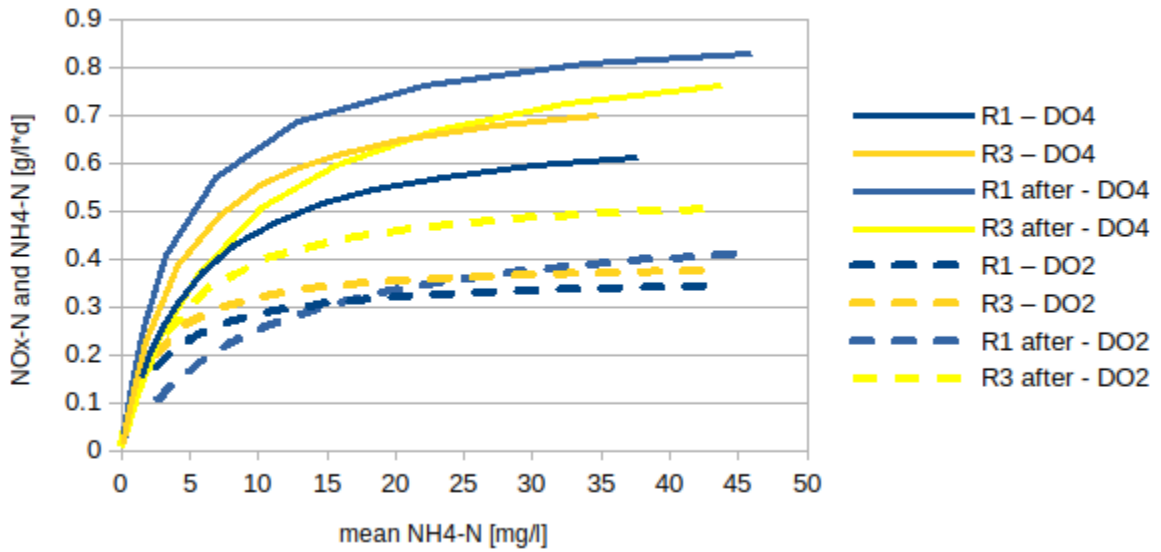
Figure 4.16. Monod-curves after the adjusted fit at 15°C with high aeration from activity studies at DO=2 (dashed lines) and DO=4 (continuous lines) before and after the loss of aggregates from R1 and R3, showing the ammonium dependency due to aggregate loss.

The retrieved Ks and μmax for both the adjusted fit and the statistical methods are represented in table Appendix 5. By comparing the fit of the Monod-curves from the two methods, it can be seen that the retrieved maximum nitrification rate from the adjusted fit is about 5-26 % higher than the statistical maximum nitrification rate, at the same time the slope of the statistical Monod-curves is often steeper at low ammonium levels (Appendix 4).

5 Discussion

To analyze the nitrification performance of the Cella technology, it was compared in sequence batch reactors (SBR) to the conventional MBBR technology. Over the course of the experiment, different activity studies were performed to investigate the ammonium and oxygen dependency of the biofilm. Additionally, samples were taken under different load, aeration and temperature conditions.

Using an SBR setup provides the possibility to control several parameters simultaneously and allows for a small setup while mimicking large-scale conditions. Nevertheless, it has to be taken into account that the biofilm is exposed to different and periodically occurring environmental extremes. One example is the high substrate concentrations at the beginning of each cycle, which can be depleted over the course of one cycle, leading to starvation of the biofilm during certain periods (Gieseke et al., 2003). This goes together with a large fluctuation of the DO depending on the availability of the substrate. These extreme changes can impact the biofilm growth and composition, which in turn could alter the results compared to a full scale or pilot set-up in continuous mode.

Additionally, the reactors were monitored by different people over the course of the experiment. Although an introduction to the sampling procedure was provided to each person to ensure sampling was as consistent as possible, small changes in the sampling procedure until day 208 cannot be excluded. Hence, the large variance in pH measurements at the beginning of the experiment could be partly based on changes in load and aeration, but also on different measurement procedures over time.

5.1 Biofilm establishment and growth

The biofilm established faster on the MBBR carriers than on the support material of the Cella. This can be seen in the quicker buildup of the nitrification rate in the MBBR reactor (Figure 4.3) as well as in the quicker reduction and stabilization of the DO in the MBBR (Figure 4.2). This could be explained by the higher shear forces on the outward growing biofilm of the Cella aggregates as also been discussed by di Biase et al. (2019). A difference in growth establishment between the Cella reactors was also observed, where biofilm established quickest in the reactor with the lowest fill rate, leading to R1>R2>R3 in terms of biofilm establishment (Figure 4.5). This is likely to be caused by the higher collision interactions in R3, due to the larger fill rate compared to R1 with the lowest fill rate. Thus, biofilm is eroded of more at R3 than at R1. The start-up time for initial biofilm development of day 12-19 lies within the timeframe other studies have shown for initial biofilm development in MBBR systems of 20 days (Chu et al., 2014; Mao et al., 2017). Hence, it can be argued that the SBR mimicked a larger scale setup in terms of growth.

By comparing the bed volume of the three Cella reactors, it can be seen that R3 had a lower bed volume than R1 and R2 during the majority of the experiment, even though it started with the largest initial fill rate. Since there was a higher fill of support material in R3, the biofilm likely had a lower load per biofilm surface, resulting in a thinner biofilm. Due to the higher initial fill rate, a higher collision force between particles could also be found in R3 compared to R1 and R2, which may lead to a denser and thinner biofilm (di Biase et al., 2019; Eberl et al., 2000). The bed volume from R3 first surpasses the bed volume from R2 during the last stable period (day 347-418), when the load of R2 is significantly lower than in R3. This shows that the biofilm is adapting to the conditions in the reactors. While a decrease in load

decreased the biofilm thickness in R2, a high load in R3 led to a continuous increase in bed volume. This continuous increase in bed volume towards the end of the experiment in R1 and R3 is not coupled to an increase in biofilm thickness (Figure 4.6 and 4.7). This could be due to the accumulation of biofilm fragments and detached biomass, which was too heavy to be pumped out with the effluent. A small fraction (< 10%) of particles like that could also be seen during microscopy. Due to the form and the biofilm growth, even a small percentage of additional particles can have a large influence on the bed volume.

A significant change in bed volume occurred on day 322, where about 9% of the total bed volume from R1 and 19% of the total bed volume from R3 were lost. If correlated with the initial fill rate, there would be approximately 2.8, 6 and 7.3 % virgin support material left after the loss in R1, R2 and R3 respectively. Consequently, this likely led to an increase in load per volume of aggregates for R1, and especially for R3 after the loss. Also, the collision forces likely decreased in both reactors, but more in R3 than in R1. The effect of the loss can be seen in the increase in oxygen consumption, leading to a lower DO in the reactors (Figure 4.2). An increase in activity can also be seen in the activity studies performed after the loss and compared to the studies before the loss (Figure 4.16). The increase in activity is higher for R1 at DO=4 to which the biofilm is acclimatized. For R3 there is no activity increase visible at DO=4. This could be due to, a balancing of nitrification rate between the large loss and that the increase in activity per biofilm surface. After the loss, the bed volume kept increasing at a similar speed as before, reaching the same bed volume as before the loss approximately 13 days later. A direct impact on the biofilm thickness was not visible due to changes in the operation settings of the reactors at day 348 and the large variation of biofilm thickness within a reactor.

At the beginning of the experiment, biofilm thickness was very similar between the three Cella reactors. Still, biofilm was always thickest in R1, which had the smallest fill rate and hence the smallest forces on the biofilm, while R3 with the highest initial fill rate and hence the largest collision forces had the thinnest biofilm. These correlations are earlier shown by di Biase et al. (2019) and Eberl et al. (2000). In the latter stages of the experiment, the biofilm thickness varied with the changes in operation of the reactor set up, where an increase in load led to an increase in biofilm thickness between day 213-347 and a decrease in load as well as a decrease in aeration led to a decrease in biofilm thickness between day 347-418 (Figure 4.6). This is especially visible for R2, which experienced the largest change between those two periods. For the K5-carriers the biofilm thickness was increasing over the course of the experiment, especially after the decrease of the temperature and the removal of the alkalinity inhibition. The increase in biofilm is most likely based on decreased activity of each single microorganisms, which requires and allows for more cells to thrive with the given ammonia concentration in the bulk-liquid. Looking at the picture from the last stable phase (Figure 4.5), the biofilm thickness ranges within the range found by Gapes & Keller (2009) and Salvetti et al. (2006) for other MBBR carriers. This implies that the operation of the MBBR reactor is comparable to other setups using MBBR.

The increase of biofilm thickness with increasing load can lead to a decrease in nitrification rate in an MBBR setup due to clogging of the MBBR carrier pores (Young et al., 2016). The Cella support material will experience no clogging, due to the external biofilm growth. This opens up the possibility of more efficient nitrification processes with increasing biofilm growth, due to the larger specific surface area available. Having a larger surface area present for nitrification could imply the possibility of obtaining a higher nitrification rate within the reactor. Similar effects were earlier shown during carrier development by Christensson and Welander (2004).

5.2 Nitrification capacity

As soon as the biofilm was growing on the support material and the carriers, the ammonium in the reactors decreased over the course of a cycle. This led to a phase at the beginning of each cycle, where there was sufficient ammonium for unlimited nitrification, but limits in oxygen. In the later part of the cycle, when ammonia had been decreased, the system was ammonia-limited. The limitation of ammonia occurred at different time points within the cycle, depending on the capacity of the biofilm as well as on the operation parameters (Appendix 2).

Differences in capacity are also visible when comparing the DO concentrations in the Cella reactors and the MBBR reactor, with a higher DO observed in R4 than in Cella reactors, even under similar aeration periods (Figure 4.2). This indicates that a larger amount of the available oxygen is used in the Cella reactors, due to a higher rate of nitrification. This supports the initial hypothesis that the Cella aggregates will behave differently compared to the MBBR carriers due to the outward growth. Thus, allowing for an increase in maximum nitrification rate.

Comparing the effluent values from the Cella reactors with the effluent values from the MBBR reactor during the two stable periods between day 153-348 (Figure 4.3.A-D) shows that the MBBR reactor (R4) was not able to nitrify the same amount as the Cella reactors. This led to lower effluent values for nitrogen compounds in the Cella reactors compared to the MBBR, even during times when the Cella reactors received higher incoming loads compared to the MBBR (maximum of 1.20 gNH_4-N/l*d for Cella and maximum of 1.06 gNH_4-N/l*d for MBBR) (Figure 4.3.A-D). It has to be noted, that the nitrification performance of the reactors might have been affected to different degrees by the limitation in alkalinity prior to day 352. Hence, it might have been possible to reach smaller effluent values, especially in the MBBR reactor (Prosser, 1990; Wang et al., 2021). Differences in the nitrification performance can also be impacted by differences in the biofilm constellation. Having different loads in the reactors implies different C:N ratios, thus the MBBR reactor might have more heterotrophs, while the Cella reactors may have a larger amount of nitrifiers due to their 1:2 C:N ratio.

There was also a difference in effluent values between the Cella reactors, which could be based on the increase of initial fill rate leading to an increase in nitrification performance. As a result, R3 was better in coping with higher loads and could quicker produce lower effluent values, when the load was increased (Figure 4.3. C).

Looking at the last stable period (day 387-421), it seemed that the average value of the ammonium effluent did not differ or was even higher in the Cella reactors compared to the average ammonium effluent in the MBBR. Notably, the nitrification potential of the MBBR reactor improved significantly after increasing the alkalinity (day 352). Additionally, the incoming load during this phase on the Cella reactors was up to twice as high as that of the MBBR reactor. Hence, only the R2 reactor should be compared to the MBBR reactor, as these two reactors were operated under the same conditions during the period after day 352. Even here, a lower effluent value is shown in the Cella reactor compared to the MBBR (Figure 4.3.B and 4.3.D).

A similar pattern can be found for the nitrate and nitrite effluent for this period (day 387-421), where the R2 Cella reactor showed a lower average effluent value compared to the R4 MBBR reactor (Figure 4.3.B and 4.3.D). Looking at the other two Cella reactors (R1 and R3) with the high load, high effluent values of nitrate and nitrite effluent were found (Figure 4.3.A and

4.3.C). These high values could indicate that a maximum nitrification performance was found for the conditions during this period which had 15°C, aeration of 3 l/min, and a load of 1.06 gNH_4-N/l*d and 1.20 gNH_4-N/l*d on R1 and R3 respectively. This is because larger effluent nitrite values can indicate that the system is loaded too high. At the same time, it is important to note that the bed volume continued to increase, and the Cella was continuously adjusting to the conditions (Figure 4.7). Hence, the system was mostly limited by oxygen availability and eventually by the volume of the reactor. As a result, the maximum nitrification rate for the Cella in general could not be determined.

5.2.1 Reactor capacity

As discussed earlier, the MBBR reactor was not able to operate at the high load the Cella was operated. So to compare the Cella process with the MBBR process, the load and aeration of R2 were reduced to match the MBBR reactor. Thus, R2 and the MBBR reactor were operated under the exact same conditions with an airflow of 5 l/min and a load of 0.60 gNH_4-N/l*d (Figure 3.2). During such operation conditions, the two reactors showed a similar nitrification performance of approximately 0.60 gNOx-N/l*d according to Figure 4.4, with a slight advantage for R2.

During the same phase R1 and R3 showed significantly higher maximum nitrification performance even though they operated under less aeration than R2 and R4. This indicates that, independent of the initial fill rate, the Cella system has a higher nitrification performance than the conventional K5-carriers. Thus, supporting the initial hypothesis that the Cella system has an advantage in nitrification due to the outwards growing biofilm, compared to a conventional MBBR. A reduction of nitrification performance in the K5-carriers due to clogging was not observed, and hence a decreased in diffusion is unlikely during this phase (Figure 4.5). Additionally, using the nitrification rate in an MBBR of up to 1.2 gNH_4-N/m²*d according to Ødegaard (2006) and the fill rate of this study of 0.4 m², a nitrification rate of 0.48 gNH4-N/l*d would be expected at 11°C. The measured nitrification performance at 15°C is approximately 0.6 gNOx-N/l*d. Therefore, it is assumed that the MBBR reactor runs at its maximum capacity under the conditions of this phase.

The higher nitrification performance is also reflected in the effluent values, where the Cella reactors can reach lower values than the MBBR due to a faster nitrification process in the reactors. This difference in nitrification performance is believed to be due to the outward growing biofilm of the Cella. Recalculating the amount of available alkalinity in the reactors during the experiment prior to day 352 also points to a possibility of buffer limitation, especially in the MBBR reactor.

Upon comparing the three Cella reactors had different fill rates, it is evident that they have very similar capacities when operated under similar conditions, with a slightly better nitrification performance in R3. The improved nitrification performance in R3 could be attributed to a denser biofilm in R3 compared to R1 and R2 (Figure 4.6). This would be supported by the findings from Hibiya et al. (2004), where biofilm density was found to decrease with increasing biofilm thickness. By that thin biofilm, with higher density and lower penetration depth, leading to a smaller diffusion coefficient, showed a higher reaction rate (Hibiya et al., 2004).

Despite differences in initial fill rate, the Cella reactors showed a similar nitrification performance in the Cella reactors, particularly during the last stable phase (day 387-421). During this phase, R1 and R3 were operated under the same conditions (Figure 3.2), with R3 having a slightly higher load (1.20 gNH_4-N/l*d) compared to R1 (1.06 gNH_4-N/l*d). While a

slight difference in average nitrification rate was observed with R1 slightly below 1 gNOx-N/l*d and R3 slightly above 1 gNOx-N/l*d (Figure 4.4). Hence, even though the Cella reactors started with different fill rates, the biofilm adapted over the course of the experiment, to overcome differences in surface area due to initial fill rates.

The reactors also showed similar behaviour, due to changes in the temperatures, even though they had different initial fill rates. This can be seen in the nitrification performance for the Cella reactors during day 243-347, where the reactors were operated with the same load as the previous period (day 153-212) but at 15°C instead of 20°C. A slight decrease in the nitrification performance can be seen for R1, R2 and R3 with the largest decrease in R3. This is going along with the findings from Hellinga et al. (1998). However, the larger decrease in R3 could be influenced by the aggregate loss on day 322.

The cycle studies were performed to investigate the maximum nitrification rate in the different systems. Comparing the results from the cycle studies with the nitrification performance in the different reactors based on the nitrate and nitrite effluent values show that there was a higher maximum nitrification rate compared to the nitrification performance within the same period, especially for the Cella reactors. While the over-all reactor performance showed a nitrification performance of maximum 1.2 gNOx-N/l*d (Figure 4.4), the highest nitrification rate reached in the cycle studies was 2.09 gNH$_4$-N/l*d (Figure 4.9.C and Appendix 3 : R3, day 204). This indicates that the maximum nitrification rate cannot be reliably measured by the effluent values. Supporting the method of using cycle studies and activity studies for the calculation of the maximum nitrification rates. Additionally, it points to that under the majority of the experiment the SBR reactors were ammonium limited, due to a lack of ammonium at the end of the cycle. Hence, the reactors most likely could have been loaded higher during the majority of the experiment and still produced low effluent values.

Comparing the maximum nitrification rate of all four reactors from the cycle studies showed that the MBBR reactor had the lowest rate of all four reactors. Additionally, the rates of the Cella reactors were very similar but with higher values in R3, which had the highest fill of support material (Appendix 3). This supports the initial hypothesis that the Cella system has an advantage in nitrification due to the outwards growing biofilm, and that the differences in initial fill rates for the Cella are of less importance.

To analyse the possible increase in nitrification rate between the Cella and the MBBR, the maximum nitrification rates from the cycle studies can be compared. For 20°C data from day 204 can be used (Appendix 3). It has to be noticed, that the Cella reactors were operated on a higher load during that time (Figure 3.2) and that there was a potential for alkalinity limitation in R4. Using the mean of ammonium and nitrite-nitrate maximum nitrification rate (Appendix 3) leading to a maximum nitrification rate of 1.91, 1.86, 2.15 and 1.37 gNOx-N/l*d for R1, R2, R3 and R4 respectively. Comparing the Cella rates with the MBBR rate shows in increase in maximum nitrification rate of 26-36%. For a comparison at 15°C, the maximum nitrification rates from the cycle studies of R2 and R4 performed on day 407, can be used. During this period, the reactors were operated under the same conditions. Using the mean of ammonium and nitrite-nitrate maximum nitrification rate (Appendix 3) leading to an increase in maximum nitrification rate of 40%. The higher difference during lower temperatures can be due to the larger flexibility of the Cella system to adapt to operation conditions compared to the MBBR. Due to the constant adaptation of the Cella to the operation conditions, a potential for larger differences in nitrification rates is given.

It can also be seen that the decrease in temperature from 20°C to 15°C on day 215 resulted in only a slight decrease in the nitrification rate in the Cella reactors, while the MBBR reactor showed a larger change (Figure 4.9). Using the Arrhenius equation with $\theta = 1.07$ (Equation 5) to calculate the expected change in nitrification rate, results in a maximum nitrification rate of 1.07 gNOx-N/l*d for the MBBR and a maximum nitrification rate of 1.4 gNOx-N/l*d for the Cella systems. It can be seen that the calculated and the measured values for the MBBR are fitting well, especially after the removal of the alkalinity limitation (day 352). The Cella systems, on a contrary, perform much better than the calculated maximum nitrification rate. This could be due to an increase in active biofilm thickness, as also found by Christensson and Welander (2004).

The last cycle study was performed after the aeration was decreased in R1 and R3, and R2 was adjusted to the same conditions as the MBBR reactor (R4). It can be seen in Figure 4.9 that even though R2 and R4 are running with the same conditions, the nitrification performance at R2 is significantly higher compared to R4, supporting the initial hypothesis that the Cella is more efficient in nitrification. At the same time comparing R1 and R3, the difference in initial fill rates (3% and 9% respectively), do not seem to lead to a difference in nitrification performance. For R1 and R3 it has to be noted that there was no difference in bed volume due to the reactor limitation and only a slight difference in load. The similarity in nitrification performance supports the initial hypothesis, that the initial fill of the Cella support material has a small impact on nitrification rates. However, it should be noted that a loss of aggregates occurred between the second and the third cycle study, leading to a reduced virgin fill of support material in R1 and R3. Additionally, there was a constant increase in bed volume even throughout the last stable phase, indicating an ongoing adaption to the operation conditions and therefore the potential for an increase in maximum nitrification performance for both R1 and R3. In contrast, the bed volume of R2 stabilized when the load was reduced in the last stable phase, indicating a reduction and potential loss of biomass due to insufficient loads compared to the existing biomass.

5.2.2 DO dependency

The activity studies indicated that there was an oxygen dependency of the nitrification rate, where an increase in DO led to an increase in the maximum nitrification rate. The activity study performed at DO=4 showed higher nitrification rates, independent of which reactor DO the biofilm was acclimatized to (Figure 4.11). This indicates that diffusion plays a major role for the maximum nitrification rate.

The relationship of an increase in DO leading to an increase in nitrification rate was not found to be solely depending on DO levels in the activity studies. An increase in DO led to an increase in nitrification rate as also found by Christensson and Welander (2004). Additionally, the increase depended also on the difference in DO the activity study was performed on and the DO the biofilm was acclimatized to in the SBR reactors. This is shown by the fact that the activity studies performed on biofilm acclimatized to lower DO levels (day 387-421) performed better in the activity study on lower DO, than the biofilm acclimatized to high DO (day 243-347)(Figure 4.11 and Appendix 5). This resulted in a smaller difference between measurements at DO=2 and DO=4 in Figure 4.11.A vs 4.11.B, comparing the same reactor. It also shows the flexibility of the biofilm to adapt to different conditions. Thus, optimizing the nitrification rate under given conditions, the adaptation could lead to a larger amount of nitrifiers in the shallow biofilm layers compared to the deeper ones. Therefore, the nitrification rate can potentially be higher under lower aeration, if the biofilm is adapted to the operation conditions. This is shown by the results of the activity studies at high aeration and low aeration and a DO=2, where R1 and R3 adapted to DO=2 performed better at lower

aeration compared to R1 and R3 at DO=2 with adaptation to high aeration (Figure 4.11). This might be due to the larger amount of active nitrification biofilm at lower aeration, due to a generally slower reaction potential and hence a longer availability of ammonium over a cycle.

The flexibility of the biofilm to adapt to different conditions was also observed through a change in the colour of the biofilm after the decrease in aeration in R1 and R3, which is an indication of changes in the microbial community. Dynamic changes in AOB populations in biofilm due to DO reduction have also been observed by Park & Noguera (2004) and Young et al. (2016).

5.2.3 Ammonium dependency
When comparing the nitrification rates from the activity studies with the nitrification potential calculated from the effluent values of the reactors, it has to be taken into account that a full bed volume is compared to 100 ml of the bed volume used in the activity studies. This corresponded to ⅓ to ⅙ of the total bed volume. By scaling up the results from the activity studies to a full bed volume, it can be seen that the maximum nitrification rates retrieved from the activity studies are much higher than the nitrification potential of the reactors (Figure 4.15.A-B and Figure 4.4). Additionally, it can be seen that the initial fill will give rise to differences in the nitrification rate, leading to a higher μmax for R3 than for R1 (Figure 4.15.B).

This can also be seen after the aggregate loss from R1 and R3 at day 322, which led to an increase in nitrification rate in R1 but not clearly in R3 (Figure 4.15). This could be due to the rapid adjustment of the biofilm to new conditions, as already seen by Gieseke et al. (2003), as well as a larger loss of support material from R3 than R1 (Figure 4.7).

Comparing the results from the cycle studies to an upscaled result of the activity studies indicates that the maximum nitrification rates in the activity studies are higher than in the cycle studies. This suggests that the activity trials are run under more favourable conditions for nitrification. This could be influences by alkalinity or mixing with fewer aggregates, leading to a thinner boundary layer (Mašić et al., 2010).

By looking at the two different methods used to calculate the Monod-curves for the activity studies, it can be seen that the adjusted fit curve results in a higher maximum nitrification rate than the statistical curve (Appendix 4). This is likely to be caused by the reduction of alkalinity during the activity study, which led to a repeated addition of buffer to the reactors based on the pH measurements. The reduced alkalinity negatively impacted the nitrification rate and led to errors in the sampling results. For the adjusted fit calculations, the knowledge about the time of the addition and the reduction of the alkalinity was included in the fitting of the curve by weighing the outliers less strongly. This was not possible for the statistical method, leading to a lower maximum nitrification rate.

Looking at the Ks values from the activity tests at high aeration shows that there was no difference in performance between the MBBR reactor and the Cella reactor with the lower initial fill rate. While R3 with the highest initial fill rate resulted in Ks less than half the size (Appendix 6). This implies that R3 has a higher affinity to ammonium, than the other reactors. This could be due to a higher concentration of nitrifiers on the outer layer of the biofilm and to the adaption of the biofilm to low ammonium levels, due to the SBR cycle depleting the ammonium quicker than the other reactors (Appendix 2). Looking at the activity studies after the aeration and load has been decreased for the Cella reactors, a different pattern can be seen (Appendix 6). Here, the affinity of the biofilm to the ammonium is highest under low DO

concentrations and lower under high DO concentrations. This implies that the reactors have been adapted to the lower DO concentrations in the SBR setup and deeper layer of the biofilm are less active. It also shows that the activation of the deeper layer is not possible within the timeframe of an activity study. Additionally, it is shown that the Cella reactor R2 and the MBBR reactor R4, which are operated under the same conditions, perform equally or only slightly better than the Cella reactors R1 and R3 under lower aeration and with higher feed. This supports the initial hypothesis, that Cella has an advantage over MBBR in nitrification.

It should be noted that the results of the activity studies may have been influenced by several other factors. For instance, were the activity studies performed on different days leading to different conditions in the reactors, due to changes in operation parameters. This may have influenced the concentration gradients of oxygen and ammonium within the biofilm, and therefore affected the activity of the microbial community in the biofilm. Thus, the differences in maximum nitrification rates between the different activity studies could be attributed to changes in the bacterial population, as already observed by Gieseke et al. (2003).

One activity study was performed on the full bed volume of the Cella reactor R2, to investigate the linearity between using 100 ml of bed volume and the full bed volume. Figure 4.13 shows that even though the activity study was performed at DO=3 the nitrification rate of the full bed volume, after adjusting to match the 100 ml, fits linearly with the two measurements at DO=2 and DO=4 performed on 100 ml bed volume. The measurement at DO=3 with the full bed is situated slightly under the linear trend. Using the results from the cycle study from day 407, shows a maximum nitrification rate adjusted to 100 ml bed volume at DO=4 of 0.4 gNOx-N/l*d. This result is lower than the measured maximum nitrification rate in the activity studies (Figure 4.11), implying a difference between cycle and activity studies. This reduction in the cycle study using the full bed could be due to an increase in boundary layer due to an increase in aggregates. Thus, could also explain the measurement slightly below the linear trend. Nevertheless, an extrapolation of the results from the activity studies to larger bed volumes should be possible.

5.3 Cella on a larger scale

Introducing external growth on the support material, by decreasing size, puts the Cella support material in a new category among biofilm-based wastewater treatment methods. The Cella process does not entirely behave as an MBBR, even though the biofilm grows on the surface of a support material. It differs from the MBBR by surrounding the whole support material and hence diffusion is possible from more than one dimension, resulting in an increase in nitrification rate.

To retain the Cella aggregates in the biological treatment, the setup for aeration and settling needs to be adjusted, as it differs from a conventional AS. This opens up for the possibility to implement Cella into an existing WWTP or to establish it as a new process for wastewater treatment. It has to be noticed that when implementing in an existing plant, it requires an initial investment. However, Cella can improve the treatment process more efficiently compared to an MBBR. Additionally, the usage of renewable by-products to produce the support material, will decrease the environmental impact of the WWTP, moving towards a circular economy.

In addition, the Cella system has an advantage over the conventional MBBR system, as it does not need an increase in fill rate to treat higher loads. This is due to the high flexibility of the outward growing biofilm, which is able to adapt to different conditions. Due to the

outward growth, an increase in maximum nitrification rate compared to the MBBR of 26-36% at 20°C and of 40% at 15°C have been found. Thus, resulting in lower effluent values for the Cella reactors. This will be beneficial in terms of the new EU- urban wastewater treatment directive, which requires lower effluent concentrations and the treatment of micro-pollutants (European Union, 2023). Even in this field, Cella has the potential to improve the wastewater treatment. This is for the first due to the long biomass retention in the treatment, allowing slow growing microorganisms to develop. Secondly, due to the outwards growing biofilm, which creates a larger surface and potentially more nieces, thus a more diverse microbial community is possible. These can contribute with a large variety of processes to remove pollutants from the water.

6 Conclusion

This study was conducted to evaluate the nitrification performance in a novel biofilm process based on external biofilm growth, looking at effects of carrier surface area and substrate limitations. For this the Cella technology, with outward growing biofilm, was compared to the conventional MBBR technology which has inward growing biofilm. After 421 days of operation including several cycle and activity studies it can be concluded that independent of aeration, temperature and load the Cella technology has an advantage over the MBBR in nitrification. This resulted in an increase in maximum nitrification rate compared to the MBBR of 26-36% at 20°C and of 40% at 15°C. Thus, resulting in lower effluent values for nitrite and ammonium in consideration of the loads but regardless of the initial fill rate.

Furthermore, by performing activity studies at different oxygen levels, it was shown that the nitrification rate depends on the oxygen levels in the reactor as well as the oxygen levels the biofilm in the Cella system is adapted to. The reduction of aeration in the reactors had a positive impact on nitrification at low DO concentrations in the activity studies, which leads to a larger activity per 100 ml aggregates. These findings support the initial hypothesis suggesting the Cella system behaves differently due to outwards growing biofilm with a higher nitrification rate and a small impact of the initial fill rate. The maximum nitrification rate of Cella was not found due to the high flexibility of the biofilm. This results in an adjustment of the biofilm to the given conditions.

The study also showed that the MBBR allowed earlier biofilm growth compared to the Cella. Within the Cella an earlier biofilm establishment was seen in the reactor with the smallest initial fill rate. Additionally, it was seen that the bed volume in the Cella reactors with high load continuously increased with increasing load, showing the flexibility of the system and the possibility to adapt to even higher loads. Hence, it can be concluded that the MBBR system had reached its maximum capacity, while the Cella system was limited by the reactor volume and the DO to reach its maximum capacity for nitrification.

7 Recommendations for future work

Comparing the maximum nitrification rate in an activity study with a full bed volume to two activity studies with 100 ml of the same bed volume showed that it is possible to extrapolate the maximum nitrification rate from 100 ml to a full SBR-reactor volume. Further research is needed to investigate if this relationship holds for extrapolation for even larger bed volumes and treatment on larger scale. Additionally, it should be investigated how the bed volume continues to increase, when there is no limitation of the reactor volume and under different aeration. If bed volume reaches the maximum reactor capacity, the set-up could be tested about development after removal of different portions of the aggregates. It should be taken into account that the increase in bed volume could be an artifact from the SBR-operation and does not occur on larger scales.

Investigations could go along with further research about the maximum nitrification rate of the Cella system. This could be tested through lowering the aeration to a minimum possible, increasing the load or decreasing the initial fill rate. This study could be used at the same time to see if a new start-up under similar conditions as in this experiment, lead to similar results. Furthermore, it would be interesting to investigate, if the increase in initial fill rate of 9% or higher, gives rise to higher nitrification rates within the Cella system, as indicated in some of the activity tests in this study. Hence, if there is a certain fill rate that divides the behaviour in different ranges.

Showing that Cella performs well in the nitrification is only the first step of ammonium removal from wastewater. Further research should investigate, if Cella could also be used for denitrification and if a combination of nitrification and denitrification in the same process is possible. This would lead to a broader use of the Cella in wastewater treatment.

8 References

Anthonisen, A. C., Loehr, R. C., Prakasam, T. B. S., & Srinath, E. G. (1976). Inhibition of nitrification by ammonia and nitrous acid. *Journal (Water Pollution Control Federation)*, 835-852. https://www.jstor.org/stable/25038971

Boltz, J. P., & Daigger, G. T. (2010). Uncertainty in bulk-liquid hydrodynamics and biofilm dynamics creates uncertainties in biofilm reactor design. *Water Science and Technology*, *61*(2), 307–316. https://doi.org/10.2166/wst.2010.829

Christensson, M., & Welander, T. (2004). Treatment of municipal wastewater in a hybrid process using a new suspended carrier with large surface area. *Water Science and Technology*, *49*(11–12), 207–214. https://doi.org/10.2166/wst.2004.0843

Chu, L., Wang, J., Quan, F., Xing, X. H., Tang, L., & Zhang, C. (2014). Modification of polyurethane foam carriers and application in a moving bed biofilm reactor. *Process Biochemistry*, *49*(11), 1979-1982. https://doi-org.ludwig.lub.lu.se/10.1016/j.procbio.2014.07.018

Coelho, P. (1993). The Alchemist. Diogenes. Zürich.

Deena, S. R., Kumar, G., Vickram, A. S., Singhania, R. R., Dong, C. D., Rohini, K., ... & Ponnusamy, V. K. (2022). Efficiency of various biofilm carriers and microbial interactions with substrate in moving bed-biofilm reactor for environmental wastewater treatment. *Bioresource technology*, *359*, 127421. https://doi-org.ludwig.lub.lu.se/10.1016/j.biortech.2022.127421

Dezotti, M., Lippel, G., & Bassin, J. P. (2018). Advanced biological processes for wastewater treatment. *Springer, İsviçre. Doi*, *10*, 978-3.

di Biase, A., Kowalski, M. S., Devlin, T. R., & Oleszkiewicz, J. A. (2019). Moving bed biofilm reactor technology in municipal wastewater treatment: A review. *Journal of Environmental Management*, *247*(May), 849–866. https://doi.org/10.1016/j.jenvman.2019.06.053

Eberl, H. J., Picioreanu, C., & Heijnen, J. J. (2000). A three-dimensional numerical study on the correlation of spatial structure, hydrodynamic conditions, and mass transfer and conversion in biofilms. *Chemical Engineering Science*. https://doi-org.ludwig.lub.lu.se/10.1016/S0009-2509(00)00169-X

Ekholm, J., De Blois, M., Persson, F., Gustavsson, D. J. I., Bengtsson, S., Van Erp, T., & Wilén, B. (2023). Case study of aerobic granular sludge and activated sludge—Energy usage, footprint, and nutrient removal. *Water Environment Research*, *95*(8), e10914. https://doi.org/10.1002/wer.10914

European Union. (2023). Urban wastewater: Council and Parliament reach a deal on new rules for more efficient treatment and monitoring. Press release 29. January 2024. https://www.consilium.europa.eu/en/press/press-releases/2024/01/29/urban-wastewater-council-and-parliament-reach-a-deal-on-new-rules-for-more-efficient-treatment-and-monitoring/ [Accessed 2024-04-22].

Fu, J., Chen, C., Wang, Y., & Chen, Y. (2010, December). Inhibition of free nitrite acid on nitrification. In *The 2nd International Conference on Information Science and Engineering* (pp. 288-290). IEEE.

Gapes, D. J., & Keller, J. (2009). Impact of oxygen mass transfer on nitrification reactions in suspended carrier reactor biofilms. *Process Biochemistry*, *44*(1), 43–53. https://doi.org/10.1016/j.procbio.2008.09.004

Gieseke, A., Bjerrum, L., Wagner, M., & Amann, R. (2003). Structure and activity of multiple nitrifying bacterial populations co‑existing in a biofilm. *Environmental Microbiology*, *5*(5), 355–369. https://doi.org/10.1046/j.1462-2920.2003.00423.x

Hellinga, C. S. A. A. J. C., Schellen, A. A. J. C., Mulder, J. W., van Loosdrecht, M. V., & Heijnen, J. J. (1998). The SHARON process: an innovative method for nitrogen removal from ammonium-rich waste water. *Water science and technology*, *37*(9), 135-142. http://dio.org/ 10.1016/S0273-1223(98)00281-9

Hem, L. J., Rusten, B., & Ødegaard, H. (1994). Nitrification in a moving bed biofilm reactor. *Water Research*, *28*(6), 1425–1433. https://doi.org/10.1016/0043-1354(94)90310-7

Hibiya, K., Nagai, J., Tsuneda, S., & Hirata, A. (2004). Simple prediction of oxygen penetration depth in biofilms for wastewater treatment. *Biochemical Engineering Journal*, *19*(1), 61–68. https://doi.org/10.1016/j.bej.2003.10.003

Juretschko, S., Timmermann, G., Schmid, M., Schleifer, K. H., Pommerening-Röser, A., Koops, H. P., & Wagner, M. (1998). Combined molecular and conventional analyses of nitrifying bacterium diversity in activated sludge: Nitrosococcus mobilis and Nitrospira-like bacteria as dominant populations. *Applied and environmental microbiology*, *64*(8), 3042-3051. https://doi-org.ludwig.lub.lu.se/10.1128/AEM.64.8.3042-3051.1998

Mao, Y., Quan, X., Zhao, H., Zhang, Y., Chen, S., Liu, T., & Quan, W. (2017). Accelerated startup of moving bed biofilm process with novel electrophilic suspended biofilm carriers. *Chemical Engineering Journal*, *315*, 364-372. https://doi-org.ludwig.lub.lu.se/10.1016/j.cej.2017.01.041

Mašić, A., Bengtsson, J., & Christensson, M. (2010). Measuring and modeling the oxygen profile in a nitrifying Moving Bed Biofilm Reactor. *Mathematical Biosciences*, *227*(1), 1–11. https://doi.org/10.1016/j.mbs.2010.05.004

Morgenroth, E. (2008). Modelling biofilm systems. In: Henze, M., van Loosdrecht, M. C. M., Ekama, G. & Brdjanovic, D. (eds). Biological Wastewater Treatment — Principles, Modelling, and Design. IWA Publishing, London.

Ødegaard, H. (2006). Innovations in wastewater treatment:–the moving bed biofilm process. *Water science and technology*, *53*(9), 17-33. https://doi-org.ludwig.lub.lu.se/10.2166/wst.2006.284

Okabe, S., Naitoh, H., Satoh, H., & Watanabe, Y. (2002). Structure and function of nitrifying biofilms as determined by molecular techniques and the use of microelectrodes. *Water Science and Technology*, *46*(1–2), 233–241. https://doi.org/10.2166/wst.2002.0482

Park, H. D., & Noguera, D. R. (2004). Evaluating the effect of dissolved oxygen on ammonia-oxidizing bacterial communities in activated sludge. Water research, 38(14-15), 3275-3286. https://doi-org.ludwig.lub.lu.se/10.1016/j.watres.2004.04.047

Pérez, J., Lotti, T., Kleerebezem, R., Picioreanu, C., & Van Loosdrecht, M. C. (2014). Outcompeting nitrite-oxidizing bacteria in single-stage nitrogen removal in sewage treatment plants: a model-based study. *Water Research*, *66*, 208-218. https://doi-org.ludwig.lub.lu.se/10.1016/j.watres.2014.08.028

Piculell, M., Suarez, C., Li, C., Christensson, M., Persson, F., Wagner, M., ... & Welander, T. (2016). The inhibitory effects of reject water on nitrifying populations grown at different biofilm thickness. *Water research*, *104*, 292-302. https://doi-org.ludwig.lub.lu.se/10.1016/j.watres.2016.08.027

Prosser, J. I. (1990). Autotrophic nitrification in bacteria. *Advances in microbial physiology*, *30*, 125-181. https://doi-org.ludwig.lub.lu.se/10.1016/S0065-2911(08)60112-5

Rusten, B., Hem, L. J., & Ødegaard, H. (1995). Nitrification of municipal wastewater in moving-bed biofilm reactors. *Water Environment Research*, *67*(1), 75–86. https://doi.org/10.2175/106143095x131213

Sánchez, O., Martí, M. C., Aspé, E., & Roeckel, M. (2001). Nitrification rates in a saline medium at different dissolved oxygen concentrations. *Biotechnology letters*, *23*, 1597-1602. https://doi.org/10.1023/A:1011977629398

Tchobanoglous, G., Metcalf & Eddy, Burton, F. L., & Stensel, H. D. (2014). Wastewater engineering : treatment and resource recovery (5th edition.). McGraw-Hill.

Wang, J., Li, L., Liu, Y., & Li, W. (2021). A review of partial nitrification in biological nitrogen removal processes: from development to application. *Biodegradation*, *32*, 229-249. https://doi.org/10.1007/s10532-021-09938-x

Young, B., Banihashemi, B., Forrest, D., Kennedy, K., Stintzi, A., & Delatolla, R. (2016). Meso and micro-scale response of post carbon removal nitrifying MBBR biofilm across carrier type and loading. *Water Research*, *91*, 235–243. https://doi.org/10.1016/j.watres.2016.01.006

Zhao, J., Liu, T., Meng, J., Hu, Z., Lu, X., Hu, S., ... & Zheng, M. (2023). Ammonium concentration determines oxygen penetration depth to impact the suppression of nitrite-oxidizing bacteria inside partial nitritation and anammox biofilms. *Chemical Engineering Journal*, *455*, 140738. https://doi.org/10.1016/j.cej.2022.140738

9 Appendix

1 Appendix solution T1 solution

Table: with recipe to prepare 1 litre of artificiel wastewater as feed.

		1 L
1	$MgSO_4$ x $7H_2O$ (g)	4.80
2	$MnCl_2$ x $2H_2O$ (g) *or*	1.60
	$MnCl_2$ x $4H_2O$ (g)	1.92
3	$CoCl_2$ x $6H_2O$ (g)	0.48
4	$NiCl_2$ x $6H_2O$ (g)	0.24
5	$ZnCl_2$ (g)	0.26
6	$CuSO_4$ x $5H_2O$ (g)	0.10
	BH_3O_3 (g)	0.00052
	Na_2MoO_4 x $2H_2O$ (g)	0.0022
	Na_2SeO_3 x $5H_2O$ (g)	0.00114
	Na_2WO_4 x $2H_2O$ (g)	0.0014
8	$FeCl_2$ x $4H_2O$ (g) *or*	1.44
	$FeSO_4$ x $7H_2O$ (g)	2.00

2 Appendix cycle studies

Cycle study day 153

R1

R3
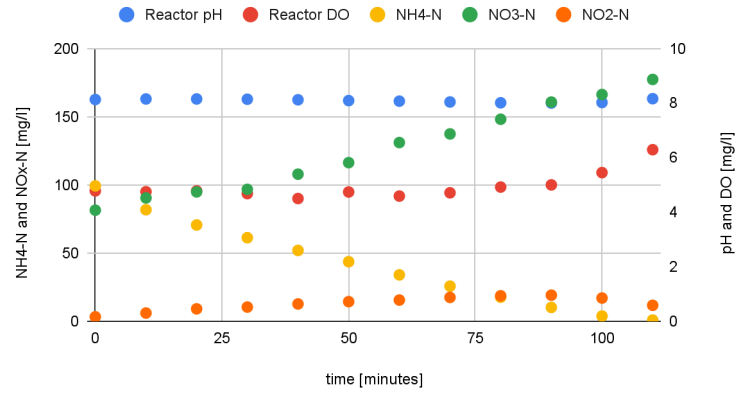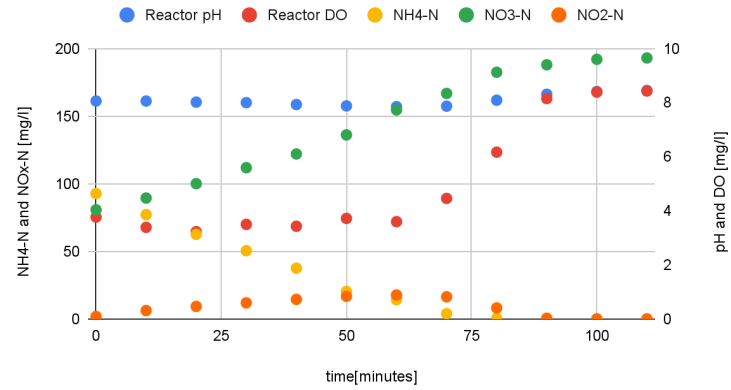
R4
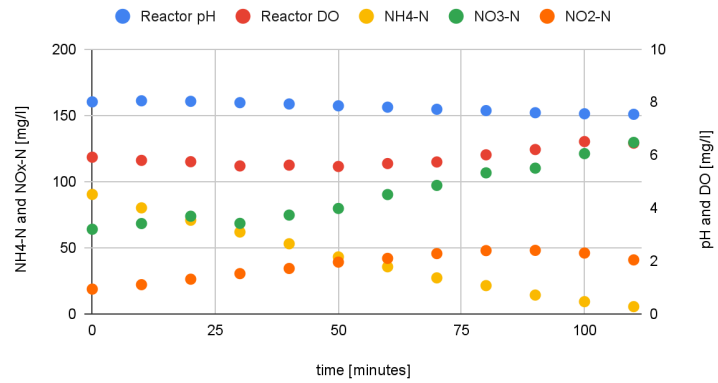
Cycle study day 204

R1

R2

R3
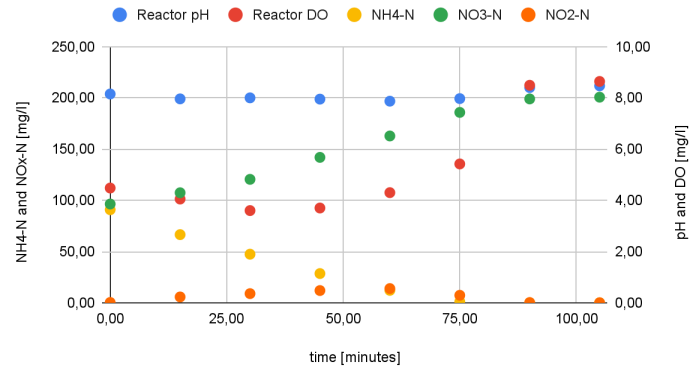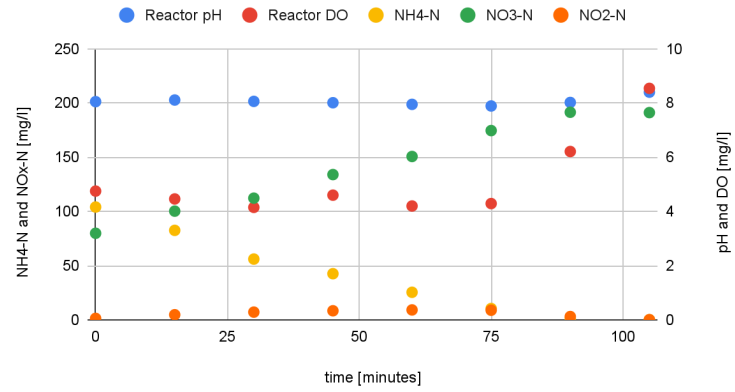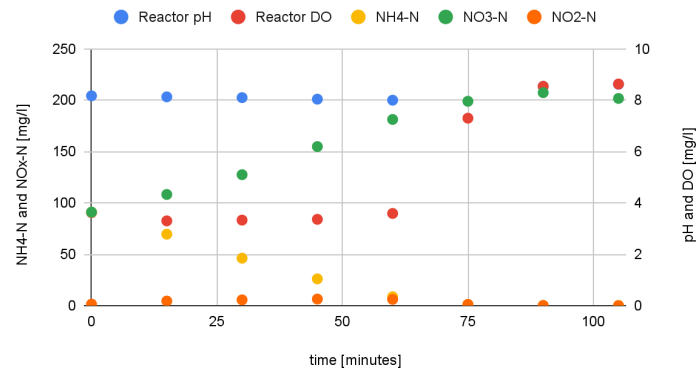
R4
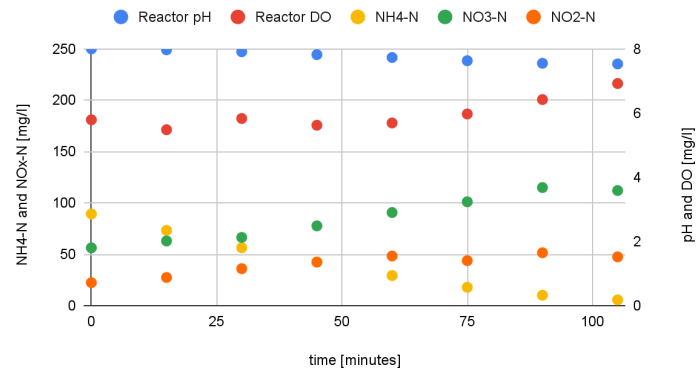
Cycle study day 286

R1

R2

R3
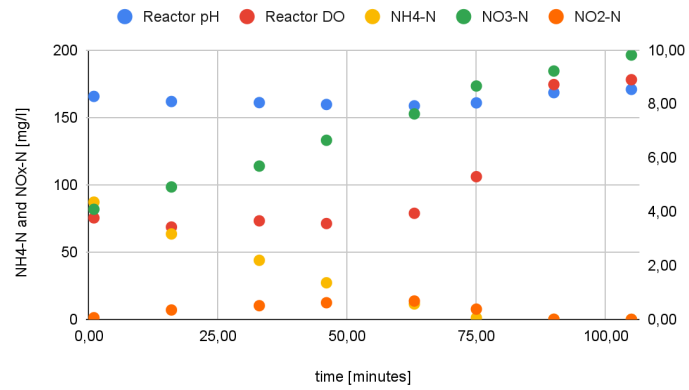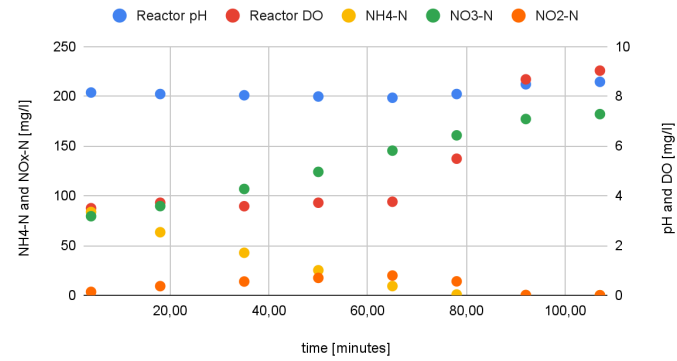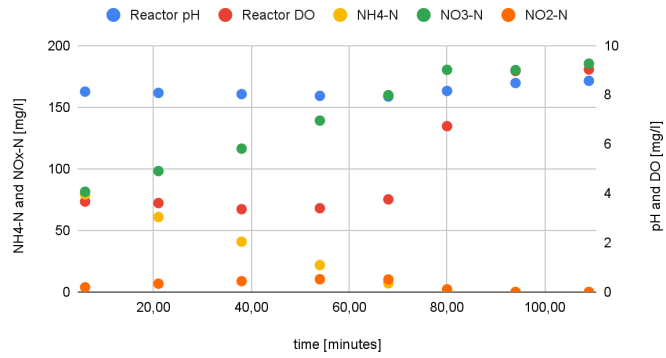
R4
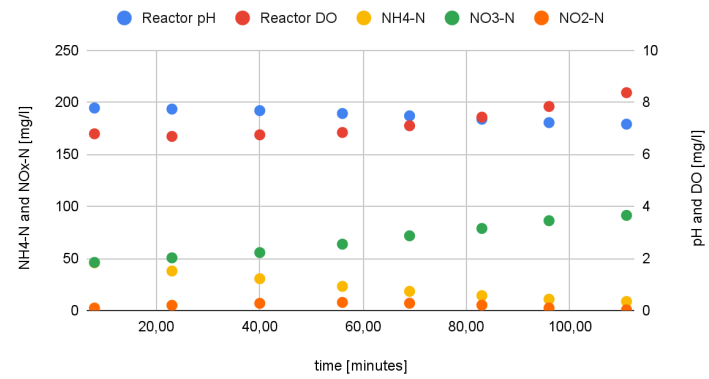
Cycle study day 407
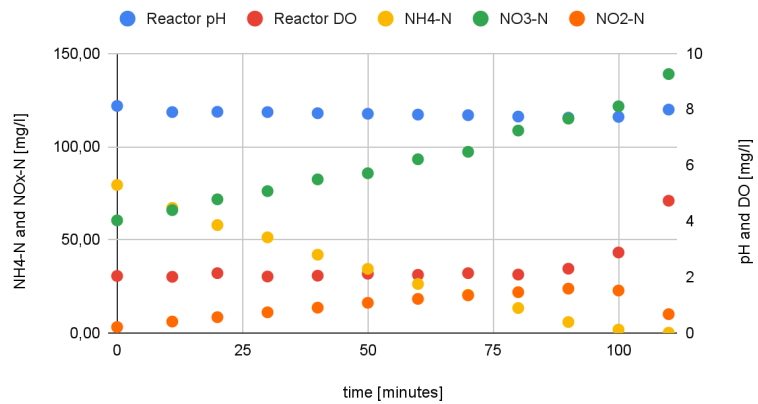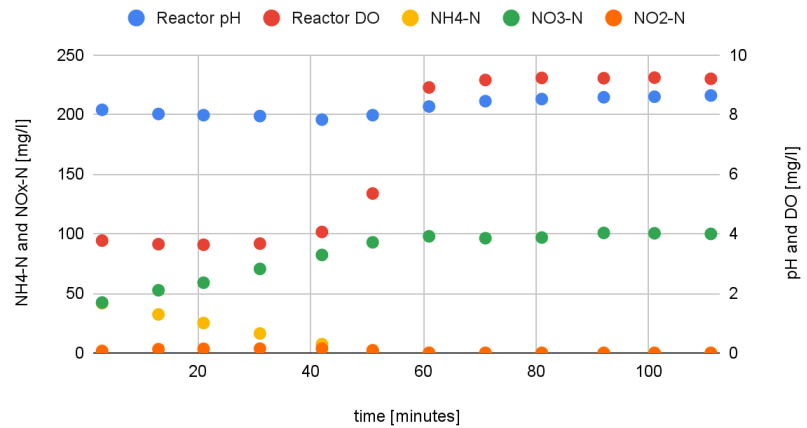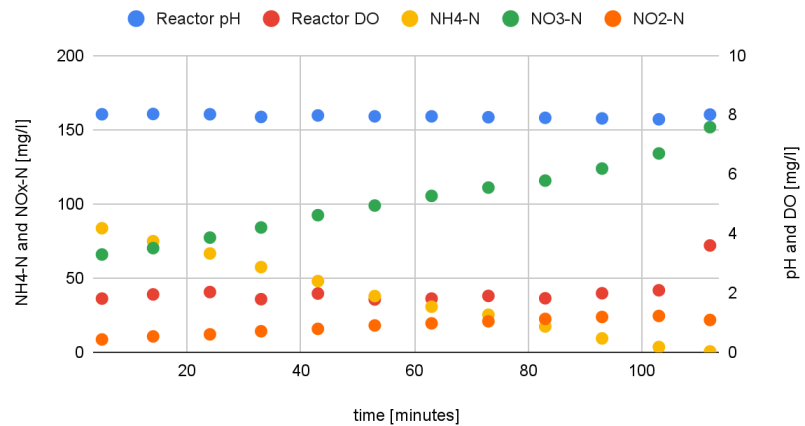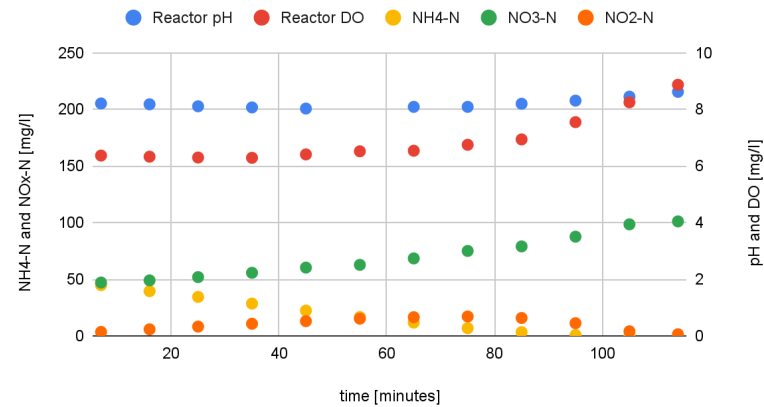
3 Appendix Cycle studies table

Table: *Maximum nitrification rates in gNOx/l*d, from the cycle studies over the course of the experiment, represented as NH$_4$-N removal and NOx-N production when NH$_4$-N > 20 mg/L.*

	R1		R2		R3		R4	
Day	**NH$_4$-N**	**NOx-N**	**NH$_4$-N**	**NOx-N**	**NH$_4$-N**	**NOx-N**	**NH$_4$-N**	**NOx-N**
153	1,28	1,51			1,84	2,11	1,18	1,25
204	1,88	1,93	1,79	1,92	2,00	2,29	1,38	1,36
286	1,66	1,91	1,63	1,86	1,58	1,93	0,53	0,64
407	1,25	1,14	1,27	1,53	1,36	1,30	0,81	0,88

4 Appendix Activity study figures

activity studies day 295

R1
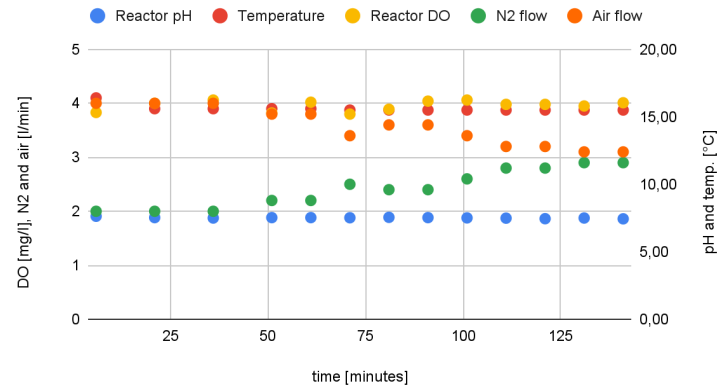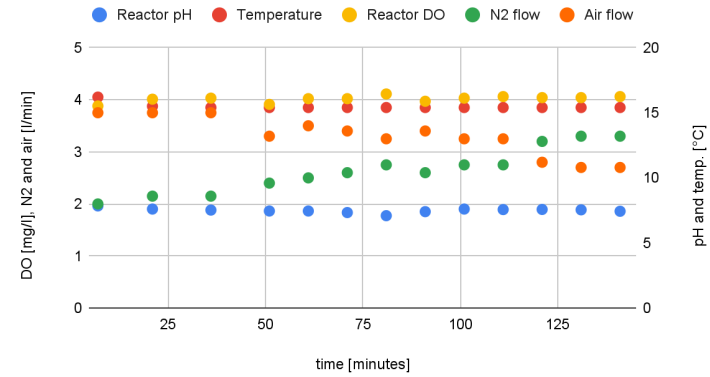
activity studies day 302

R2

R3

R4
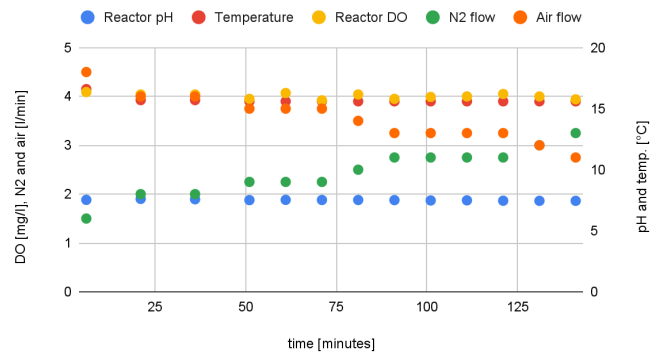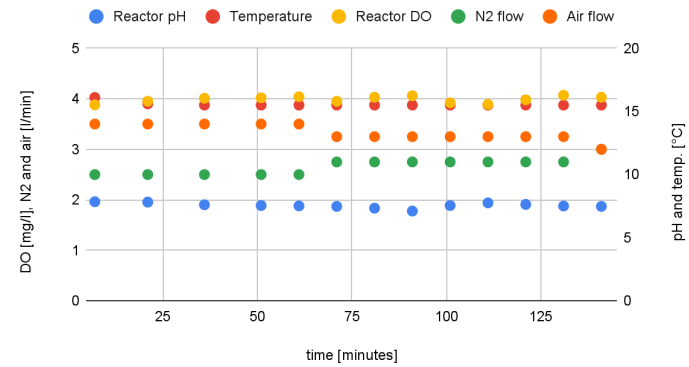
activity studies day 310

R1
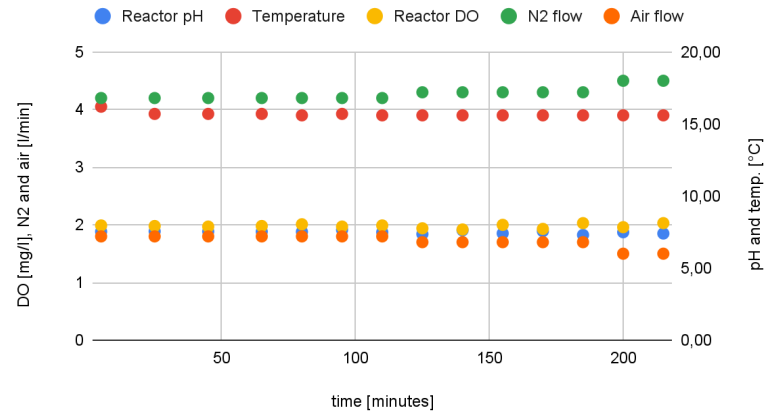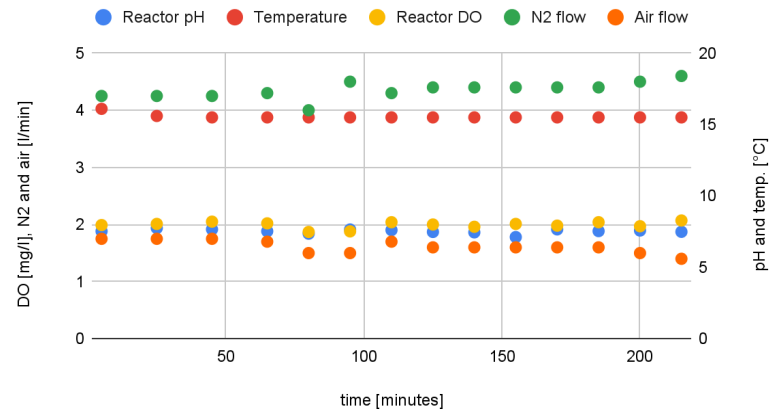
activity studies day 337

R3

R1

R3
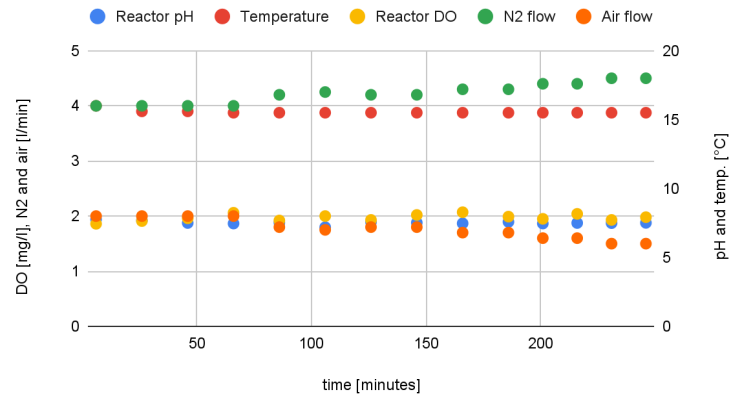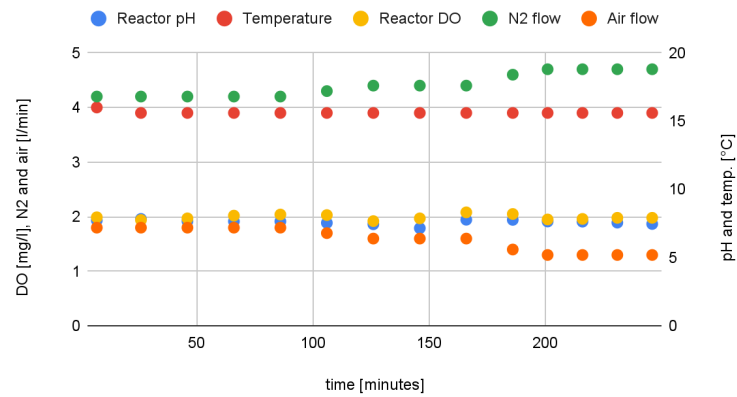
activity studies day 344

R1

R3
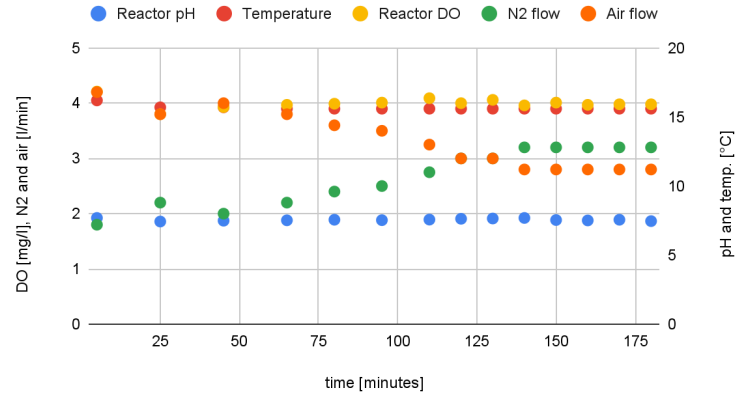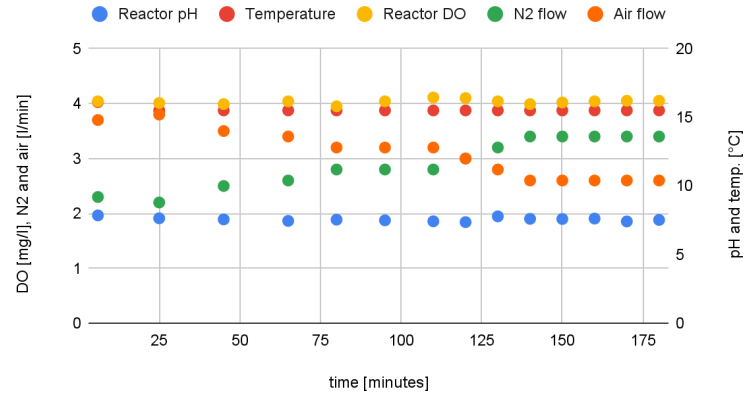
activity studies day 412

R2

R4
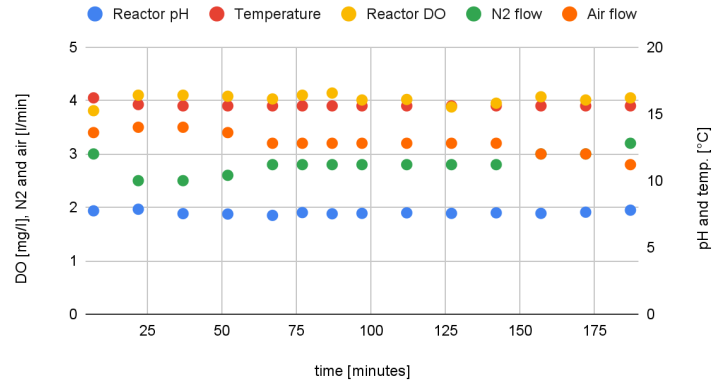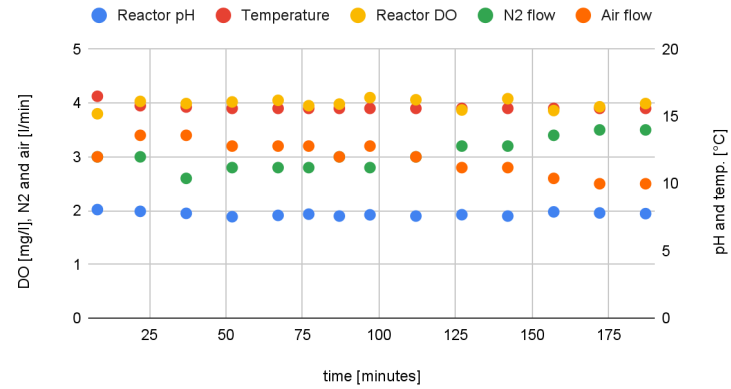
activity studies day 414

R2

R4
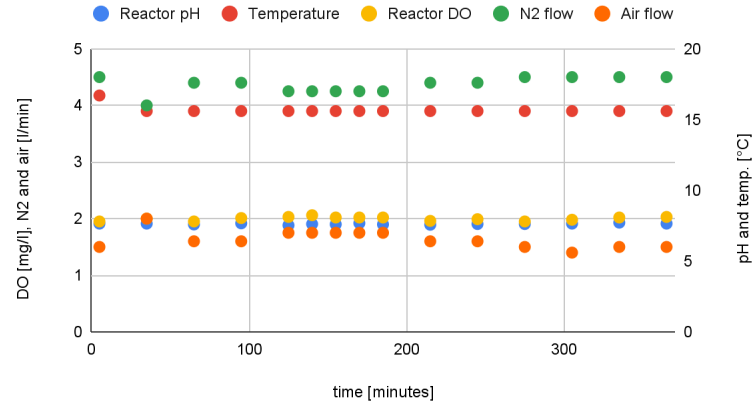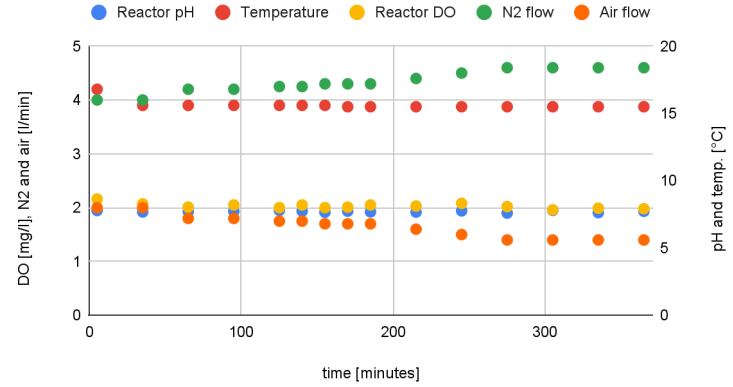
activity studies day 419

R1
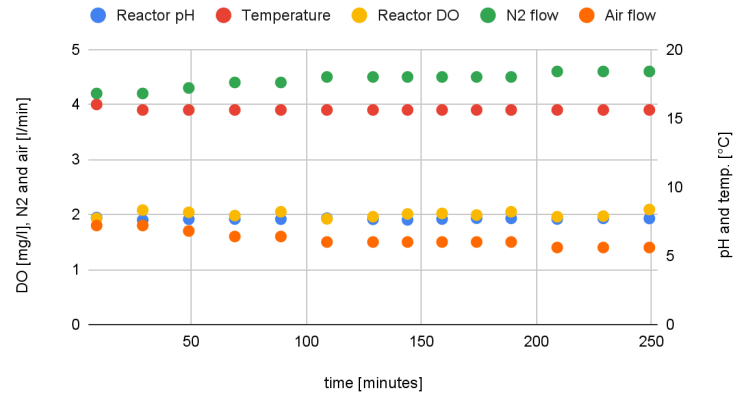
R3
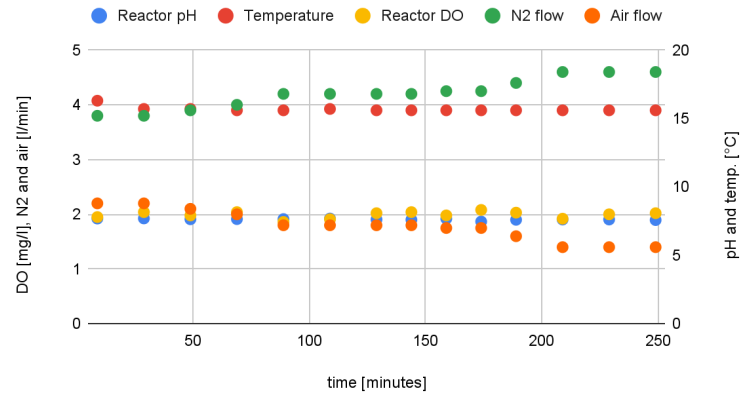
activity study with full bed volume day 419

R2
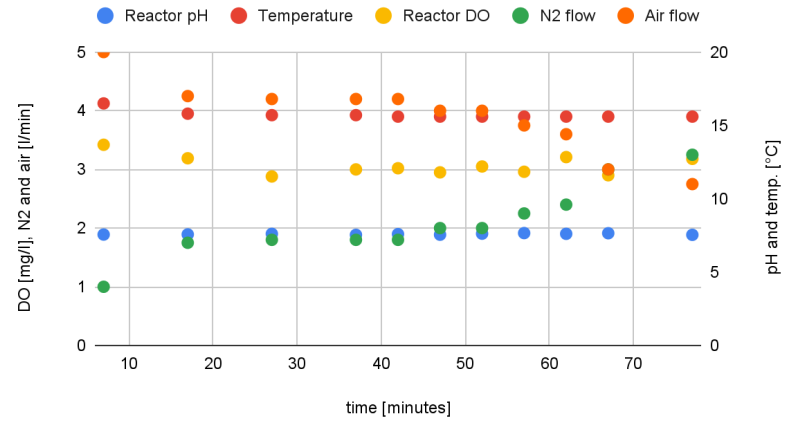
activity studies day 421

R1
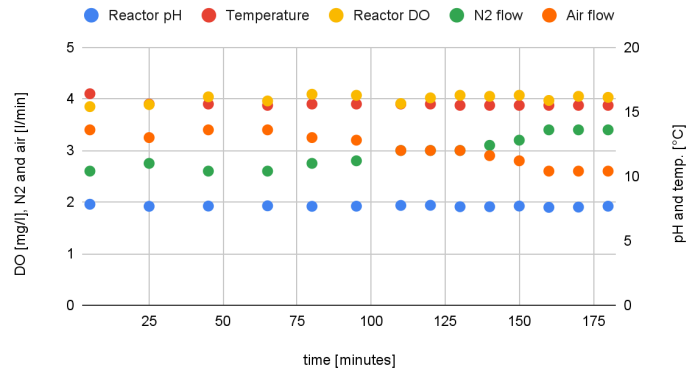
R3
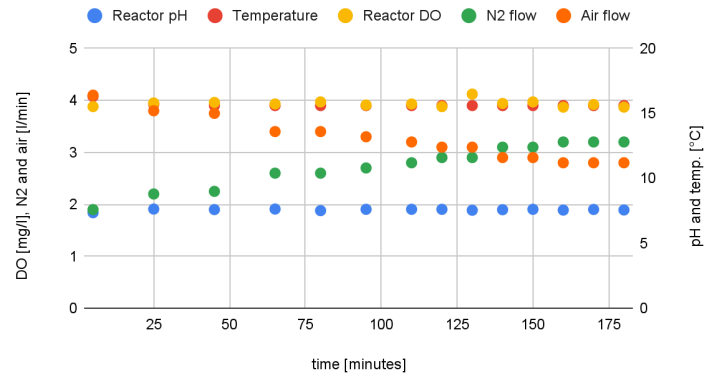
5 Appendix Monod curves

R1 - DO4 - day 295
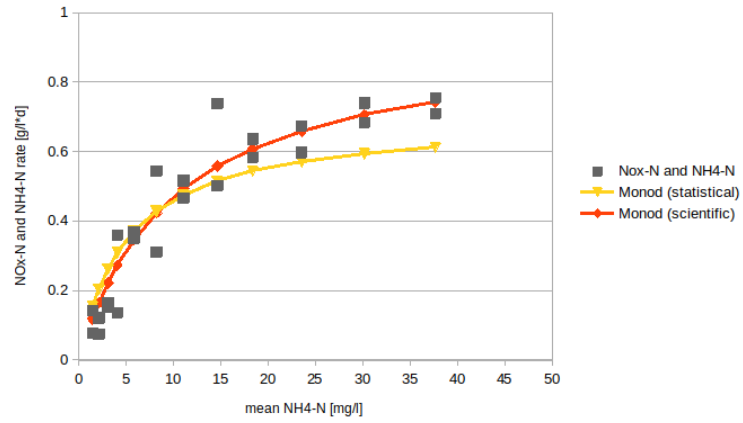
R3 - DO4 - day 295
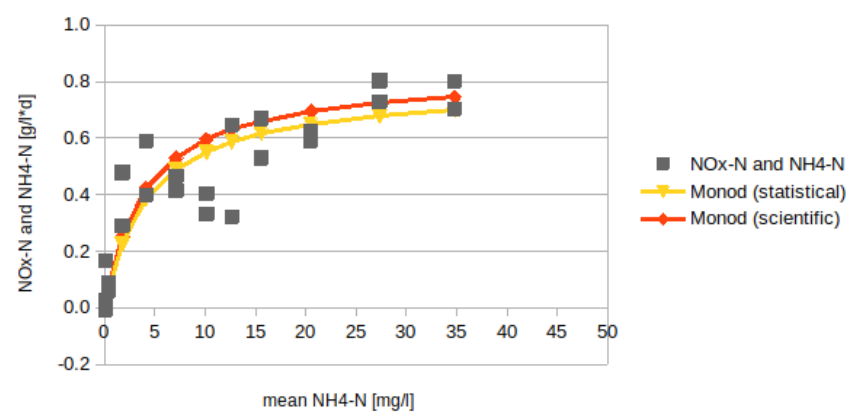
R2-DO4-day 302
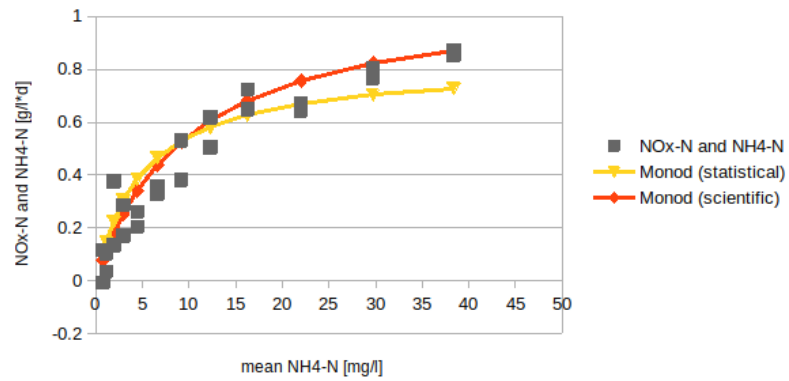
R4-DO4-day 302
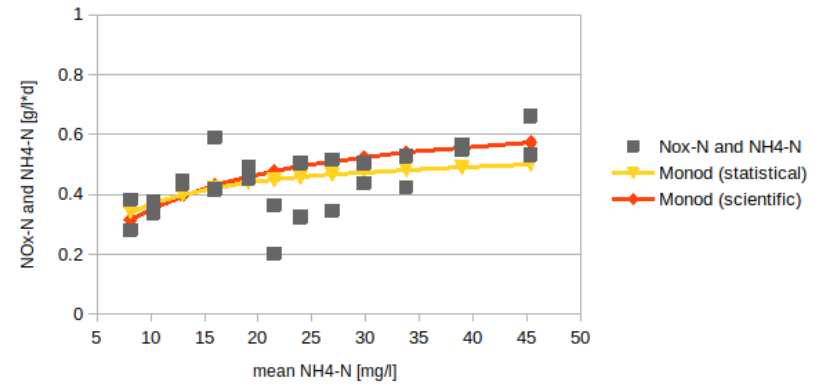
R1 - DO2 - day 310
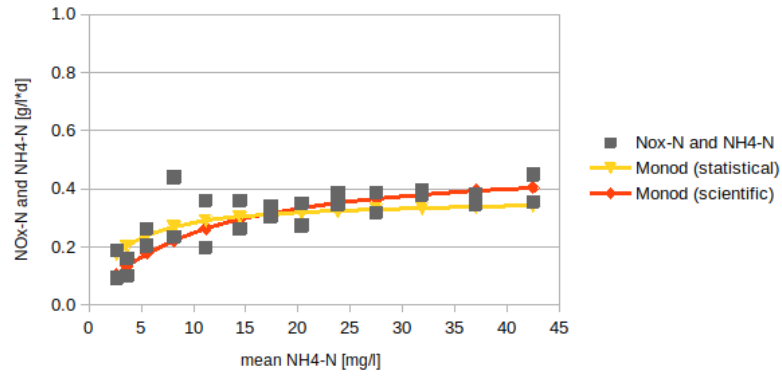
R3 - DO2 - day 310
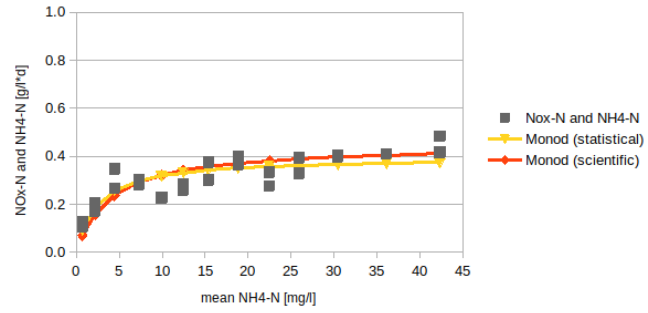
R1 after aggregate loss - DO2 - day 337
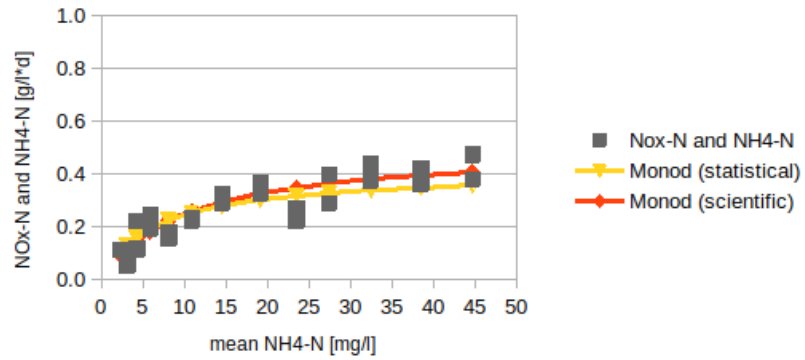
R3 after aggregate loss - DO2 - day 337
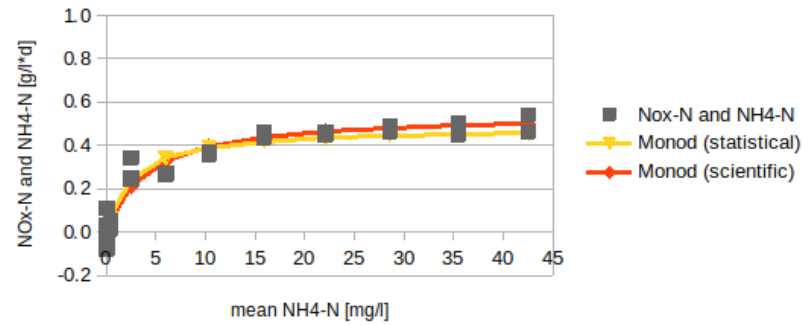
R1 after aggregate loss - DO4 - day 344
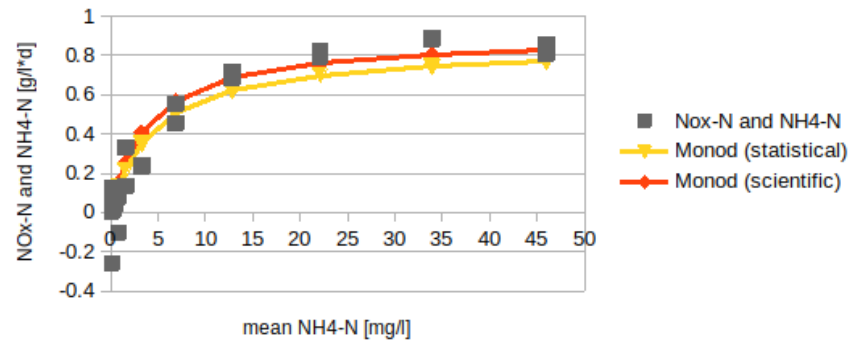
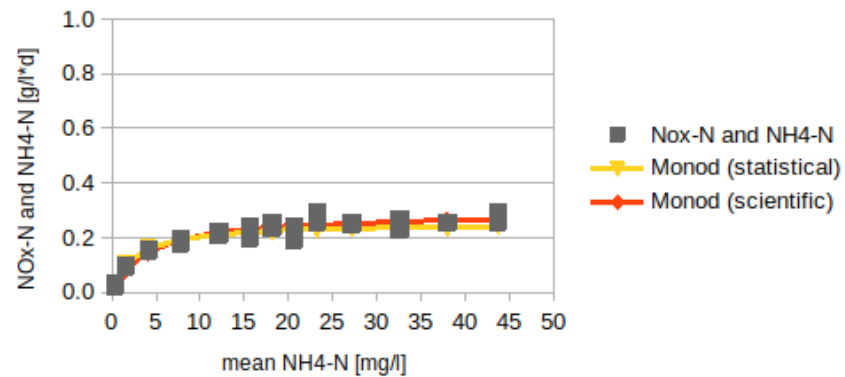R3 after aggregate loss - DO4 - day 344
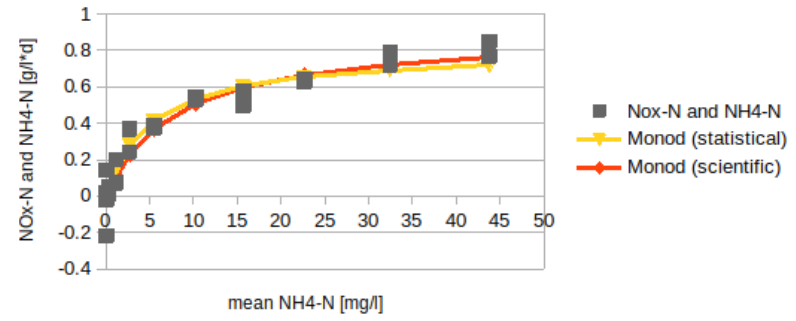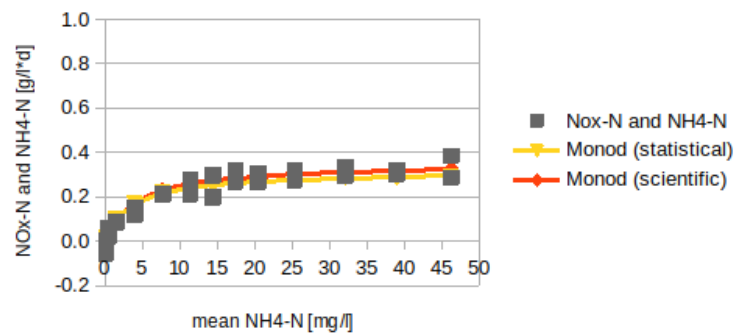
R2 - DO4 - day 412
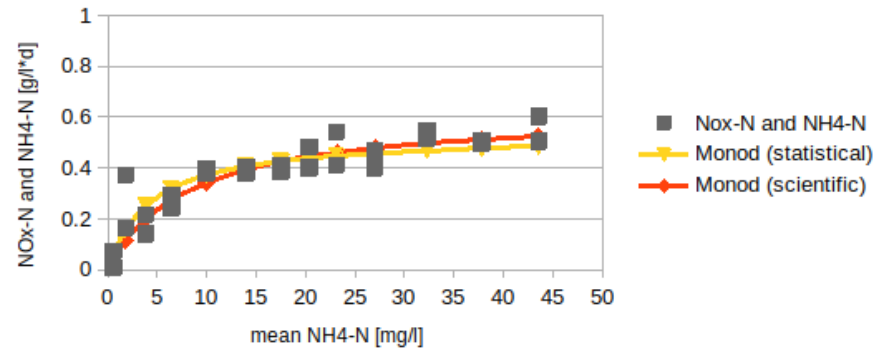
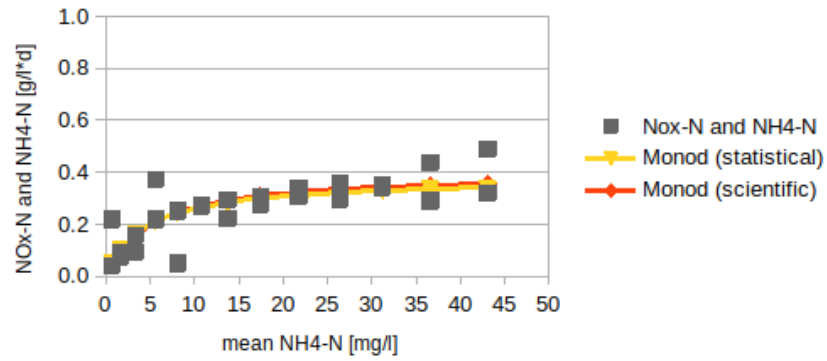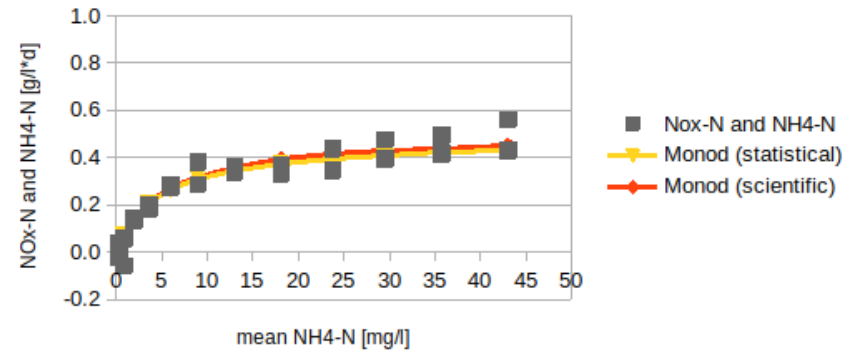R4 - DO4 - day 412
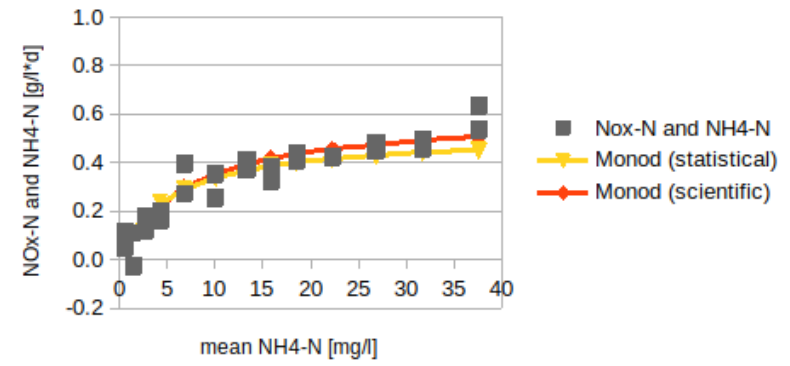
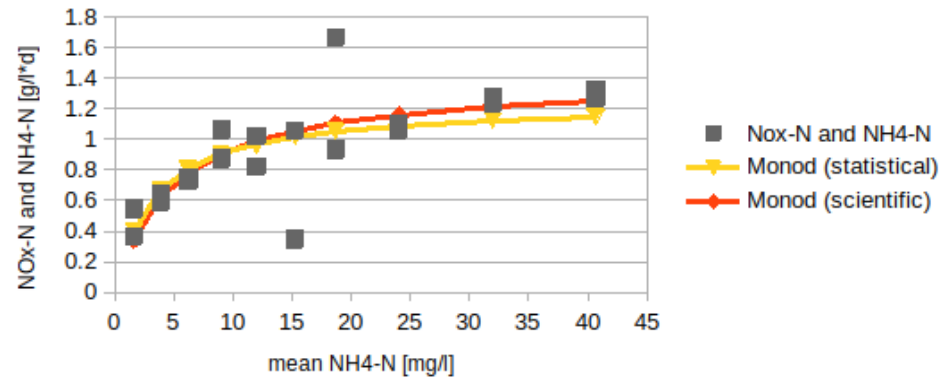R1 - DO4 - day 421
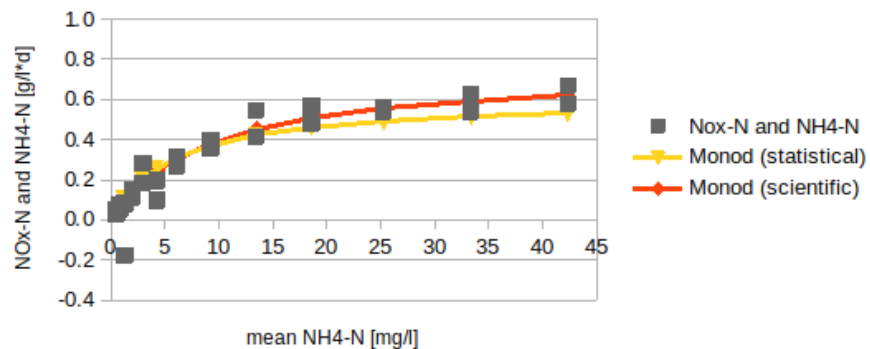
R3 - DO4 - day 421
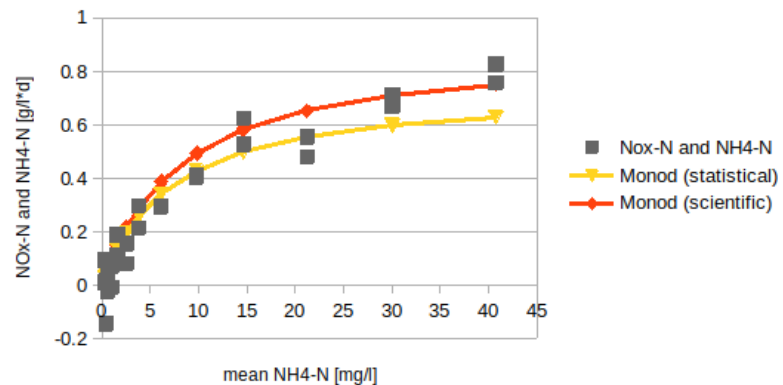
R2 - DO2 - day 414

R4 - DO2 - day 414

R1 - DO2 - day 419

R3 - DO2 - day 419

## R2 full bed volume - DO3 - day 419

6 Appendix Table summary activity studies

*Table: Ks and **μ**max values from the Monod curves calculated after the adjusted fit and the statistical method. For the statistical method the MSPE is shown. Values for the calculations are retrieved from activity studies at 15 °C performed at DO=2 and DO=4. Information about the DO in the experiment (DO in reactor) as well as the DO the activity study was performed under (DO in act. study) are shown.*

day	reactor	DO in act. study	Ks adjusted fit	umax adjusted fit	Ks statistical	umax statistical	MSPE statistical	Do in reactor	Info
295	R1	4	10	0,94	5,1	0,70	0,20	4	
295	R3	4	4	0,83	4,3	0,79	0,22	4	
302	R4	4	10	0,70	5,1	0,56	0,18	4	
302	R2	4	10	1,10	5,1	0,83	0,21	7	
310	R1	2	10	0,50	2,9	0,37	0,06	4	
310	R3	2	4	0,45	2,4	0,40	0,05	4	
337	R1	2	10	0,50	6,6	0,41	0,06	4	after aggregate loss
337	R3	2	4	0,55	2,5	0,49	0,05	4	after aggregate loss
344	R1	4	4	0,90	4,6	0,85	0,11	4	after aggregate loss
344	R3	4	8	0,90	5,1	0,80	0,07	4	after aggregate loss
412	R2	4	8	0,62	4,2	0,53	0,07	4	
412	R4	4	7	0,60	5,2	0,51	0,06	6	
414	R2	2	4	0,29	2,3	0,26	0,02	4	
414	R4	2	4	0,35	3,4	0,32	0,04	6	
419	R1	2	5	0,40	4,3	0,38	0,07	2	
419	R3	2	5	0,50	4,7	0,48	0,05	2	
419	R2	3	5	1,40	3,4	1,25	0,20	4	all carriers
421	R1	4	9	0,75	5,8	0,61	0,08	2	
421	R3	4	8	0,90	7,1	0,74	0,08	2	

7 Appendix Figure Monod curves after statistical method

Statistical method day 295-310
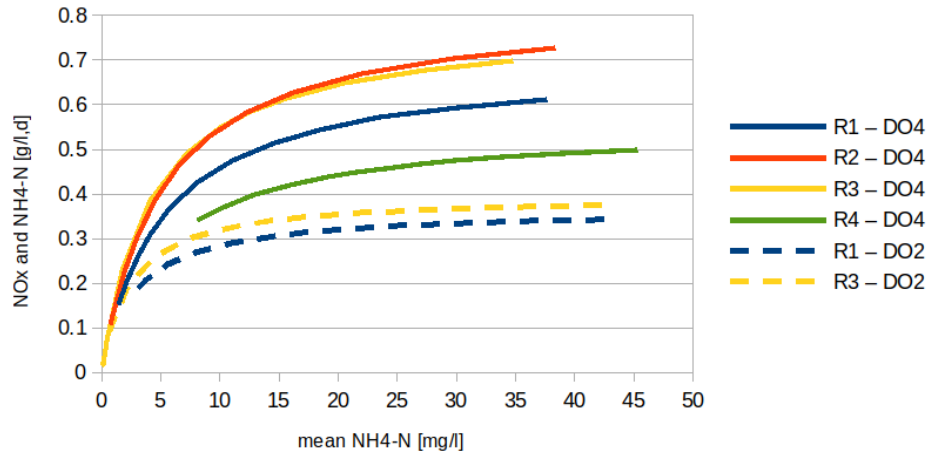
Statistical method day 412-421
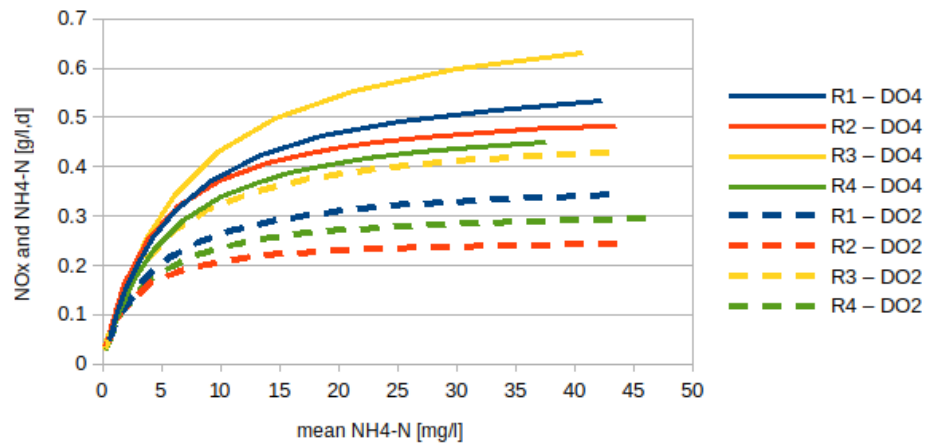
Statistical method at high aeration, day 264-310 and 337-344